

**T.R.  
SAKARYA UNIVERSITY  
GRADUATE SCHOOL OF NATURAL AND APPLIED SCIENCES**

**SYNTHESIS OF AION, MgAION AND MgAl<sub>2</sub>O<sub>4</sub> POWDERS USING  
THERMO-CHEMICAL METHOD**

**PhD THESIS**

**Hamza BOUSSEBHA**

**Metallurgy and Materials Engineering Department**

**MARCH 2023**



**T.R.  
SAKARYA UNIVERSITY  
GRADUATE SCHOOL OF NATURAL AND APPLIED SCIENCES**

**SYNTHESIS OF AION, MgAION AND MgAl<sub>2</sub>O<sub>4</sub> POWDERS USING  
THERMO-CHEMICAL METHOD**

**PhD THESIS**

**Hamza BOUSSEBHA**

**Metallurgy and Materials Engineering Department**

**Thesis Advisor: Prof. Dr. Ali Osman KURT**

**MARCH 2023**



The thesis work titled “Synthesis of AlON, MgAlON and MgAl<sub>2</sub>O<sub>4</sub> powders using thermo-chemical method” prepared by Hamza Boussebha, was accepted by the following jury on 22/03/2023 unanimously as a PhD THESIS in Sakarya University Graduate School of Natural and Applied Sciences, Metallurgy and Materials Engineering department.

### Thesis Jury

- Jury Member :**      **Prof. Dr. Ali Osman KURT (Advisor)** .....  
Sakarya University
- Jury Member :**      **Prof. Dr. Abdil ÖZDEMİR** .....  
Sakarya University
- Jury Member :**      **Prof. Dr. Kenan YILDIZ** .....  
Sakarya University
- Head of Jury :**      **Prof. Dr. Ramazan YILMAZ** .....  
Sakarya University of Applied Science
- Jury Member :**      **Prof. Dr. Figen KAYA** .....  
Yıldız Technical University



## **STATEMENT OF COMPLIANCE WITH THE ETHICAL PRINCIPLES AND RULES**

I declare that the thesis work titled " TECHNICAL CERAMIC NANO POWDER SYNTHESIS AND PROCESS OPTIMIZATION USING THERMO-MECHANOCHEMICAL METHOD", which I have prepared in accordance with Sakarya University Graduate School of Natural and Applied Sciences regulations and Higher Education Institutions Scientific Research and Publication Ethics Directive, belongs to me, is an original work, I have acted in accordance with the regulations and directives mentioned above at all stages of my study, I did not get the innovations and results contained in the thesis from anywhere else, I duly cited the references for the works I used in my thesis, I did not submit this thesis to another scientific committee for academic purposes and to obtain a title, in accordance with the articles 9/2 and 22/2 of the Sakarya University Graduate Education and Training Regulation published in the Official Gazette dated 20.04.2016, a report was received in accordance with the criteria determined by the graduate school using the plagiarism software program to which Sakarya University is a subscriber, I accept all kinds of legal responsibility that may arise in case of a situation contrary to this statement.

(15/03/2023)

Hamza Boussebha



*To my mother who was my driving force to seek higher education and my father  
whose pride has always been in our achievements.*



## ACKNOWLEDGMENTS

It is with much pleasure that I dedicate this PhD dissertation to all those who have been alongside me in this journey. Above all come my parents for devoting their lives to help me achieve the highest level of education and constantly pushing me to pursue greatness in life. Then my beloved and fellow PhD candidate, Salome Tsikarishvili who has been by my side from the first day I took this challenge, my sister and also fellow PhD candidate Meriem Boussebha for her unconditional support that I have always had in my heart and never doubted, my PhD advisor Prof. Ali O. Kurt without whom this thesis and study would not have been completed in the finest way possible, then all those who helped me during my research, my laboratory partners Sinan Bakan and Betül Özdemir, our research team members Assoc. Prof. Nuray Canıkoğlu and Assoc. Prof. Ayşe Şükran Demirkıran, defense jury members Prof. Abdil Özdemir, Prof. Cuma Bindal, Prof. Kenan Yıldız, Prof. Ramazan Yılmaz and Prof. Figen Kaya provided me with invaluable insights about my research, our department XRD and SEM technicians Murat Kazancı, SARGEM laboratory technician Mesut Aydemir, Sakarya University for providing financial support through BAP grant No 2020-7-25-82, and not forgetting the European Ceramic Society represented by Véronique Huart and the American Ceramic Society represented by Amanda Engin, both of which granted me financial support to attend international conferences. In the end, this single page acknowledgement section would never sum up the massive support I have had throughout the years and therefore, I am grateful to all those whose names I forgot to mention. I dedicate this work to all of you.

Hamza Boussebha



## TABLE OF CONTENTS

	<u>Page</u>
<b>ACKNOWLEDGMENTS</b> .....	<b>ix</b>
<b>TABLE OF CONTENTS</b> .....	<b>xi</b>
<b>ABBREVIATIONS</b> .....	<b>xiii</b>
<b>SYMBOLS</b> .....	<b>xv</b>
<b>LIST OF TABLES</b> .....	<b>xvii</b>
<b>LIST OF FIGURES</b> .....	<b>xix</b>
<b>SUMMARY</b> .....	<b>xxiii</b>
<b>ÖZET</b> .....	<b>xxv</b>
<b>1. INTRODUCTION</b> .....	<b>1</b>
<b>2. LITERATURE REVIEW</b> .....	<b>5</b>
2.1. Historical Background.....	5
2.2. Phase Diagrams and Crystal Structure .....	6
2.2.1. MgAl <sub>2</sub> O <sub>4</sub> spinel .....	6
2.2.2. AlON .....	8
2.2.3. MgAlON .....	13
2.3. Properties of MAS, AlON and MgAlON.....	17
2.3.1. Mechanical properties .....	17
2.3.1.1. Magnesium aluminate (spinel).....	17
2.3.1.2. Aluminum oxynitride .....	18
2.3.1.3. MgAlON .....	19
2.3.2. Optical properties .....	20
2.4. Synthesis Methods.....	21
2.4.1. Spinel .....	22
2.4.1.1. Sol-Gel .....	22
2.4.1.2. Solid state reaction .....	23
2.4.2. AlON.....	24
2.4.2.1. Carbothermal reduction nitridation .....	24
Reducing agents .....	27
Particle size .....	27
2.4.2.2. Other synthesis methods .....	28
2.4.2.3. Forming mechanism.....	29
2.4.3. MgAlON .....	30
2.4.3.1. Formation mechanism.....	31
2.5. Densification of MAS, AlON and MgAlON for Transparent Windows .....	32
2.5.1. Factors controlling densification.....	33
2.5.1.1. Ball milling .....	33
2.5.1.2. Sintering additives.....	34
<b>3. EXPERIMENTAL PROCEDURE</b> .....	<b>37</b>
3.1. Powder and Reaction Temperature Selection .....	37
3.1.1. Magnesium aluminate .....	38
3.1.2. AlON.....	41

3.1.3. MgAlON.....	44
3.2. Experimental Design .....	45
3.2.1. The DTM furnace.....	45
3.2.2. Gas use .....	47
3.2.3. Heating plan .....	48
3.3. Characterization methods .....	52
3.3.1. X-ray diffraction (XRD).....	53
3.3.2. Scanning electron microscopy (SEM).....	53
3.3.3. Field emission scanning electron microscope (FESEM) .....	54
3.3.4. Particle distribution analyses.....	54
<b>4. RESULTS AND DISCUSSIONS .....</b>	<b>57</b>
4.1. Characterization Results .....	57
4.1.1. Magnesium aluminate spinel.....	57
4.1.1.1. Results of XRD analyses .....	58
4.1.1.2. Scanning electron microscopy results .....	64
4.1.2. Aluminum oxynitride .....	66
4.1.2.1. XRD analyses results .....	66
4.1.2.2. Scanning electron microscopy .....	76
4.1.3. Magnesium aluminum oxynitride .....	79
4.1.3.1. XRD analyses results .....	80
4.1.3.2. Scanning electron microscopy results .....	85
4.1.3.3. Particle size distribution results.....	87
4.2. Discussions .....	90
4.2.1. Magnesium aluminate spinel.....	90
4.2.2. Aluminum oxynitride .....	91
4.2.3. Magnesium aluminum oxynitride .....	94
<b>5. CONCLUSION AND RECOMMENDATIONS .....</b>	<b>97</b>
5.1. Recommendations .....	99
<b>REFERENCES .....</b>	<b>101</b>
<b>CURRICULUM VITAE .....</b>	<b>113</b>

## **ABBREVIATIONS**

<b>CP</b>	: Cold Pressing
<b>CRN</b>	: Carbothermal Reduction Nitridation
<b>DTM</b>	: Dynamic Thermochemical Method
<b>FC</b>	: Facial Cubic
<b>FCC</b>	: Facial Centered Cubic
<b>FESEM</b>	: Field Emission Scanning Electron Microscopy
<b>GG</b>	: Gas-Gas Reaction
<b>HIP</b>	: Hot Isostatic Pressing
<b>HP</b>	: Hot Pressing
<b>MAS</b>	: Magnesium Aluminate Spinel
<b>NRL</b>	: Naval Research Laboratory
<b>rpm</b>	: Revolution per Minute
<b>SEM</b>	: Scanning Electron Microscopy
<b>SG</b>	: Solid-Gas Reaction
<b>SHS</b>	: Self High Temperature Synthesis
<b>SPS</b>	: Self Propagating Synthesis
<b>SS</b>	: Solid-Solid Reaction
<b>XRD</b>	: X Ray Diffraction



## SYMBOLS

$^{\circ}\text{C}$	: Degree Celsius
$^{\circ}\text{C}/\text{m}$	: Degree Celsius per minute
$\text{\AA}$	: Angstrom
$a$	: Lattice parameter
$\text{Al}$	: Aluminum
$\text{Al}(\text{OH})_3$	: Aluminum Hydroxide
$\text{Al}_2\text{O}_3$	: Alumina
$\text{AlN}$	: Aluminum Nitride
$\text{AlON}$	: Aluminum Oxynitride
$\text{Ar}$	: Argon
$\text{C}$	: Carbon
$\text{C}_3\text{H}_8$	: Propene
$\text{g}/\text{cm}^3$	: Grammes per Cubic Meter
$\text{GG}$	: Gas-Gas Reaction
$\text{GPa}$	: Giga Pascal
$\text{h}$	: Hour
$\text{IR}$	: Infrared
$\text{L}$	: Length
$\text{l}/\text{m}$	: Liter per Minute
$\text{LiF}$	: Lithium Florid
$\text{Mg}$	: Magnesium
$\text{Mg}(\text{OH})_2$	: Magnesium Hydroxide
$\text{MgAl}_2\text{O}_4$	: Magnesium Aluminate
$\text{MgAlON}$	: Magnesium Aluminum Oxynitride
$\text{MgO}$	: Magnesia
$\text{MPa}$	: Mega Pascal
$\text{N}_2$	: Nitrogen

<b>NH<sub>3</sub></b>	: Ammonia
<b>O<sub>2</sub></b>	: Oxygen
<b>P</b>	: Pressure
<b>RN</b>	: Reduction Nitridation
<b>T</b>	: Transmission
<b>UV</b>	: Ultraviolet
<b>X</b>	: Catanionic Vacancy
<b>Y</b>	: Young Modulus
<b>μ</b>	: Poisson Ratio
<b>μm</b>	: Micrometer
<b>Φ</b>	: Diameter

## LIST OF TABLES

	<u>Page</u>
<b>Table 2.1.</b> The existing phases in the experimental Al <sub>2</sub> O <sub>3</sub> -AlN phase diagram as given by McCauley .....	10
<b>Table 2.2.</b> MgAlON formulas with comparisons between experimental and calculated parameters .....	14
<b>Table 2.3.</b> Mechanical properties of MAS collected from different studies .....	17
<b>Table 2.4.</b> Physical and mechanical properties of transparent AlON .....	18
<b>Table 2.5.</b> Mechanical properties of MgAlON collected from different studies.....	19
<b>Table 3.1.</b> The chemical composition of Al(OH) <sub>3</sub> used, as obtained from the producing company. ....	38
<b>Table 3.2.</b> The chemical composition of Mg(OH) <sub>2</sub> used as obtained from the producing company.....	39
<b>Table 3.3.</b> The general gas flow plan in AlON synthesis.....	48
<b>Table 3.4.</b> The heating plans investigated in the synthesis of MgAl <sub>2</sub> O <sub>4</sub> .....	49
<b>Table 3.5.</b> The heating plans investigated in the synthesis of AlON .....	49
<b>Table 3.6.</b> The heating plans investigated in the synthesis of MgAlON.....	51
<b>Table 4.1.</b> Heating plans of experiments with varying parameters comparing to that of the optimum result. ....	71



## LIST OF FIGURES

	<u>Page</u>
<b>Figure 2.1.</b> MgO-Al <sub>2</sub> O <sub>3</sub> binary phase diagram.....	6
<b>Figure 2.2.</b> Spinel unit cell illustration with MgO <sub>4</sub> tetrahedra sites in violet and AlO <sub>6</sub> octahedra in blue .....	7
<b>Figure 2.3.</b> MgO-Al <sub>2</sub> O <sub>3</sub> phase diagram showing MgO rich spinel phase at high temperature.....	8
<b>Figure 2.4.</b> AlN-Al <sub>2</sub> O <sub>3</sub> phase diagram presented by McCauley and Corbin .....	9
<b>Figure 2.5.</b> Crystal structure, bonding and phase variation in the AlN-Al <sub>2</sub> O <sub>3</sub> system	11
<b>Figure 2.6.</b> Representation of Al <sub>23</sub> O <sub>27</sub> N <sub>5</sub> crystal model .....	12
<b>Figure 2.7.</b> MgO-AlN-Al <sub>2</sub> O <sub>3</sub> system phase diagram as given by willems et. al.....	12
<b>Figure 2.8.</b> Experimental MgO-AlN-Al <sub>2</sub> O <sub>3</sub> phase diagram as presented by Granon et. al.....	13
<b>Figure 2.9.</b> MgAlON crystal model with low nitrogen content .....	16
<b>Figure 2.10.</b> MgAlON crystal model with high nitrogen content .....	16
<b>Figure 2.11.</b> Stability regions of AlON at 1600°C and 1750°C (dot and solid lines respectively) as function of partial pressure of (a) O <sub>2</sub> and N <sub>2</sub> , and (b) O <sub>2</sub> and Al suboxides in an atmosphere with constant N <sub>2</sub> pressure PN <sub>2</sub> =N <sub>2</sub> .	25
<b>Figure 2.12.</b> AlON forming mechanism.....	30
<b>Figure 2.13.</b> MgAlON evolution in Al-Al <sub>2</sub> O <sub>3</sub> -MgO-N <sub>2</sub> system. ....	31
<b>Figure 2.14.</b> MgAlON formation mechanism in the C-Al <sub>2</sub> O <sub>3</sub> -MgO system.....	32
<b>Figure 3.1.</b> SEM analysis (a) and XRD pattern (b) of Al(OH) <sub>3</sub> raw material.....	39
<b>Figure 3.2.</b> SEM analysis (a) and XRD pattern (b) of Mg(OH) <sub>2</sub> material. ....	39
<b>Figure 3.3.</b> Thermodynamic modal of the reaction of 2 moles of Al(OH) <sub>3</sub> with 1 mole of Mg(OH) <sub>2</sub> under Ar atmosphere between 100°C and 1500°C.....	40
<b>Figure 3.4.</b> A photograph showing the prepared granules before charging into the reactor.....	41
<b>Figure 3.5.</b> Thermodynamic modal of the reaction of Al(OH) <sub>3</sub> at 1450°C under NH <sub>3</sub> + 5% C <sub>3</sub> H <sub>8</sub> . ....	42
<b>Figure 3.6.</b> Thermodynamic modal of the reaction of Al(OH) <sub>3</sub> under N <sub>2</sub> + 5% C <sub>3</sub> H <sub>8</sub> at 1450°C. ....	43
<b>Figure 3.7.</b> Thermodynamic modal of the reaction of Al(OH) <sub>3</sub> + 21C under N <sub>2</sub> with 1500°C as a completion temperature. ....	44
<b>Figure 3.8.</b> Schematic representation of the DTM process .....	46
<b>Figure 3.9.</b> The DTM modified rotary furnace. ....	46
<b>Figure 3.10.</b> ALICAT brand MFCs for gas mixing used in the synthesis process. ..	47
<b>Figure 3.11.</b> Graphical representation of the AlON heating plan .....	48
<b>Figure 3.12.</b> Rigaku D/MAX/2200-PC device used in the characterization of powders. ....	52
<b>Figure 3.13.</b> JEOL, model 6060 LV, USA scanning electron microscope used in the characterization. ....	53
<b>Figure 3.14.</b> FESEM used in the characterization of the synthesized powders .....	54

<b>Figure 3.15.</b> MICROTRAC S3500 size characterization device used in the determination of the size distribution.....	55
<b>Figure 4.1.</b> A photograph showing the obtained powder after the synthesis (a) using alumina balls and (b) without balls. ....	57
<b>Figure 4.2.</b> XRD patterns of powders synthesized for 1h at 1300°C, 1400°C and 1500°C.....	58
<b>Figure 4.3.</b> XRD patterns of spinel powder synthesized at 1500° for 1h, 1.5h and 2h. ....	59
<b>Figure 4.4.</b> A computer screenshot of MAUD program used to quantify the proportion of phases in the synthesis of magnesium aluminate.....	60
<b>Figure 4.5.</b> XRD pattern corresponding to powders synthesized at 1500°C for 1.5h at 2rpm tube rotation (no balls used).....	61
<b>Figure 4.6.</b> XRD pattern of powders synthesized at 1400°C for 1.5h in presence of 10B/P using alumina balls comparing to that obtained at 1500°C for 1.5h. Reactor speed in both test was 2 rpm. ....	62
<b>Figure 4.7.</b> XRD results of powder synthesized at 1500°C for 1.5h at 2rpm. ....	63
<b>Figure 4.8.</b> Alumina balls after being used in the synthesis of spinel powder at 1500°C for 1.5h with at 2rpm. (B/P was 20.) Satellite formation clearly visible on the balls indicates alumina deposition.....	63
<b>Figure 4.9.</b> SEM micrograph illustrating the powder morphology of spinel powder synthesized at 1500°C for 1.5h. ....	64
<b>Figure 4.10.</b> SEM micrograph illustrating the powder morphology of spinel powder synthesized at 1500°C for 2h. ....	64
<b>Figure 4.11.</b> SEM micrograph of spinel powder synthesized at 1500°C for 1.5h at 2rpm. Figure “b” is the enlargement of image “a”.....	65
<b>Figure 4.12.</b> XRD pattern of AlN powders synthesized via gas reduction nitridation at 1450°C for 1h.....	67
<b>Figure 4.13.</b> XRD pattern of powders synthesized at 1450°C for 1h at 2rpm. ....	68
<b>Figure 4.14.</b> XRD patterns of powders synthesized at 1500°C for 2h at 4rpm.....	68
<b>Figure 4.15.</b> XRD pattern for two-steps synthesis performed at 1100°C followed by continuous heating and holding at 1500°C with varying holding time of the first step. ....	69
<b>Figure 4.16.</b> AlON forming mechanism as given by Xie et al.....	70
<b>Figure 4.17.</b> XRD patterns of powder obtained with a two steps synthesis at 1100°C for 1.25h followed by a second holding at 1500°C under different conditions. ....	72
<b>Figure 4.18.</b> Powders synthesized under the same conditions (two-steps continuous heating at 1100 °C for 1.25h then 2h at 1500 °C).....	73
<b>Figure 4.19.</b> XRD patterns of powders synthesized at 1500°C for 2 h, after holding at 1100 °C for 1.25h under different atmospheres. ....	74
<b>Figure 4.20.</b> Powder synthesized from AlN and Al(OH) <sub>3</sub> mixture at 1500 °C for 2h under 1 liter per minute N <sub>2</sub> gas flow. ....	75
<b>Figure 4.21.</b> Powder synthesized at 1500°C for 2h with an intermediate holding at 1100°C for 1.25h under flow of NH <sub>3</sub> + 4% C <sub>3</sub> H <sub>8</sub> gas mixture with different conditions. ....	76
<b>Figure 4.22.</b> FESEM images of powders obtained under NH <sub>3</sub> + 4% C <sub>3</sub> H <sub>8</sub> atmosphere at 1450°C for 1h, statically (a) versus that obtained via DTM at 2rpm (b). ....	77
<b>Figure 4.23.</b> SEM micrographs illustrating morphologies of powder synthesized at 1500°C for 2h at 4rpm after holding at 1100°C for: A) 1h B) 1.5h.....	78

<b>Figure 4.24.</b> FESEM micrographs illustrating morphologies of powders synthesized at 1500°C for 2h at 4rpm after holding at 1100°C for 1.25h. Image b is the enlargement of image a. ....	79
<b>Figure 4.25.</b> XRD pattern of powder synthesized at 1500°C for 2h under N <sub>2</sub> .....	80
<b>Figure 4.26.</b> XRD pattern of powders synthesized dynamically under N <sub>2</sub> atmosphere compared to MgAl <sub>2</sub> O <sub>4</sub> obtained in a static system under Ar. ....	81
<b>Figure 4.27.</b> Representation of MgAlON formation as given by Chen et al.....	81
<b>Figure 4.28.</b> XRD patterns of powders synthesized at 1500°C for 1h in NH <sub>3</sub> + 1% C <sub>3</sub> H <sub>8</sub> at 2rpm. ....	82
<b>Figure 4.29.</b> XRD patterns of powders obtained in DTM method under NH <sub>3</sub> + 1% C <sub>3</sub> H <sub>8</sub> at 1500°C for 1h and 2h.....	82
<b>Figure 4.30.</b> XRD patterns of powders synthesized using DTM method at 1500°C for 2h at 2 rpm comparing to MgAl <sub>2</sub> O <sub>4</sub> obtained statically at 1500°C for 2h.	83
<b>Figure 4.31.</b> XRD patterns of powders obtained at 1500 °C for 2h under NH <sub>3</sub> + 1% C <sub>3</sub> H <sub>8</sub> in both static and dynamic system. ....	84
<b>Figure 4.32.</b> XRD patterns of powders synthesize under NH <sub>3</sub> + 1% C <sub>3</sub> H <sub>8</sub> atmosphere. ....	84
<b>Figure 4.33.</b> FESEM images of powders obtained after 2h at 1500°C under NH <sub>3</sub> + 1% C <sub>3</sub> H <sub>8</sub> at (a) 2rpm and (b) statically.....	86
<b>Figure 4.34.</b> FESEM images of powders obtained after 2h at 1500°C under NH <sub>3</sub> at (a) 2rpm and (b) statically. ....	86
<b>Figure 4.35.</b> FESEM images of powders obtained after 1h at 1500°C under NH <sub>3</sub> + 1% C <sub>3</sub> H <sub>8</sub> at 2rpm. ....	87
<b>Figure 4.36.</b> Particle size distribution of powders obtained at 1500°C for 2h under NH <sub>3</sub> + 1% C <sub>3</sub> H <sub>8</sub> synthesized (a) statically versus (b) that obtained at 2rpm. ....	88
<b>Figure 4.37.</b> Particle size distribution of powders obtained at 1500°C for 2h under NH <sub>3</sub> synthesized at 2rpm.....	89
<b>Figure 4.38.</b> Particle size distribution of powders obtained at 1500°C for 1h after holding at 1100°C for 1h under NH <sub>3</sub> + 1% C <sub>3</sub> H <sub>8</sub> synthesized at 2rpm.....	89



## **SYNTHESIS OF AION, MgAION AND MgAl<sub>2</sub>O<sub>4</sub> POWDERS USING THERMO-CHEMICAL METHOD**

### **SUMMARY**

Due to their major importance in the field of armor and transparent infrared windows, aluminum oxynitride (AION), magnesium aluminate, also known as spinel (MgAl<sub>2</sub>O<sub>4</sub>) and magnesium aluminum oxynitride (MgAION) have always been subject to research due to the limitations of their manufacturing processes. The interest of synthesizing fine powders of these ceramics at intermediate temperatures, aims to decrease the high cost of the final products, as well as, providing promising commercial methods to produce their powders. AION powders are commercially unavailable and can only be found as a ready to use products, produced via direct sintering of submicron aluminum oxide (Al<sub>2</sub>O<sub>3</sub>) and aluminum nitride (AlN) at temperatures exceeding 1850°C. This process has the disadvantage of raising the cost of the product together with the fact that many companies whose arsenal of equipment allows them to design their own parts, will not have the flexibility of purchasing aluminum oxynitride powders and manufacturing their own products. Unlike AION, spinel can be found commercially as powder and has already been manufactured and sold worldwide but a limited number of companies. Nevertheless, the production process as well as the cost of production are still major issues that cause a significant increase in the price of the product to provide spinel powders with high purity and fine particles. MgAION has been presenting itself as an intriguing technical ceramic since it perfectly mimics AION with properties as close as its parent phase. This is due to the that magnesium aluminum oxynitride is considered as a magnesium stabilized AION with a slightly lower stability temperature without a major loss in the mechanical and optical properties of aluminum oxynitride. With that in hand, there has always been an interest in investigating the synthesis of these ceramics via different methods to optimize their synthesis processes or even providing novel approaches to obtain their powders. In the last years, an innovative approach that can be considered as a modified carbothermal reduction nitridation (CRN) has been investigated in the synthesis of technical ceramics and has been deemed effective in providing powders that can be readily used in their as-synthesized form. “Dynamic / Thermochemical Method” (DTM) is the denomination used to describe this approach. In this process, the reduction and nitridation reactions take a place in a moving system that provides constant motion to the synthesis allowing the reaction to proceed and be accomplished in a relatively shorter time than usually needed in the convention CRN method as well as the massive advantage of relatively lowering the reaction temperature. In this PhD thesis, the optimization of these technical ceramics’ synthesis has been investigated via the DTM process. The obtained results showed that a temperature of 1500°C was sufficient to fully synthesize MgAION powders from aluminum and magnesium hydroxides (Al(OH)<sub>3</sub> and Mg(OH)<sub>2</sub>, respectively) in gas mixtures, without any solid carbon added. It has also been found that more than 50% conversion to AION could be achieved at an unprecedented temperature of 1500°C with submicron particles. Conversely, AION and MgAION whose syntheses via the dynamic thermochemical method was

successful,  $\text{MgAl}_2\text{O}_4$  had better results in the static synthesis comparing to its dynamic counterpart. The obtained results were characterized via X-ray diffraction (XRD), scanning electron microscopy (SEM), field emission scanning electron microscopy (FESEM) and particle size distribution. The obtained results were explained and some recommendations for further investigation and optimization of the results we provided.

## TERMO-KİMYASAL YÖNTEMLE AION, MgAION VE MgAl<sub>2</sub>O<sub>4</sub> TOZ ÜRETİMİ

### ÖZET

Alüminyum oksinitrür (AION), magnezyum alüminat (MgAl<sub>2</sub>O<sub>4</sub>) ve magnezyum alüminyum oksinitrür (MgAION) spinel yapıya sahip olup zırh ve şeffaf kızılötesi pencereler gibi uygulama alanlarındaki önemi nedeniyle birçok araştırmaya konu olmuştur. Bu seramik malzemelere ait tozların çok küçük tane boyutunda 1600°C ve altı sıcaklıklarda sentezlenmesi, bunlardan elde edilecek ürün maliyetlerinin azaltılmasının yanında üretim kolaylığı sağlaması nedeniyle ilgi kaynağı olmaktadır. AION seramik malzemeler ticari olarak toz formunda mevcut değildir. Bu seramik malzemeler mikron altı boyutlarda alüminyum oksit (Al<sub>2</sub>O<sub>3</sub>) ve alüminyum nitrit (AlN) tozlarının 1900°C'yi aşan sıcaklıklarda ve çoğunlukla gaz basınçlı sistemde birlikte sinterlenmesi ile elde edilen şekilli parça/ürün formunda bulunmaktadır. Yüksek maliyetli söz konusu işlem bu malzemelerin üretimi önündeki en büyük engeli oluşturmaktadır. AION'un aksine MgAl<sub>2</sub>O<sub>4</sub> (spinel) yapı ise toz formunda tedarik edilebilmektedir. Ancak, söz konusu toz malzemeyi yüksek saflıkta sağlanabilen üretici firma sayısı sınırlıdır. Bununla birlikte yüksek saflıkta ve ince parçacıklı spinel tozlarının elde edilebilmesi için kullanılan mevcut toz üretim yaklaşımları halen çok pahalı sistemlerdir. MgAION seramik fazı ise AION'e yakın özelliklerde olup birçok açıdan AION ile aynı niteliklere sahip ancak daha fazla tercih edilen bir malzemedir. Bunun nedeni, daha düşük sıcaklık kararlılığına sahip olmakla birlikte magnezyum alüminyum oksinitrürün, alüminyum oksinitrürün mekanik ve optik özelliklerine yakın bir davranış göstermesi nedeniyle magnezyumla kararlaştırılmış AION olarak kabul edilmesindedir. Bu nedenle bu malzemelerin toz üretim süreçlerini optimize etmek amaçlı farklı metot ve yöntemler ve yenilikçi yaklaşımlara olan ihtiyaç daima mevcut olmuştur.

Son yıllarda teknik seramik toz sentezinde modifiye karbotermal indirgeme nitrüleme (DTM) olarak da değerlendirilebilecek yenilikçi bir yaklaşım araştırılmış ve nitelikli teknik seramik tozlarının bu yöntemle kolayca elde edilebileceği görülmüştür. Bu yenilikçi toz üretim sisteminde indirgeme ve nitrüleme reaksiyonları daha etkili gerçekleşmekte ve geleneksel KİTİN yöntemine kıyasla daha kısa sürelerde ve morfolojik açıdan avantajlı tozlar elde edilebilmektedir. Bu teknikte seramik toz sentez süreçlerinin optimizasyonu, reaksiyonun hareketli bir sistemde yer aldığı yeni bir karbotermal indirgeme nitrüleme (KTİN) yöntemi olan Dinamik / Termokimyasal Metod (DTM) aracılığıyla gerçekleştirilmektedir. DTM, toz sentezinin bir döner fırın / döner tip reaktör içerisinde gerçekleştiği, reaksiyonun nispeten daha kısa sürede tamamlanmasına izin veren ve sentezlenmiş formlarında kolayca kullanılabilen ince tozlar sunan modifiye edilmiş bir karbotermal indirgeme metodudur.

Bu tez çalışmasında söz konusu teknik (DTM) kullanılarak AION, MgAl<sub>2</sub>O<sub>4</sub> ve MgAION toz üretimleri araştırılmıştır. Hammadde olarak Mg(OH)<sub>2</sub> ve Al(OH)<sub>3</sub> tozları kullanılmıştır. Deneysel çalışmalara başlanılmadan önce ilgili hammadde oranları ile kullanılacak indirgeyici ve süpürücü gazların belirlenmesi ve gerekli reaksiyon

sıcaklıklarının tespiti amaçlı *FactSage 7.0* yazılımından yararlanılarak termokimyasal modelleme çalışmaları yapılmıştır. Bu tez çalışmasını özgün kılan ve literatüre katkı sağlayan bir diğer unsur karbotermik indirgeme işlem süreçlerinde sistemde katı karbon yerine indirgeyici gaz(lar) kullanılmış olmasıdır. Hassas gaz akışları MFC (gas mass flow controller) marifeti ile özel tasarlanmış bir gaz karışım aparatı üzerinden bir mikroişlemci yardımı ile bilgisayarlı sağlanmıştır. Spinel toz üretiminde argon gazı ve AlON toz sentezinde amonyak ve propan karışım gazları kullanılmıştır. MgAlON tozu üretimlerinde ise azot ve amonyak gaz karışımlarından yararlanılmıştır.

Spinel ve MgAlON tozu üretimi süreçlerinde tek kademe, AlON tozu sentezinde ise tek veya çoklu kademe ısıtma rejimleri uygulanmıştır. Spinel tozunun (magnezyum alüminatın) sentezi 1300°C ile 1500°C sıcaklıkları arasında farklı tutma sürelerinde hem statik hem de dinamik sistemde gerçekleştirilmiştir. AlON tozu sentezi farklı sıcaklıklarda çalışılmış; örneğin, 1100°C'de ilk bekleme akabinde 1500°C'ye çıkıp burada reaksiyonun tamamlanması beklenmek suretiyle iki kademe yapılan ısıtma rejimi ile en iyi sonuca ulaşılmıştır. MgAlON tozu üretiminde ise tek kademe ısı rejimi ile örneğin 1500°C'de 2 saat beklemek tam dönüşüm için yeterli olmuştur.

Bu çalışma ile DTM kullanılarak amonyak veya amonyak ve propan gaz karışımı kullanarak Al(OH)<sub>3</sub> ve Mg(OH)<sub>2</sub>'nin MgAlON'a tam dönüşümü literatürle kıyaslandığında çok daha düşük sıcaklıklarda (1500°C'de) gerçekleştirilmiştir. MgAlON'un ucuz hammaddelerden 1500°C'de sentezi, hem başlangıç tozlarının düşük maliyeti hem de ara sentez sıcaklığı üretim maliyetinin düşürülmesine yardımcı olabileceğinden, yöntemin olası ticarileşmesine kapı açabileceği değerlendirilmektedir. Hâlihazırda MgAlON ve AlON gibi kullanıma hazır pencereler piyasada bulunmamaktadır. Buna karşılık, magnezyum alüminyum oksinitrür, çalışmalarda yalnızca olası bir ikame ve üretimi birçok zorlukla sınırlanan daha ucuz bir alüminyum oksinitrür formu olarak sunulmaktadır.

Ayrıca, bu çalışma sonrasında ilk defa 1500°C'de amonyak ve propan gaz karışımı altında Al(OH)<sub>3</sub>'ten AlON'a %50'den fazla dönüşüm sağlanmıştır. Literatürde AlON'un katı hal sentezinin alüminyum oksinitrürün kararsızlığı nedeniyle 1640°C'nin altında ulaşılamaz olduğu raporlanmakta iken bu çalışma ile 1500°C'de dönüşümün gerçekleşebileceği gösterilmiştir. 1500°C'de AlON'a kısmi dönüşüm iki nedenden dolayı çok olumlu bir sonuç olarak kabul edilebilir: Birincisi, 1640°C'nin altında alüminyum oksinitrürün elde edilemeyeceği belirtilmektedir. İkinci olarak, araştırma imkânları 1500°C'nin üzerinde çalışılmasına izin vermemiştir. Daha yüksek sıcaklıklarda örneğin 1550°C veya 1600°C'de test (DTM) yapılmasının mümkün olması durumunda tam dönüşümün gerçekleşebilme olasılığı yüksek olarak değerlendirilmiştir. Tüm bunlara ilave olarak termokimyasal işlemler öncesinde hammaddenin / alüminyum hidroksitin öğütülmesi gibi farklı ön-işlem aşamaları sonrası yapının geçiş alüminasına dönüşmesinin ve dolayısıyla AlON'a tam bir dönüşüm sağlama potansiyelinin artacağı değerlendirilmektedir.

AlON ve MgAlON'dan farklı olarak, dinamik termokimyasal yöntem, statik sistemde elde edilenlerden daha iyi sonuçlar sağlamada etkili değildi. Bu, dinamik yöntemin nitrürler veya oksitlerden ziyade oksinitrür bileşiğinin sentezini desteklemesi gerçeğiyle açıklandı.

Toz morfolojisi ile ilgili olarak, önceki çalışmalarımızda DTM'nin daha iyi bir toz morfolojisi sağlamada etkili olduğu kabul edilirken, incelenen seramik tozlarından sadece bir tanesi sinterleme için pozitif olarak kabul edilebilecek bir morfolojiye sahiptir. Buna karşılık, hem spinel hem de magnezyum alüminyum oksinitrürün her

ikisi de homojen olmayan boyutta kaba bir toz tane boyutu vermiştir. Çalışılan dinamik sistem ve hemen hemen tüm parametreler aynı olduğu için bu morfolojinin nedeninin magnezyum içermesi olduğu sonucuna varılmıştır.

Bu tez çalışması DTM ile MgAlON toz sentezinin literatüre kıyasla çok daha düşük sıcaklıklarda mümkün olabildiği gösterilmiş ayrıca, AlON'un ise 1640°C'nin altında oluşamayacağı önermesi çürütülecek sonuçlara ulaşılmıştır. Yapılan çalışmada 1500°C'de mikron altı bir boyutta ve %50'den daha fazla miktarda AlON`na dönüşüm sağlanmıştır. Elde edilen tozlar genel anlamda homojen bir yapıya sahiptir.

Spinel sentezi ile ilgili olarak, spinel sentezi için geleneksel ham maddeler (Al<sub>2</sub>O<sub>3</sub> ve MgO) kullanılarak dinamik yöntemin, ara dönüşüm olarak elde edilmek yerine, ana spinel oluşturucu bileşikler kullanıldığında bir fark olup olmadığını belirlemek için daha fazla araştırılması gerektiğine inanılmaktadır.

AlON durumunda, dinamik sistem aracılığıyla 1600°C'de oluşumunun araştırılmasının önemini vurgulamak hayati önem taşımaktadır. AlON'un kararsız kabul edildiği bir sıcaklıkta %50'den fazla dönüşümün gerçekleştirilmiş olması, mevcut kararlılık sıcaklığının altında olası sentez şansını yükseltmektedir.

MgAlON tozları bu çalışma ile tümüyle sentezlenebilmiştir. Bununla birlikte toz morfolojisinin geliştirilmesi üzerine çalışmalar gerçekleştirilebilir. Bu kapsamda hammaddelerin DTM öncesi tane küçültme de dâhil ön işlemlere tabi tutmak suretiyle nihai ürün morfolojisi üzerine etkileri araştırılabilir.

Elde edilen tozların kullanılabilirliği / sinterlenebilirliğinin ve sentezlenen tozlardan oluşan bir ürünün özelliklerinin araştırılması da önerilen çalışmalar arasındadır. Bu durum yeni yaklaşımla sentezlenen tozların kalitesinin tam olarak anlaşılmasını sağlayacaktır. Elde edilen sonuçlar, 1500°C'lik bir sıcaklığın, alüminyum ve magnezyum hidroksitlerden (sırasıyla Al(OH)<sub>3</sub> ve Mg(Al)<sub>2</sub>) spinel ve MgAlON tozlarının herhangi bir karbon eklenmeden gaz karışımlarında tamamen sentezlenmesi için yeterli olduğunu göstermiştir. AlON tozu üretiminde ise Al(OH)<sub>3</sub>`ten DTM ile 1500°C`de %50`den fazla dönüşüm sağlanabilmiştir.



## 1. INTRODUCTION

Over the last century, a technological revolution has led to a growing advancement in the field of materials science. These advancements were driven by different purposes such as national security (military), technological and economic dominance, as well as providing better choices for industry and its advancement. Hence, the elaboration of new materials with variety of properties that can be functional in different kind of use, has always been a target.

The merging of good mechanical and optical properties was one of the aims of much research, as to exploit the transparency of hard materials, giving birth to whole new field of research, that carried the name of: Optical ceramics.

Optical transparency refers to the property related to the transmittance of electromagnetic waves, with the least reflection and absorption. Thus, any obstacle that interrupts the transmittance of these waves results a lower transparency [1]. Since the interruptions of transmittance occurs as a result of absorption and scattering of electromagnetic radiation, attaining the highest percentage of transparency, requires the least absorption and scattering [2]. The absorption in a material is subject to different factors. These factors can be intrinsic as the bond strength and vibration energy of atoms, which can be increased as a result of radiation. Electrons too, are affected with radiation as they can be excited to jump from filled shells to unfilled higher ones [1]. These previously mentioned phenomena necessitate an energy which is dictated by the band gap theory. The difference of energy in the visible region is 3.102 eV, and thus, a material with a larger band gap than 3 eV is suspect to become transparent [2]. Additionally, there are extrinsic factors that also provoke a limitation of transparency such as porosity, secondary phases and grain boundaries [3]. Consequently, the obtention of highly transparent ceramics, requires: First, a choice of a material with band gap energy greater than 3.102 eV. Second a limitation of all sources of electromagnetic radiations absorption and scattering.

Transparent ceramics are advanced ceramics which had much of attention as being of interest for diverse applications such as lamp envelope, domes, windows and

transparent armor. Advanced ceramics can be obtained via particulate materials technology, in which sometimes, a certain porosity and very low impurities are tolerable when the production cost is to be maintained low. Nevertheless, for highly transparent ceramics, the powder must be of a high purity and the microstructure has to be carefully controlled during sintering to avoid all light scattering sources such as inclusions, secondary phases and porosity [3]. This means complex synthesis routes making the cost extremely high.

The manufacturing of optical ceramics obeys mostly to four important factors which are the degree of transmission, the polycrystalline isotropy, mechanical properties and limitations of manufacturing (size and cost). These factors are all influenced by the choice of system that delivers a compromise in matters of best possible properties and the least manufacturing limitations. The systems that are susceptible to operate at the visible wavelength can be single crystal, polycrystalline or amorphous, and their number is very limited. These include sapphire single crystal, aluminum oxide (alumina), yttrium oxide (yttria), magnesium aluminate (spinel), aluminum oxynitride (AlON), recrystallized glass and glass [2].

Sapphire single crystal is a chemically stable compound. It has a band gap energy of 9eV, making it a good insulator. Optically, it has a wide transmission range spanning the ultraviolet visible and infrared regions and remains transparent even under high radiation doses and high energy electron beams [4]. Sapphire single crystals can be obtained via crystal growing techniques such as Czochralski technique and the heat exchanger method [5]. However, these techniques do not offer net shapes and it is difficult to obtain curved surfaces which are preferred for windows.

Polycrystalline alumina is one of the best ceramics that possess excellent mechanical properties from hardness to fracture toughness and flexural strength. It can be obtained using conventional ceramic processing techniques. However, its birefringent nature, makes getting a good transparency very hard, limiting polycrystalline alumina's optical properties to be a translucent material [3].

Spinel ( $MgAl_2O_4$ ) is a cubic crystalline material that combines ruggedness and excellent transmission ranging from the ultraviolet (0.2  $\mu m$ ) to the mid-infrared (5  $\mu m$ ) region, which makes of spinel an excellent choice for military uses and commercial infrared windows applications [6]. It is, however, very difficult to obtain single crystal

spinel since the techniques are hard to control, time-consuming and expensive [7]. Additionally, obtaining dimensions greater than a few millimeters via traditional technique, is very hard due to its high melting temperature of 2135°C [8]. On the other hand, polycrystalline spinel can be obtained via hot pressing of powders. Nevertheless, due to the inhomogeneous mixing of sintering aids, an inhomogeneous structure with opaque regions, can engender transmission problems [9]. The US Naval Research Laboratory (NRL) has developed a technique to homogenize the sintering aids mixing by coating each powder particle with lithium fluoride (LiF), leading to high transparency after sintering [9].

The last 20 years has known the introduction of aluminum oxynitride (AlON) as a spinel competitor in the field of transparent ceramics destined for military uses. AlON has excellent properties, in addition to its excellent optical characteristics [10], it possesses a hardness close to that of single crystal sapphire, making it the hardest commercially available polycrystalline material [11]. Furthermore, AlON has a very good mechanical strength and resistance to both chemical attacks [12] and radiation [13]. A fully densified AlON can reach a transmittance band ranging from ultraviolet (a wavelength about 0.2  $\mu\text{m}$ , UV), to mid-infrared (about 5.0  $\mu\text{m}$ , IR) [14]. Besides the excellent transmittance, AlON has a great optical clarity (over 98 %) and very low haze (less than 2 %) in the visible wavelengths [11].

Magnesium aluminum oxynitride (MgAlON) has a spinel structure similar to that of AlON. It is well considered as a magnesium stabilized AlON, with almost the same mechanical and optical properties. The advantage that MgAlON holds over AlON lays within its forming temperature of 1400°C [15] and its stability temperature 1600°C [16], whereas aluminum oxynitride starts forming at 1600°C [17], and has been reported to only be stable above 1700°C [17-21].

In this thesis, we aim to apply a modified approach to synthesize the previously mentioned ceramics, as to deliver an affordable method that can be applied commercially. The root that was used is based on the traditional carbothermal reduction nitridation (CRN) with a difference of performing the synthesis in a rotating system which gives a dynamic nature to the CRN process, which helps homogenize the temperature of the reactant leading to shortened holding time and relatively lower temperature. In addition, it has been shown that this method provides a better powder morphology. This method has been deemed efficient in the synthesis of different

nitrides and borides [22-25]. Hence, a rising interest to investigate its efficiency in the synthesis of transparent ceramic powders led to this work.

## 2. LITERATURE REVIEW

### 2.1. Historical Background

As stated before, the development of transparent ceramics emerges from military and economic purposes. Magnesium aluminum spinel (MAS), AlON and MgAlON are amongst the best systems, presenting themselves as the best candidates to produce transparent ceramic windows.

Single crystal magnesium aluminate spinel occurs naturally. Originally, it has no color, yet it can include colors ranging from red to pink, indigo, green, purple, blue, violet or black, as a result of impurities that play the role of pigment. Due to the similarity of colors, spinel had been mistaken for rubies and sapphire, until it was first differentiated from them in 1908 [7]. With chemical formula of  $AB_2X_4$ , the group of minerals sharing this same formula and crystallizing in the face centered cubic (FCC) system, was named after spinel [7,26]. In the years that follow, the possible transparency of spinel had given rise to massive research to elaborate a practical route for its synthesis, especially in the United States (US), where  $MgAl_2O_4$  was shown to exhibit a good transparency and mechanical strength in the late 1960s at the North Carolina State University [27]. Nonetheless, not until 1980 had a high purity spinel powder been produced, giving rise to many projects and governmental funding in the United States, from which laboratories as Coors Ceramics, Raytheon Research Division, Alpha Optical Systems, TA&T and Surmet, has benefited to optimize the synthesis of spinel [28].

Dissimilar to spinel, AlON doesn't occur naturally and can only be obtained via combination of other compounds or synthesis. The first glimpse of aluminum oxide nitride dates to 1946 when Yamaguchi stated a possible existence of a spinel form of alumina may be stabilized above  $1000^\circ\text{C}$  by reducing aluminum (Al) ions from  $Al^{3+}$  to  $Al^{+1}$  or  $Al^{+2}$  [29-31]. Nevertheless, Yamaguchi came back in 1959 with paper proposing an AlN- $Al_2O_3$  formula for the new spinel, with a believe that the reduction to the spinel-like form results from nitrogen incorporation [30]. Various research has been carried out ever since, however, rising interests in SiAlON led to AlON becoming

a major interest [31]. In 1979, McCauley and Corbin presented the first model of transparent AlON opening the door to many future investigations to optimize the synthesis and manufacturing process [32].

AlON however, has been very difficult to obtain under 1740°C, and has been stated to be thermodynamically unstable under 1640°C [21,33]. In attempts to stabilize AlON under lower temperatures, MgAlON made appearance in the 1990s by introducing MgO to the AlN-Al<sub>2</sub>O<sub>3</sub> [34], and has been subject to research ever since.

## 2.2. Phase Diagrams and Crystal Structure

### 2.2.1. MgAl<sub>2</sub>O<sub>4</sub> spinel

Magnesium aluminate spinel is the intermediate compound that forms in the MgO and Al<sub>2</sub>O<sub>3</sub> binary system. With both being refractories having melting temperatures of 2825°C and 2054°C, and densities of 3.58g/cm<sup>3</sup> and 3.997g/cm<sup>3</sup>, respectively, spinel is formed with a melting temperature of 2122°C, and a density of 3.578g/cm<sup>3</sup> [7]. Figure 2.1 illustrates a representation of the MgO-Al<sub>2</sub>O<sub>3</sub> binary system.

It can be seen that two eutectoid systems are formed, MgO-MgAl<sub>2</sub>O<sub>4</sub> in which the eutectoid point is at a molar percentage of 36% Al<sub>2</sub>O<sub>3</sub> at 1985°C, whereas the one of MgAl<sub>2</sub>O<sub>4</sub>-Al<sub>2</sub>O<sub>3</sub> takes place at 1994°C and an Al<sub>2</sub>O<sub>3</sub> of 79%. Spinel, on the other hand, is the intermediate phase that separates both with a melting point of 2122°C.

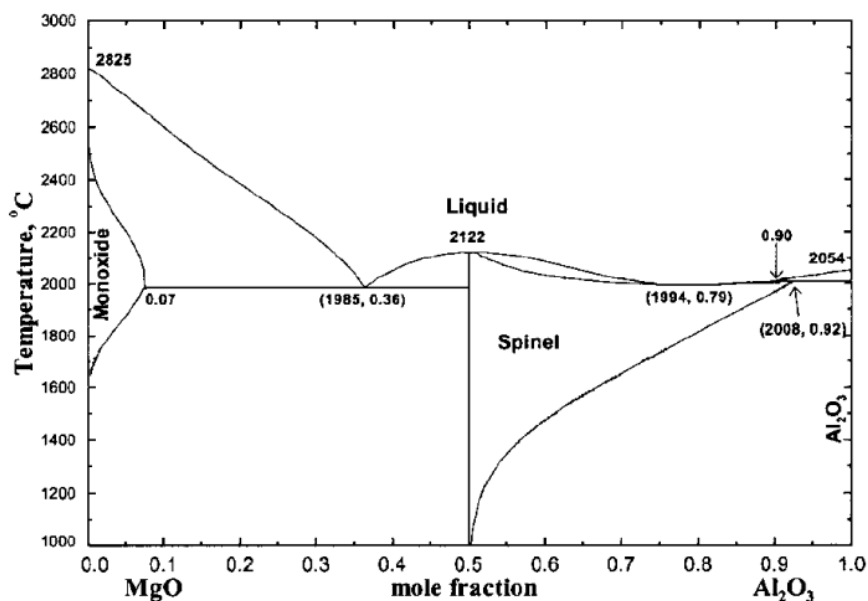
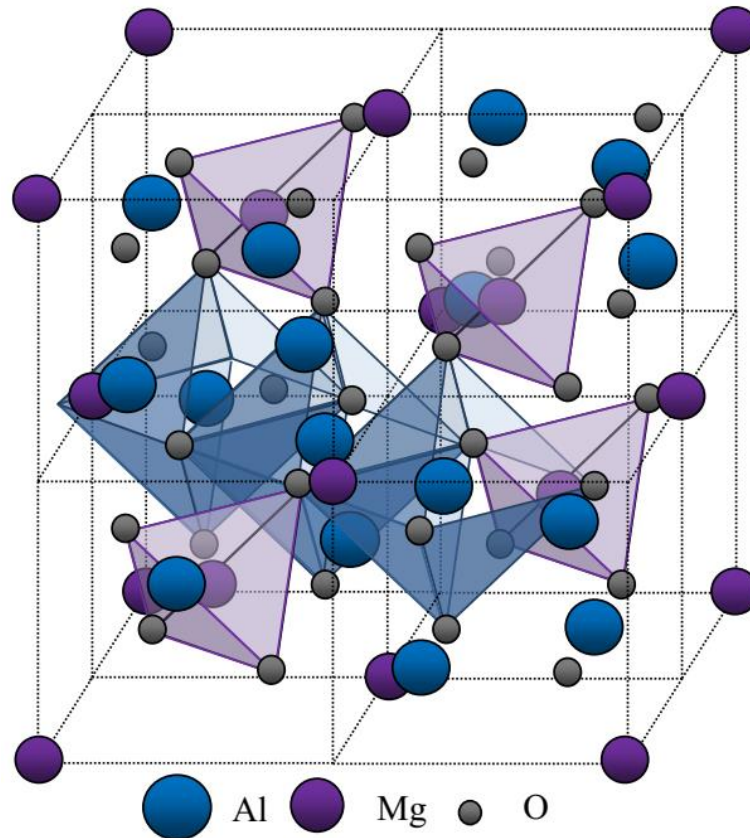


Figure 2.1. MgO-Al<sub>2</sub>O<sub>3</sub> binary phase diagram. [35]

Magnesium aluminate spinel has been shown to crystallize in the  $Fd\bar{3}m$  cubic system, while its parent compounds,  $MgO$  and  $Al_2O_3$ , crystallize in a cubic,  $Fm\bar{3}m$  space group and the hexagonal system of  $R\bar{3}c$  space group, respectively [7].

The unit cell of spinel comprises eight  $MgAl_2O_4$  molecules [36-37], in which magnesium has four neighboring oxygen atoms to form  $MgO_4$  tetrahedra, besides  $AlO_6$  octahedra where aluminum is surrounded with six atoms of oxygen.



**Figure 2.2.** Spinel unit cell illustration with  $MgO_4$  tetrahedra sites in violet and  $AlO_6$  octahedra in blue. [7]

The general formula of magnesium aluminate spinel  $Mg_8Al_{16}O_{32}$ , with 32 oxygen anions being cubic face centered, which forms eight molecules of  $MgAl_2O_4$  [37]. This explains the origin of the  $AB_2O_4$  spinel expression as a simplification by division on 8, the number of molecules in a spinel unit cell.

Minh [7] adapted an illustration of  $MgAl_2O_4$  unit cell from Nishikawa's work [38] over spinel group crystal, in which both  $MgO_4$  tetrahedra and  $AlO_6$  octahedra sites are visible (Figure 2.2).

It is relevant to mention that another representation of the spinel phase diagram exists, in which a MgO rich compound is present at high temperatures (Figure 2.3).

The presumption of the MgO rich solution is based on the degree of magnesia precipitation in the solid solution being lower than that of  $\text{Al}_2\text{O}_3$  resulting an MgO rich solution. Nevertheless, the non-existence of a calculated lattice parameter variation when MgO dissolves into  $\text{MgAl}_2\text{O}_4$  results the dissent over the magnesia rich solution formation [7].

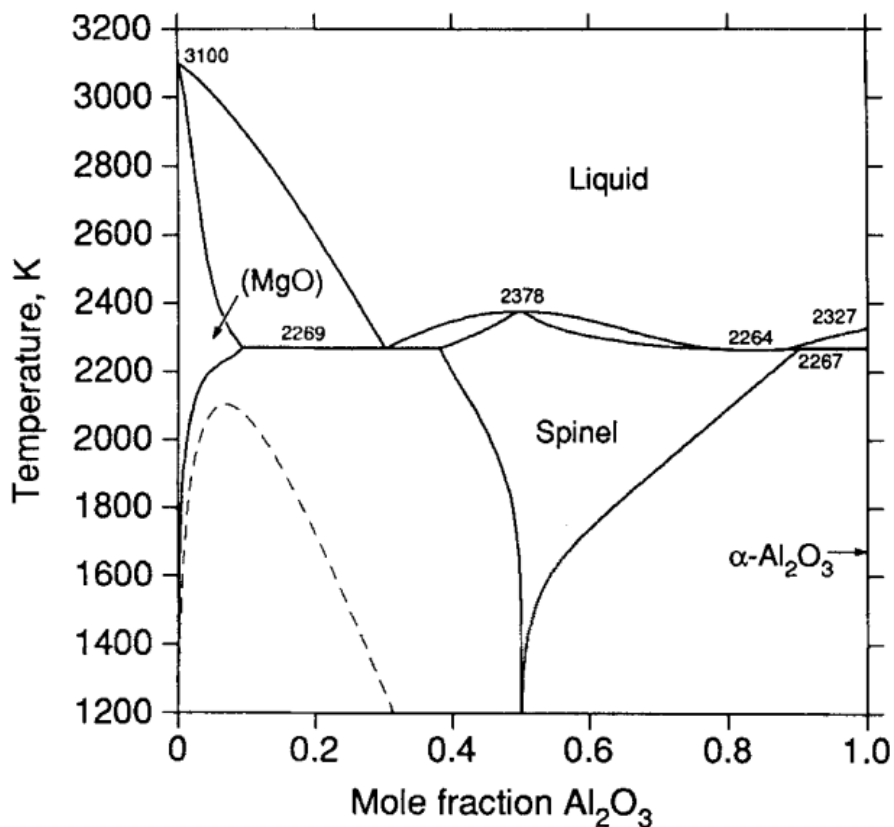


**Figure 2.3.** MgO- $\text{Al}_2\text{O}_3$  phase diagram showing MgO rich spinel phase at high temperature. [39]

### 2.2.2. AlON

Aluminum oxynitride has been considered as the best choice for transparent windows as it perfectly merges good mechanicals properties with outstanding optical characteristics. AlON is considered the hardest commercially available polycrystalline material with a hardness close to that of single crystal sapphire [11]. The transmittance band of fully densified AlON extends from the ultraviolet (a wavelength about 0,2  $\mu\text{m}$ , UV), to mid-infrared (about 5,0  $\mu\text{m}$ , IR) [14]. Moreover, the optical clarity of AlON is over 98% with a very low haze of less than 2% in the visible wavelengths [11].

Hence, aluminum oxynitride can be considered as a nitrogen stabilized cubic alumina, to which much of AlON's properties are similar. Due to its cubic structure, if processed in a proper way, dense polycrystalline AlON can be fully transparent.

AlON is a cubic spinel structure, its crystal structure is of the Fd3M space group type [40]. According to the model given by McCauley [2], AlON maintains the concentration of aluminum cation constant, with a varying concentration of nitrogen and oxygen anion. Labbe [41] stated that the percentage of nitrogen affects the cell parameter of AlON in which "a" the cell parameter, obeys the equation 2.1.

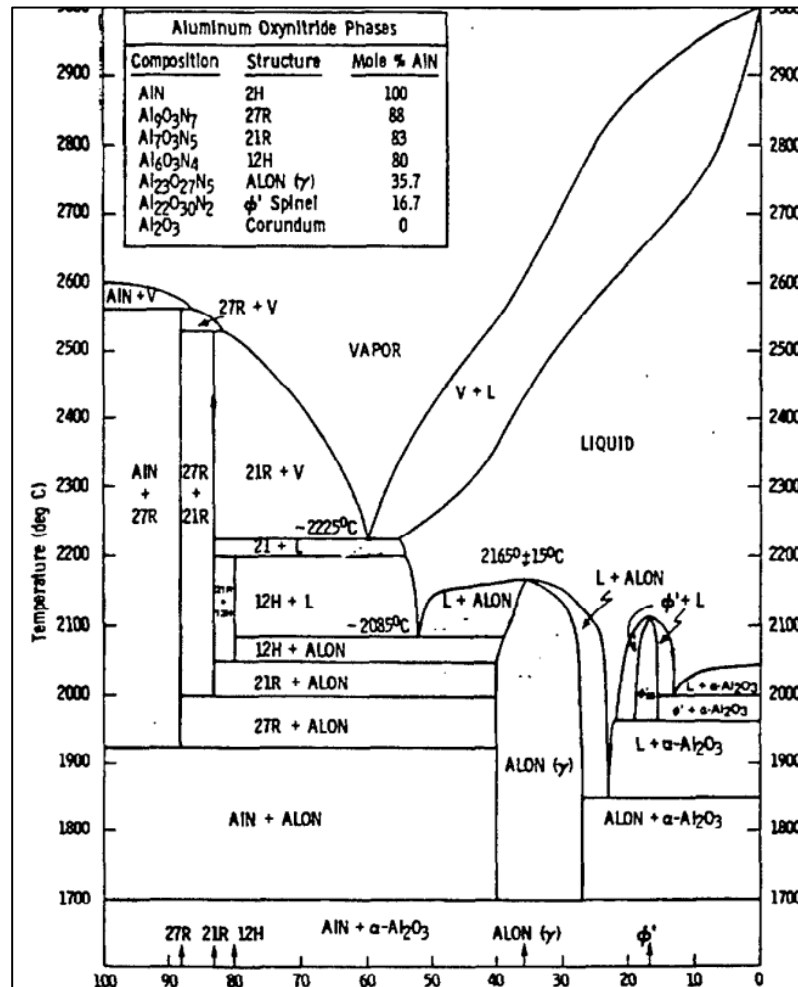


Figure 2.4. AlN-Al<sub>2</sub>O<sub>3</sub> phase diagram presented by McCauley and Corbin. [18,31,43]

$$a \text{ (Å)} = 7.914 + 0.117x \quad \text{where } 18\% < x < 32\% \quad (2.1)$$

The charge balance in the structure is dictated by Pauling's rule [42], due to the nitrogen replacement of oxygen, an imbalance of the local charge is induced. In order to hold this balance, the coordination of aluminum atom is shifted from six to four [2].

This model presented by McCauley incorporates a formula that defines the composition of aluminum oxynitride as given in equation (2.2) [2,10,32].

$$Al_{(64+x)}O_{(32-x)}N_x \quad (0 < x < 8) \quad (2.2)$$

It has been suggested that  $x = 5$  represents the optimum stability in the stoichiometric formula. Hence,  $Al_{23}O_{27}N_5$  was considered as the best stoichiometric form of aluminum oxynitride. McCauley and Corbin [32] stated that AlON is a cubic spinel in the  $Al_2O_3$ -AlN binary system (figure 2.4).

Its composition is centered at 35.7 mol% AlN, which matches the  $Al_{23}O_{27}N_5$  stoichiometric formula, the formula can as well be given as  $5AlN-9Al_2O_3$ . It can also be seen in the diagram that AlON does not exist below  $1700^\circ C$ ; however, alumina in its  $\alpha$  form is present beside aluminum nitride. Willems [21] summarized the studies that attempted to verify AlON stability at low temperatures. It has been found that in most cases AlON can emerge beside its constituents, starting from  $1580^\circ C$ . Nonetheless, it is highly instable, and quickly decomposes back to  $Al_2O_3$  and AlN.

Besides the three main phases in the phase diagram, stable AlON,  $Al_2O_3$  and AlN, there exist other compounds, which can be considered as intermediate. McCauley [18] reviewed the existing phases in the  $Al_2O_3$ -AlN diagram as presented in table 2.1, whereas figure 2.2 provides a summary of the phase equilibrium in existence, together with the variation of bonding and atomic structure in the AlN- $Al_2O_3$  diagram as given by McCauley and Corbin [43].

**Table 2.1.** The existing phases in the experimental  $Al_2O_3$ -AlN phase diagram as given by McCauley. [18]

AlN-AlON Region	AlON Region	AlON- $Al_2O_3$ Region
1 $Al_2O_3$ : 4 AlN = 12H		13 $Al_2O_3$ : 1 AlN = $\phi$ $Al_2O_3$
1 $Al_2O_3$ : 5 AlN = 21R		9 $Al_2O_3$ : 1 AlN = $\delta$ $Al_2O_3$
	9 $Al_2O_3$ : 5 AlN = $Al_{23}O_{27}N_5$	
1 $Al_2O_3$ : 7 AlN = 27R		10 $Al_2O_3$ : 2 AlN = $\zeta$ $Al_2O_3$ or $\phi'$ $Al_2O_3$ / $Al_{22}O_{30}N_2$
1 $Al_2O_3$ : 14 AlN = 32H		

It can be seen in the table that the AlN-Al<sub>2</sub>O<sub>3</sub> region includes different compounds as 12H, 21R, 27R and 32H in which the stoichiometric balance is in favor of AlN against Al<sub>2</sub>O<sub>3</sub> with a ratio starting from 1:4 then enlarging to 1:14. Although these compounds have an Al<sub>x</sub>O<sub>y</sub>N<sub>z</sub> formula, they do not represent the oxynitride in question, but rather, AlN polytypoids. The other side incorporates an Al<sub>2</sub>O<sub>3</sub> balanced stoichiometric, while in between,  $\gamma$ -AlON is present between an AlN mole% of 27 to 40, with an ideal stoichiometry of 9 alumina to 5 AlN.

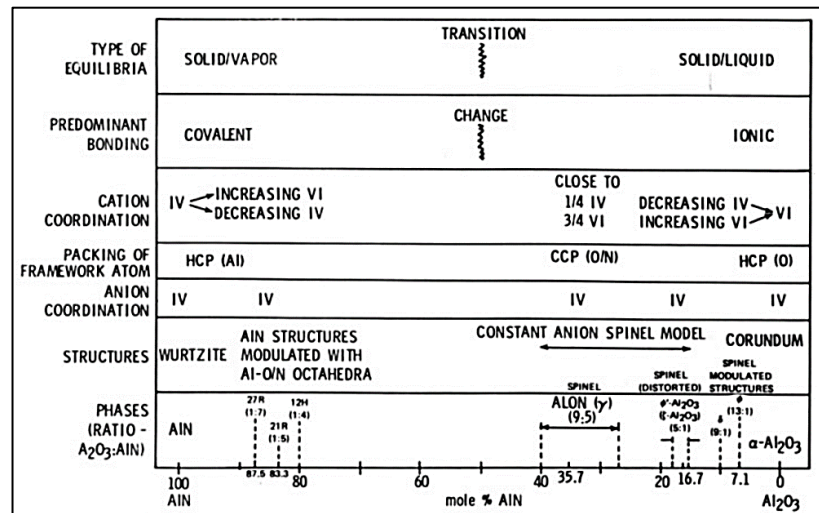


**Figure 2.5.** Crystal structure, bonding and phase variation in the AlN-Al<sub>2</sub>O<sub>3</sub> system. [18]

As it has been stated, AlON is a spinel of the Fd3m space group. It is generally known that the spinel group holds an AB<sub>2</sub>X<sub>4</sub> formula [26]. Yet, AlON is considered as a spinel since the Fd3m space group, had been assigned to spinels [40,44-45]. The model presented by McCauley and Corbin suggests a constant aluminum cation concentration, whereas both concentrations of oxygen and nitrogen are varying [2]. With the electronegativity of aluminum, oxygen and nitrogen being, 1.5, 3.5 and 3.0 respectively, the application of Pauling rule, suggested a predicted ionic character of AlON at 56% [18]. Clearly, a charge imbalance is initiated with oxygen substitution into AlN or nitrogen in Al<sub>2</sub>O<sub>3</sub>.

Thus, a suggestion had been made by McCauley [46] which has been later confirmed by Tabary [47], that the imbalance is annihilated by anion coordination shifting from six to four around aluminum, resulting a spinel structure deriving from the  $\alpha$ -Al<sub>2</sub>O<sub>3</sub> based phase, in which cations are shared between octahedral and tetrahedral coordination. Hence, AlON unit cell comprises 8 Al cations in the tetrahedral sites

and 15 Al in the 16 octahedral ones, with 1 vacancy left [18]. This makes the equation of the ideal AlON as given in equation (2.3).

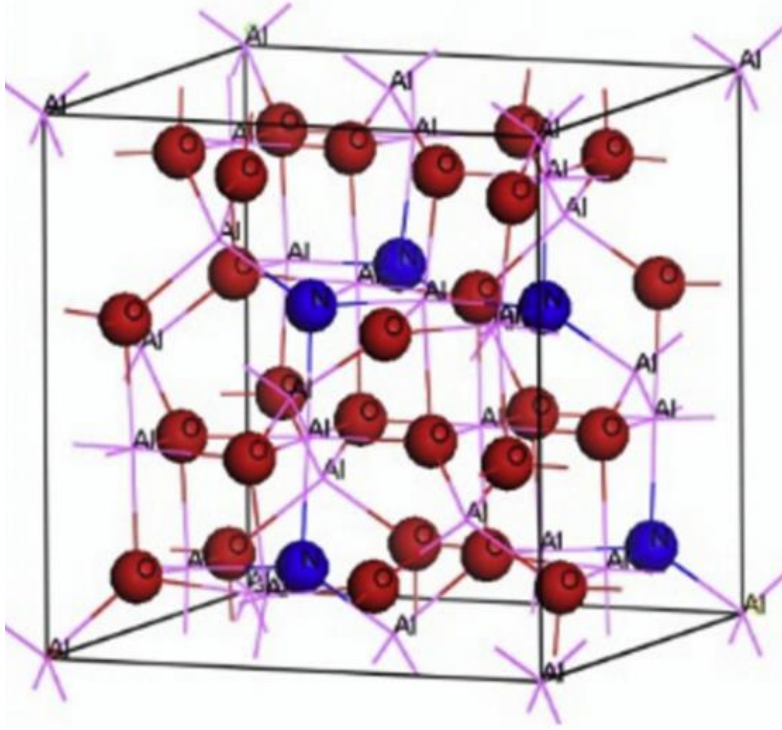


**Figure 2.6.** Representation of  $Al_{23}O_{27}N_5$  crystal model. [48]

Based on this understanding of AlON crystal structure, many works have tried to present a crystal structure representation of the oxynitride [49-51]. Figure 2.6 illustrates an AlON model, in which octahedral sites have Al vacancies on them with oxygen being the sole neighbor, whereas nitrogen atoms are distantly distributed.

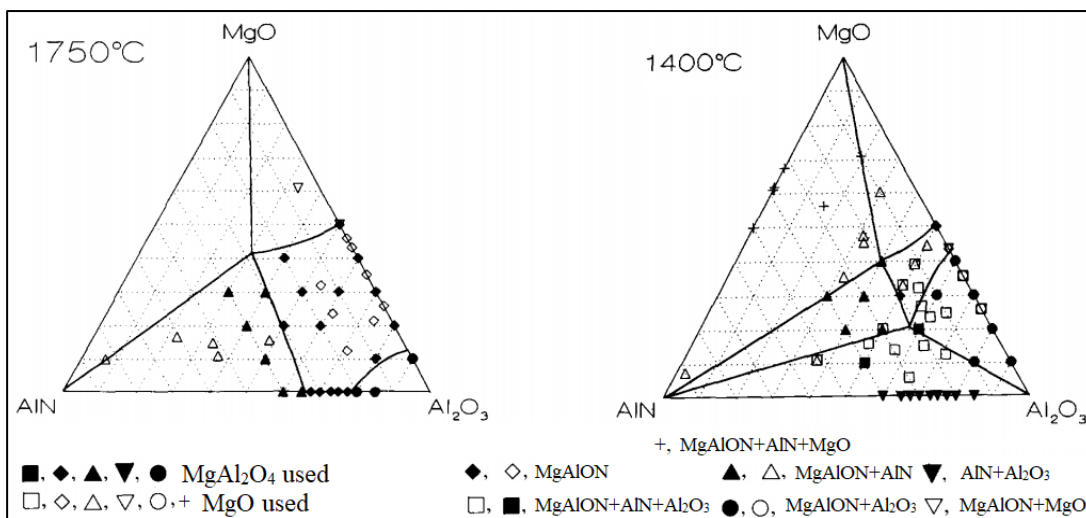


**Figure 2.7.** MgO-AlN-Al<sub>2</sub>O<sub>3</sub> system phase diagram as given by willems et. al. [34]

Despite being a great choice for a transparency and mechanical strength compromise, aluminum oxynitride has been reported to be instable below 1640°C since it can quickly decompose to its main constituents, AlN and Al<sub>2</sub>O<sub>3</sub> [21,34], additionally, recent research suggested a temperature of 1750°C to obtain a full conversion to aluminum oxynitride [17].

### 2.2.3. MgAlON

Due to the elevated temperatures required to stabilize AlON, which highly affects the production cost, a need for a method to obtain AlON at lower temperatures emerged, opening the gate for the introduction of MgAlON. The first idea made appearance with K.H. Jack's work on SiAlON [52], who determined an equilibrium of the Mg-Si-Al-O-N system at 1800°C, followed by an extension of knowledge and a better understanding of magnesium aluminum oxynitride with the work of Willems et. al. [34] who proposed MgO or MgAl<sub>2</sub>O<sub>4</sub> as stabilizers for AlON, to give MgAlON.

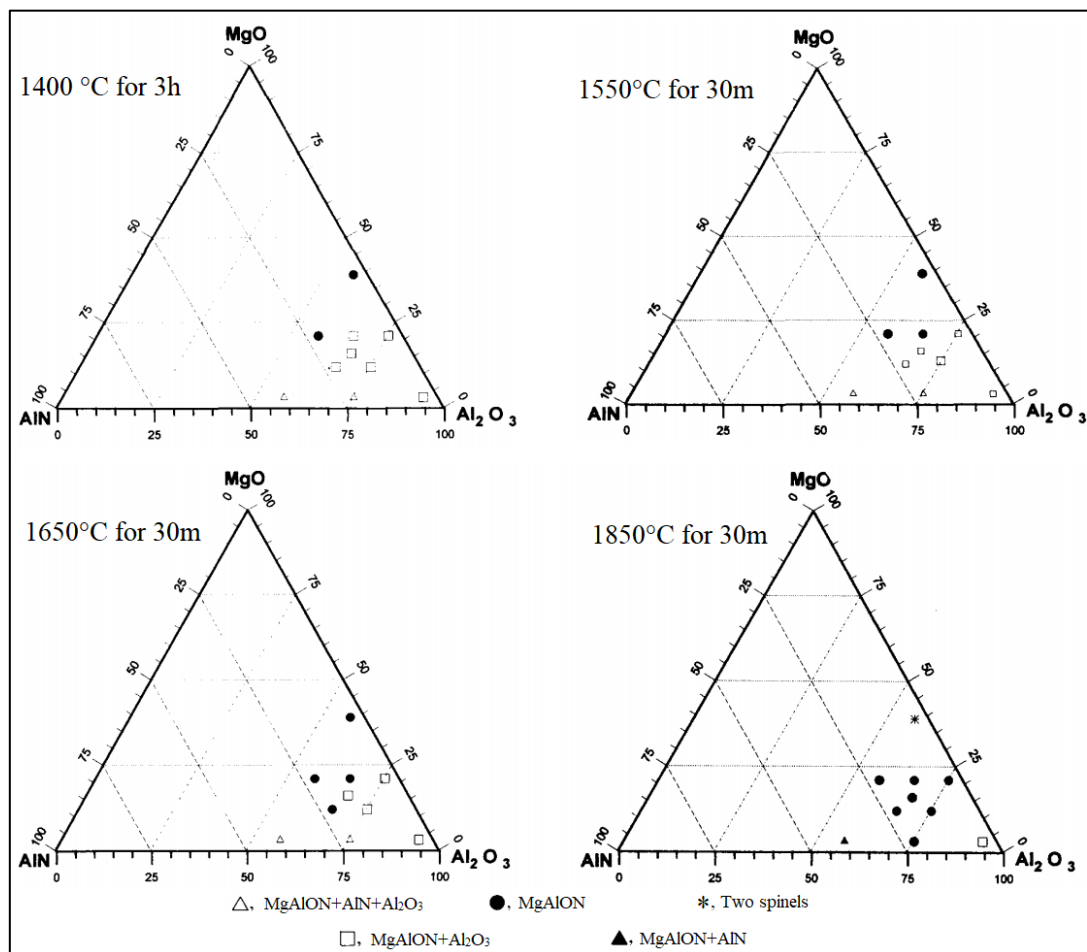


**Figure 2.8.** Experimental MgO-AlN-Al<sub>2</sub>O<sub>3</sub> phase diagram as presented by Granon et. al. [53]

Since MgAlON emerged from AlON stabilization, no formal accepted phase diagram exists; but rather, different experimental ternary diagrams consisting of an MgO-Al<sub>2</sub>O<sub>3</sub>-AlN system, are proposed. Figure 2.7 illustrates experimental MgAlON phase diagram as given by Willems et. al. [34].

It was found that at lower temperatures, MgAlON can exist in the Al<sub>2</sub>O<sub>3</sub>-MgO system regions provided that a holding time exceeding 24h is performed, whereas at elevated temperatures, MgAlON extends towards the Al<sub>2</sub>O<sub>3</sub>-AlN system, with a lower holding time needed. It has been shown as well that the lattice parameter of MgAlON is highly affected by the composition and can be represented with formula (2.4) [34].

$$a \text{ (nm)} = 0.7900 + 0.0160x + 0.0206y \quad (2.4)$$

Where  $a$  is the lattice parameter, while  $x$  and  $y$  represent the mole fractions of AlN and MgO respectively.

**Table 2.2.** MgAlON formulas with comparisons between experimental and calculated parameters. [53]

MgAlON formula	Experimental value (Å°)	Calculated value (Å°)
Mg <sub>0.376</sub> Al <sub>2.54</sub> X <sub>0.084</sub> O <sub>3.628</sub> N <sub>0.372</sub>	7.992	8.007
Mg <sub>0.200</sub> Al <sub>2.71</sub> X <sub>0.090</sub> O <sub>3.469</sub> N <sub>0.530</sub>	7.985	7.985
Mg <sub>0.360</sub> Al <sub>2.478</sub> X <sub>0.162</sub> O <sub>3.846</sub> N <sub>0.154</sub>	7.992	7.992
Mg <sub>0.386</sub> Al <sub>2.522</sub> X <sub>0.092</sub> O <sub>3.662</sub> N <sub>0.338</sub>	7.997	8.008
Mg <sub>0.415</sub> Al <sub>2.579</sub> X <sub>0.005</sub> O <sub>3.432</sub> N <sub>0.568</sub>	8.016	8.020
Mg <sub>0.769</sub> Al <sub>2.219</sub> X <sub>0.012</sub> O <sub>3.805</sub> N <sub>0.195</sub>	8.065	8.061
Mg <sub>0.438</sub> Al <sub>2.492</sub> X <sub>0.070</sub> O <sub>3.649</sub> N <sub>0.351</sub>	8.009	8.017
Mg <sub>0.649</sub> Al <sub>2.313</sub> X <sub>0.038</sub> O <sub>3.763</sub> N <sub>0.236</sub>	8.051	8.045

X: Cationic vacancy

Other than the diagram proposed by Willems, there exist other experimental diagrams, that differ with the molar ratio of compounds used to obtain MgAlON. Figure 2.8 represent different experimental diagrams of the MgO-AlN-Al<sub>2</sub>O<sub>3</sub> system as given by Granon et. al. [53]. It can be seen from the diagrams that MgAlON region extends with

increasing temperatures. Additionally, the holding time necessary to achieve a full conversion to MgAlON, decreases with the augmentation of temperature.

Not dissimilar to their predecessors' work, Granon et al. confirmed the varying lattice parameter of MgAlON with the difference in the composition. Based on their calculations using formula (2.5), various MgAlON compositions were presented with different lattice parameter for each. The results are given in table 2.2. Additionally, it was found that in order to achieve a stabilization of aluminum oxynitride at 1400°C, an average 25% MgO or 50% MgAl<sub>2</sub>O<sub>4</sub> need to be added. Hence, the properties of MgAlON obtained at lower temperature, was suggested to be closer to MgAl<sub>2</sub>O<sub>4</sub> than AlON [53].

$$a (A^\circ) = 7.900 + 0.375(MgO) + 0.150(AlN) \quad (2.5)$$

MgAlON formulas presented in table 2.2, are not the only ones in existence. Many recent studies have been reporting different compositions (e.g. Liu et al. [54] Mg<sub>0.1</sub>Al<sub>1.53</sub>O<sub>1.89</sub>N<sub>0.27</sub> and Zong et al. [55] Mg<sub>0.27</sub>Al<sub>2.58</sub>O<sub>3.73</sub>N<sub>0.27</sub>), which indicates that different compositions can always be determined.

Morey [56] worked on the presentation of a MgAlON formula similar to that presented by McCauley (Eq. 2.2). via substituting aluminum cation in Eq. (2.6) to obtain Eq (2.7) with a lower vacancy number.



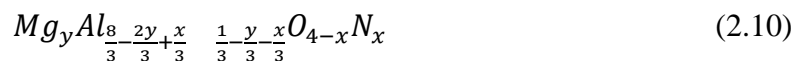
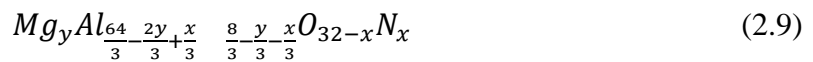
Where  $8/3$  refer to aluminum vacancies.



Via substitution of oxygen anion in Eq (2.6) with nitrogen and increasing the aluminum to preserve electroneutrality and thus, lowering cationic vacancies, we get



With a simultaneous substitution, MgAlON general formula can be written as given in Eq. (2.9), which can be simplified as Eq. (2.10).



Morey et. al. [57] studied the crystal structure of MgAlON to conclude that the sites in magnesium aluminum oxynitride structure are highly affected by the varying nitrogen concentration. Unlike AlON in which nitrogen is randomly distributed [50], the distribution of nitrogen atoms in MgAlON is dictated by its incompatibility with magnesium as neighbors, and thus, a segregation of AlN<sub>4</sub> evolves. Figures 2.9 and 2.10 illustrates models of low and high nitrogen MgAlON respectively, as given by Morey et. al.

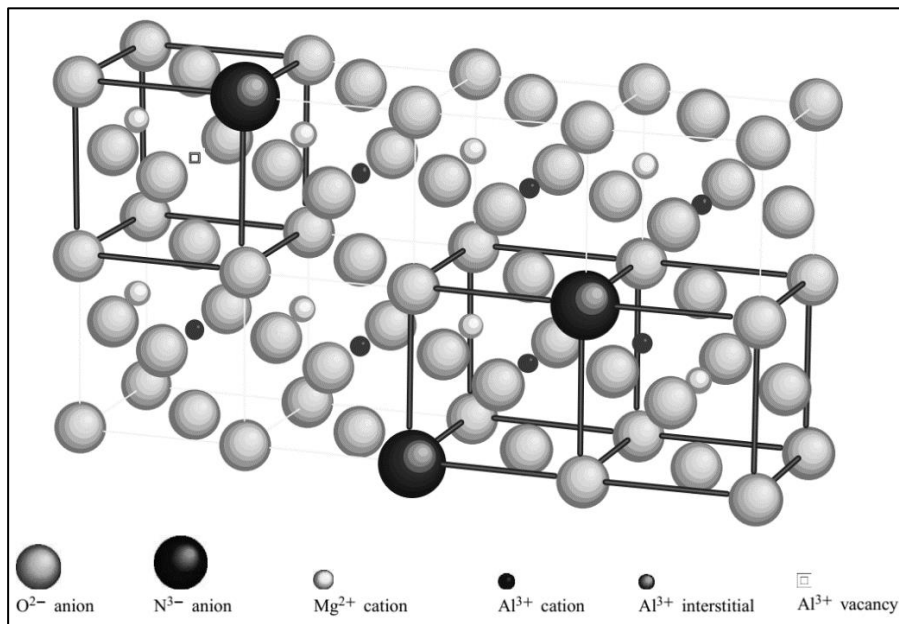


**Figure 2.9.** MgAlON crystal model with low nitrogen content. [57]

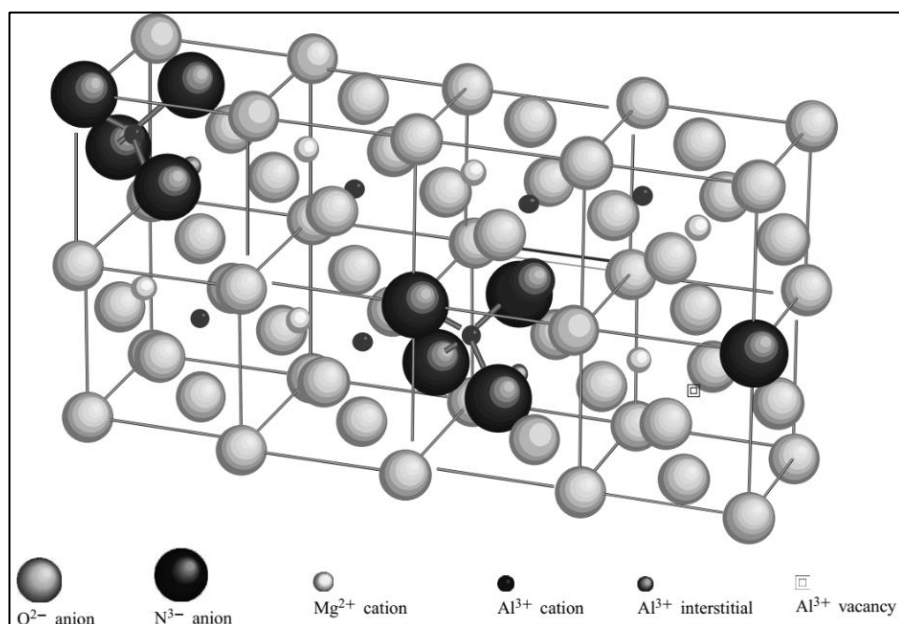


**Figure 2.10.** MgAlON crystal model with high nitrogen content. [57]

## 2.3. Properties of MAS, AlON and MgAlON

### 2.3.1. Mechanical properties

#### 2.3.1.1. Magnesium aluminate (spinel)

Being a candidate for armor windows applications, elite mechanical properties are mandatory for MAS. Mechanical characteristics are known to be highly dependent on many factors, from the purity of the raw powders to the fabrication techniques, consolidation conditions, the microstructure, grain size of the final product...etc. The mechanical properties of spinel have been reported to be highly influenced by the composition [37]. This was also pointed in [58] where it was stated that  $n$  value changes in the formula  $MgO_nAl_2O_3$ , influence the properties of MAS.

Additionally, despite the isotropic optical properties of MAS, its hardness was found to be anisotropic as a result of its crystal structure as well as the primary slip systems which accumulate dislocations when indented, where polycrystalline spinel's hardness is strongly dependent on the microstructure, but not the orientation of indentation [7]. Mitchell [58] reported that slip in single crystal spinel, takes place on {111} and {110} planes, as well as {100}, while all follow the <110> direction.

Hardness is not the only property that can be affected by the primary slip plans. Cui et al. [59] demonstrated that the fracture toughness as well, can be affected with orientation. It has been found that the fracture toughness of the {110}/{100} boundary orientation is 43% higher than that of the {111}/{100}.

**Table 2.3.** Mechanical properties of MAS collected from different studies.

Properties	Single Crystal MAS	Polycrystalline MAS
Young's Modulus (GPa)	295; 303; 308* [7]	277 [11]
Bulk Modulus (GPa)	197; 204; 206* [7]	192 [7]
Shear Modulus (GPa)	118; 121; 123* [7]	110 [7]
Poisson Ratio	0.25 [11]	0.26 [37]
Fracture Toughness (MPa m <sup>1/2</sup> )	1.46; 1.55; 1.71** [59]	1.2 ~ 1.3 [60]
Hardness (Kg/mm <sup>2</sup> )	1760 – 1830 [61]	1450 – 1650*** [11]

\* For  $n$  values of 1, 2.6 and 3.5 respectively

\*\* For {100} <100>; {110} <110>; {111} <110> respectively

\*\*\* Knoop<sub>200g</sub>

Furthermore, grain size has been found to have an influence on the mechanical properties of MAS. Tokariev et al. [62] studied the effect of grain size on the mechanical properties and found that spinel of coarse grains exhibits lower strength and an increased sensitivity of slow crack growth.

Table 2.3 summarizes the main mechanical properties of both single crystal and polycrystalline spinel, collected from both theoretical and experimental data found in different studies.

### 2.3.1.2. Aluminum oxynitride

Despite having a cubic spinel lattice similar to its magnesium aluminate counterpart, AlON holds the mechanical superiority over MAS due to their differences of bonding and bonding strength, which promotes aluminum oxynitride to have higher hardness and elastic modulus than magnesium aluminate [11].

**Table 2.4.** Physical and mechanical properties of transparent AlON.

Al <sub>23</sub> O <sub>27</sub> N <sub>5</sub> Properties	
Density (g cm <sup>-3</sup> )	3.71
Lattice Parameter (Å)	7.947
Melting Point (°C)	2140
Young Modulus E (GPa)	323
Shear Modulus G (MPa)	130
Poisson's Ratio $\mu$	0.24
Flexural Strength (4pt test) (MPa)	300 ±34.47
Hardness Knoop (Kg/mm <sup>2</sup> )	1950
Fracture Toughness (MPam <sup>1/2</sup> )	2.0

Both bulk and shear moduli were found to increase with increasing nitrogen molar percentage due to a stronger Al-N bonding versus that of Al-O [2]. It has been stated that  $\gamma$ -AlON is the hardest polycrystalline material commercially available, with a hardness close to that of single crystal sapphire [11].

Previous measurement of AlON hardness showed a dependency on the applied load. The fracture strength was found to decrease above 1000°C, with an approximate value of 200MPa, whereas young's module varies between 323 and 332 GPa [63].

The experimental mechanical properties of AlON are summarized in table 2.4 as found by Hartnett et al. [64].

Willems [63] reviewed the fracture strength of AlON that had been investigated and found a highest value of 300 MPa at room temperature for 3-point bending whereas the highest fracture strength for a 4-point test was determined as 307 MPa, highlighting that the specimens of with higher values had fracture origins at large grains while that of low values subjects originated at porous or unreacted regions.

**Table 2.5.** Mechanical properties of MgAlON collected from different studies.

	Young Modulus (GPa)	Vickers Hardness (GPa)	Flexural Strength (MPa)	Fracture Toughness (MPa m <sup>1/2</sup> )
MgAlON	325.5 [65]	13.39 / 13.72 [65]	274 [65]	2.46 / 2.33 [65]
γ-AlON	323 [64]	15	310	2.0
MgAl <sub>2</sub> O <sub>4</sub>	277 [11]	12 – 15	100 – 300	1.5 – 2.2

### 2.3.1.3. MgAlON

Owing to the variety of magnesium aluminum oxynitride formulas, the physical properties of this spinel type ceramic can be enhanced by the introduction of different atoms in the cation or anion sites, or both [66]. Furthermore, being a quaternary compound, the anion and cation sites of MgAlON include two distinct types of constituent atoms, and therefore, its physical properties differ from those of MgAl<sub>2</sub>O<sub>4</sub> and AlON.

Lui et al. studied the mechanical properties of MgAlON comparing to γ-AlON and MgAl<sub>2</sub>O<sub>4</sub> to find characteristics closely similar to that of aluminum oxynitride, while Ma et al. studied the mechanical properties of magnesium aluminum oxynitride separately, using a nanoindentation method. The mechanical properties of MgAlON in comparison with γ-AlON and MgAl<sub>2</sub>O<sub>4</sub> are summarized in Table 2.5.

### 2.3.2. Optical properties

Being candidates for sapphire replacement as transparent armor windows, the optical characteristics are viewed as the most important together with mechanical properties.  $\text{MgAl}_2\text{O}_4$ ,  $\gamma\text{-AlON}$  and  $\text{MgAlON}$  exhibit excellent transparency ranging from the ultraviolet to mid infrared.

Transparency refers to light waves allowed through a body with the least absorption, scattering or reflection [11]. Vu [7] reported an equation for the calculation of the transmittance  $T$  (given by equation 2.11) as the spectral radian power  $P_\lambda$  transmitted through a path of a length  $l$ , divided by the spectral radian power  $P_\lambda^0$  incident on a body.

$$T = \frac{P_\lambda}{P_\lambda^0} \quad (2.11)$$

When it comes to transmittance, the structure of the sample on which light is incident, must be carefully controlled, since any presence of impurities, secondary phases, inclusions, grain boundaries or defects, would negatively affect light transmission. For instance, it has been found that a nano-scale porosity (50 – 100 nm) of an amount less than 0.01% in a 5mm thick sample, could have a negative effect on infrared transmittance [67].

The transmission of magnesium aluminate spinel ranges from the ultraviolet (0.2 $\mu\text{m}$ ) to the mid-infrared (5 $\mu\text{m}$ ) [6]. It has been reported that the optical properties of  $\text{MgAl}_2\text{O}_4$  are theoretically the same for both single crystal and polycrystalline structures [7]. The experimental results of Blodgett et al. [68] demonstrated that the transmittance values of single crystal sapphire, at wavelengths of 632.8 nm and 3.39  $\mu\text{m}$ , are 86% and 88% respectively, whereas polycrystalline spinel transmittance measurements gave 82% and 88% at the same wavelengths respectively.

In practice, the transmittance of spinel is highly sensitive to any defects in the structure with pores, surface condition and grain boundaries being the major factors to cause a deterioration of the optical properties. Additionally, microcracks along grain boundaries in sintered spinel bodies were reported to cause a loss of transmittance. Equation (2.12) expresses the microcracks dependency of transmittance  $T$  in polycrystalline spinel [7].

$$T \cong (1 - R)^2 \exp(-\beta' S_v^{Mc} t) \quad (2.12)$$

$\beta'$  is a constant,  $S_v^{Mc}$  is the surface area of microcracked grain boundaries per unit volume,  $t$  is the thickness of the body and  $R$  the reflectance which is expressed with equation (2.13).

$$R \cong \frac{(\bar{n}-n_a)^2}{(\bar{n}+n_a)^2} \quad (2.13)$$

$\bar{n}$  is the reflective index of single crystalline spinel while  $n_a$  is the reflective index of the air ( $\cong 1$ ).

Almost similarly to MAS, AION exhibits a useful transmittance extending from 0.22 $\mu$ m to 5.2 $\mu$ m [69]. In matters of haze and optical clarity, which refer the amount of light scattered at large and small angles respectively, the figures are  $\geq 2\%$  and  $98 \leq$  respectively [11]. These characteristics are highly dependent on certain factors, which are determined by the fabrication technique, such as grain boundaries, pores, inclusion of a secondary phase and surface properties [70].

It is important to understand that aluminum oxynitride is considered as more advantageous ceramic than spinel due to its mechanical properties. It is true that spinel can reach higher transparency than AION can reach. Nevertheless, when coupled with mechanical properties, aluminum oxynitride takes the lead instead of MAS. Therefore, AION makes a better choice for applications in which infrared transparency and high mechanical properties are needed.

In the case of MgAION, no extensive studies have been carried out to investigate its transparency comparing to AION due to the fact that its consideration rose from the need to find a substitute to aluminum oxynitride whose production limitations make it an expensive material to purchase.

Additionally, being a magnesium stabilized aluminum oxynitride, the optical properties of magnesium aluminum oxynitride are relatively similar to that of its parent phase. Hence, there was more focus in the literature on how to obtain MgAION instead of studying its properties in comparison to that of AION.

#### **2.4. Synthesis Methods**

Being transparent ceramics, MAS, AION and MgAION require highly sensitive approaches when it comes to their fabrication. This is due to the detrimental effects that can be caused by any defect (pores, inclusions, grain boundaries...etc).

Commercially, these ceramics are mainly fabricated through sintering of high-quality powders ( $\text{MgO}$  and  $\text{Al}_2\text{O}_3$  for  $\text{MgAl}_2\text{O}_4$ ;  $\text{AlN}$  and  $\text{Al}_2\text{O}_3$  for  $\text{AlON}$  and  $\text{MgO}$ ,  $\text{AlN}$  and  $\text{Al}_2\text{O}_3$  for  $\text{MgAlON}$ ) at high temperatures. Nonetheless, the high cost of these powders added to the nature of the system used in densification results in extremely expensive products. Hence, powder synthesis presented itself as an attractive subject for researchers to provide a ready-to-use powders of those ceramics.

There exist different techniques to produce MAS,  $\text{AlON}$  and  $\text{MgAlON}$  powders. However, carbothermal reduction (and subsequent nitridation for nitrides and oxynitride powders) has been widely reported as the most preferable method due to its simplicity and efficiency [17]. In what follows, the synthesis methods of each of the studied ceramics are reviewed.

### **2.4.1. Spinel**

The synthesis methods of ceramic powders vary from mechanical destined to produce traditional ceramics or those not necessitating elite properties, to chemical methods, originally adapted for the fabrication of advanced ceramic powders, involving meticulously controlled conditions as to obtain the desired powder characteristics [7].

Being an advanced ceramic for transparent windows usage, MAS is supposed to have high purity and excellent particle qualities since the slightest existence of impurities or defects can engender a detrimental effect on transparency as well as the mechanical properties. For example, a residual porosity exceeding 0.01% can result in limited transparency [71]. Thus, high purity starting materials as well as advanced processing techniques are required to assure high quality powders.

The synthesis methods of spinel vary from sol-gel to solid state reactions like that of  $\text{MgO}/\text{Al}_2\text{O}_3$  or  $\text{Mg}$  and  $\text{Al}$  bearing precursors [72]. In addition, spinel can be obtained via mechanical routes such as high energy ball-milling or mechanical activation [73]. In what follows the synthesis techniques of spinel are discussed.

#### **2.4.1.1. Sol-Gel**

Considered as the popular method, sol-gel can provide the needed purity to synthesize high purity MAS powders due to its advantage in controlling the characteristics of powders [72]. Spinel powders can be obtained from aluminum and magnesium bearing precursors, mainly alkoxides [74-75], nitrates [76-77] and sulfates [78-79]. Freeze-

drying of aluminum isopropoxide and magnesium methoxide precursors, was used to prepare MAS as part of the alkoxide method resulting in high sinterability powders [74]. Bickmore et. al. [80] synthesized a nanosized MAS powder from an Al/Mg double alkoxide precursors using spray flame pyrolysis. Sanjabi et. al. [81] obtained nanocrystalline  $MgAl_2O_4$  powders from aluminum and magnesium nitrates, citric acid, and diethylene glycol monoethyl ether. McHale et. al. [82] used freeze drying to synthesize nanocrystalline spinel from nitrate-based precursors. Schreyeck et. al. [78] reported the synthesis of MAS powders from sulfate-based precursors ( $MgSO_4 \cdot 7H_2O$  and  $NH_4Al(SO_4)_2 \cdot 12H_2O$ ) with higher crystallite size than that of the oxide. Additionally, the former method was found to provide a higher purity than the later in less severe conditions.

#### **2.4.1.2. Solid state reaction**

With purity being a crucial factor in the production of magnesium aluminate powders for transparent windows applications, the sol-gel method presented itself as the popular method owing to its advantages with regards to purity. Nevertheless, this process cannot be considered when it concerns mass production such as that for the use of spinel as refractory. Hence, the solid-state reaction method of Mg and Al bearing oxides, hydroxides and carbonates is chosen over its sol-gel counterpart [72]. Radishevskaya et. al. [83] reported the synthesis of 99% purity submicron  $MgAl_2O_4$  powders via the self-propagating high temperature synthesis method (SHS), from an MgO-Al<sub>2</sub>O<sub>3</sub>-Al system. Similarly, Gorshkov et. al. [84] studied the optimum synthesis conditions of MAS via SHS method. In a different method, Domanski et. al. synthesized 99% purity MAS powders at room temperature using a mechanochemical synthesis method [85].

In different methods MAS could be directly obtained as final product using solid state simultaneous reaction sintering methods yielding high purity spinel for optical use. Zhihui et. al [86] studied the effect of mechanical activation of Al<sub>2</sub>O<sub>3</sub> on the reaction sintering of alumina and magnesia to obtain magnesium aluminate spinel. Meir et. al. [87] reported transparent spinel obtained via spark plasma sintering method (SPS) of MgO-Al<sub>2</sub>O<sub>3</sub> mixture.

## 2.4.2. AlON

Unlike magnesium aluminate spinel, which can be used both for transparent windows production involving strictly controlled synthesis conditions as well as a refractory material in which powders with average properties are used, aluminum oxynitride is mainly used for its optical properties because of which the processing conditions must be carefully controlled to avoid any impurity or defects. Thus, high purity starting materials (AlN and Al<sub>2</sub>O<sub>3</sub>) are used. Carbothermal reduction nitridation is the most popular synthesis method AlON due to its simplicity. Nevertheless, other techniques such as direct nitridation and sol-gel methods have been reported. Additionally, AlON, whose powders are not available commercially to date, is available in the market as a ready-to-use product obtained via reaction sintering of high purity AlN and Al<sub>2</sub>O<sub>3</sub> using hot isostatic pressing (HIP) [88], hot pressing (HP) [89] or spark plasma sintering [90].

### 2.4.2.1. Carbothermal reduction nitridation

AlON synthesis via carbothermal reduction nitridation has been the widely used and the well-studied method since its introduction for the oxynitride powder production as a substitute to direct sintering process of AlN and Al<sub>2</sub>O<sub>3</sub>. The advantages of CRN lays within its cost and simplicity. However, the remaining carbon, which needs further processing, has always limited the transparency of the final product [17].

Many researches were carried out on the synthesis of AlON via CRN with the aim of optimizing it and providing a better understanding of its mechanism [16-21]. Xiumin et. al. [17] synthesized AlON with a two-step carbothermal reduction nitridation (CRN) method. This method, which had been first developed by both Hartnett et. al. [64], then optimized by Zheng et. al. [20] via pre-calcinating a mixture of alumina and carbon between 1500°C and 1600°C in nitrogen atmosphere to produce Al<sub>2</sub>O<sub>3</sub>-AlN composites followed by heating between 1680°C and 1820°C in order to obtain AlON powder providing a better homogeneity [64]. According to Xiumin et al. [17] before AlON's formation, Al<sub>2</sub>O<sub>3</sub> are covered with an unsealed layer of AlN containing holes and cracks caused by the negative volume expansion of the Al<sub>2</sub>O<sub>3</sub> to AlN transformation ( $\Delta V_E = -2,1\%$ ). As the temperature exceeds 1650°C, AlON begins to form by gas diffusion in form of Al<sub>(g)</sub>, O<sub>2</sub> and N<sub>2</sub> through the AlN layer cracks and holes. The same research team presented multiple equilibrium states leading to the

formation of AION through solid-state reaction, gas-solid reaction, and gas phase reaction. These equilibrium states are given as the follows:

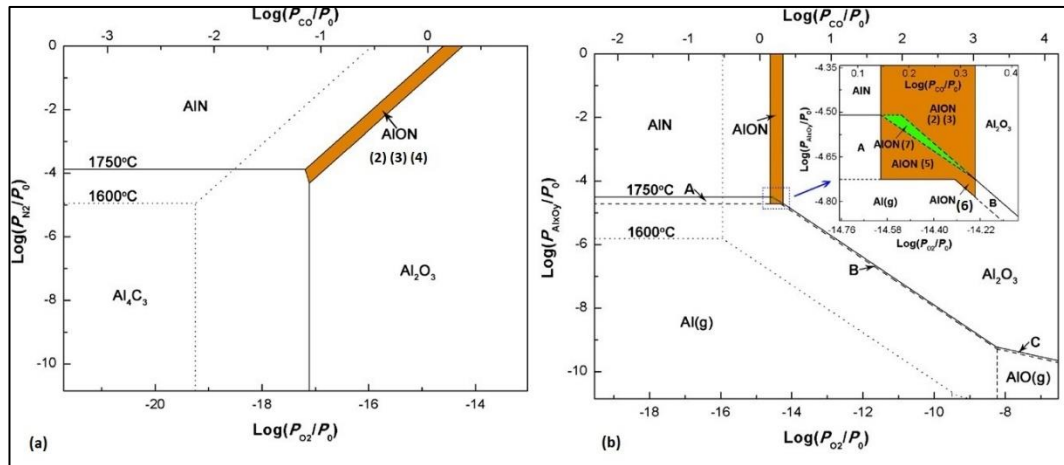
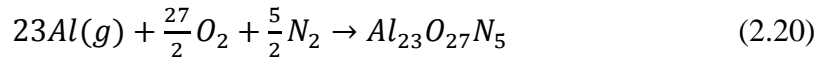
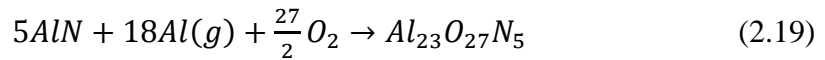
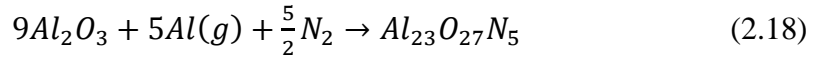
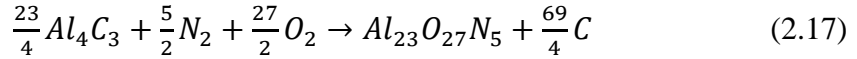
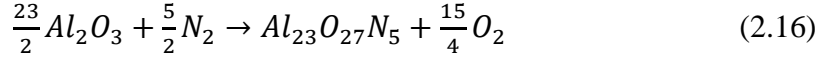
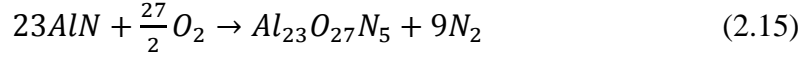
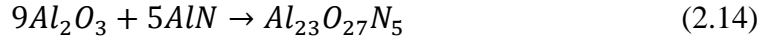
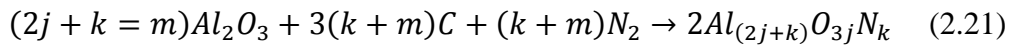


**Figure 2.11.** Stability regions of AION at 1600°C and 1750°C (dot and solid lines respectively) as function of partial pressure of (a) O<sub>2</sub> and N<sub>2</sub>, and (b) O<sub>2</sub> and Al suboxides in an atmosphere with constant N<sub>2</sub> pressure P<sub>N2</sub>=N<sub>2</sub>. [17]

It has been reported that AION doesn't form under 1600°C due to its thermodynamic instability with a full stability reached at 1750°C in a narrow range provided that O<sub>2</sub> and N<sub>2</sub> gas species are involved as shown in Figure 2.11(a) in which reactions 2.15, 2.16 and 2.17 can be found. However, when aluminum suboxide vapor species with an almost constant nitrogen pressure P<sub>N2</sub> ≈ P<sub>0</sub> are considered, reactions 2.18, 2.19 and 2.20 may take place under a defined oxygen and aluminum gas pressure Figure 2.11(b).

In most of the reviewed papers,  $\gamma$ - $\text{Al}_2\text{O}_3$  was preferentially chosen to synthesize AlON. It has been reported that  $\gamma$ - $\text{Al}_2\text{O}_3$  possesses the best reactivity that allows AlN to be formed at lower temperatures in comparison with other precursors [92-97]. Yamakawa et. al. [95] explained the better reactivity of  $\gamma$ - $\text{Al}_2\text{O}_3$  with its tetrahedral  $\text{AlO}_4$  sites being preferentially nitrated comparing to the octahedral  $\text{AlO}_6$  sites of the  $\alpha$ - $\text{Al}_2\text{O}_3$ . As  $\gamma$ - $\text{Al}_2\text{O}_3$  contains both  $\text{AlO}_4$  and  $\text{AlO}_6$ , while only the stable  $\text{AlO}_6$  are in existence in  $\alpha$ - $\text{Al}_2\text{O}_3$ , the synthesis behavior of the former was suggested to be better than  $\alpha$ - $\text{Al}_2\text{O}_3$ . For this reason, many researchers choose  $\gamma$ - $\text{Al}_2\text{O}_3$  as a reactant in synthesis of AlON via CRN method.

In practice, the exact proportion of AlN to  $\text{Al}_2\text{O}_3$  needed to obtain  $\gamma$ -AlON is difficult to achieve during reduction process. However, having an excess of AlN has been reported to be easier to obtain via stopping the transformation of alumina into AlN. Xinayang et. al. [98] presented a method to calculate first the amount of AlN in the mixture. Zheng et. al. [20] reported that the mixture treated by carbothermal reduction can contain AlN +  $\text{Al}_2\text{O}_3$ , AlN +  $\text{Al}_2\text{O}_3$  + AlON, or pure AlN depending on preliminary composition, temperature, time of soaking and the atmosphere. Thus, AlN may be present as AlN,  $\gamma$ -AlON or both. The following equation was presented to calculate the amount of AlN [98]:



$$\downarrow = (j\text{Al}_2\text{O}_3 + k\text{AlN}) + 2m\text{AlN} + 3(k + m)\text{CO} \quad (2.22)$$

$$\sim 2j\text{Al}_2\text{O}_3 + 2(k + m)\text{AlN}' + 3(k + m)$$

$$\text{CO} [(j \geq 0, k > 0, m \geq 0), \text{AlN}': \text{All forms of AlN}]$$

The post-reaction weight change is expressed with equation (2.23):

$$\left\{ \begin{array}{l} \text{Al}_2\text{O}_3 \sim 2\text{AlN}' \quad \Delta m \\ 102 \quad 2 \times 41 \quad 102 - 2 \times 41 = 20 \\ x \quad \quad \quad M_{\text{Al}_2\text{O}_3} - M_m \end{array} \right. \quad (2.23)$$

$$\Rightarrow x = 4.1 \times (M_{\text{Al}_2\text{O}_3} - M_m)$$

$x$ : Weight of AlN',  $M_{Al_2O_3}$ : weight of starting Al<sub>2</sub>O<sub>3</sub> powders,  $M_m$ : weight of the mixture  $\Delta m$ : Weight change between reactant Al<sub>2</sub>O<sub>3</sub> powders and resultant AlN' powders [98].

Thus, the weight of Al<sub>2</sub>O<sub>3</sub> powders to be added into the mixture in order to obtain pure AlON powders is given with equation (2.24):

$$\omega = \frac{x}{M_{add} + M_m}$$

$$\Rightarrow M_{add} = x/\omega - M_m = 4.1 \times (M_{Al_2O_3} - M_m)/\omega - M_m \quad (2.24)$$

### Reducing agents

Carbon black is considered as the standardized reducer in CRN methods however many reducing agent can be adapted in order to obtain AlON powders via the carbothermal reduction nitridation process. Xinayang et al. [98] used organic sucrose as a reducer instead of carbon black following a two-step method in which  $\gamma$ -Al<sub>2</sub>O<sub>3</sub> was used as a starting powder. Sucrose was found to be more effective in nitriding and hindering the agglomeration of powders. In their results, after 4h of heating at 1500°C, there was a partial nitridation giving (after carbon removal) a commercial-like grey AlN powders, unlike the brown AlN powders obtained when carbon black is used. The rest converted to  $\alpha$  and  $\gamma$  phase. The AlN powder's color was explained as Al<sub>2</sub>O<sub>3</sub> are covered with carbon at 900°C when sucrose is used, making the area of nitridation large. While in case of carbon black use, it infiltrates between particles giving a small nitridation area. It was also suggested that carbon layers help avoiding agglomeration of AlN-Al<sub>2</sub>O<sub>3</sub> composite powders. A further heating at 1750°C for 4h of the mixture of  $\gamma$ -Al<sub>2</sub>O<sub>3</sub> and AlN powders gives white  $\gamma$ -AlON powders of 1 – 2  $\mu$ m size [98]. Propane has been suggested as a reducing agent in the carbothermal reduction nitridation in which it has been found to have a positive accelerating effect on the nitridation with an addition of a small amount of (C<sub>3</sub>H<sub>8</sub>) [93,95].

### Particle size

Particle size is an important factor in powder synthesis since a reduced powder size of the reactant to a nano scale raises the specific energy lowering the sintering temperatures [99]. In the reviewed literature, the particle size of AlON powders

obtained via CRN was large and needed further processing. Qiang et. al. [19] used ball milling in order to lower the powder size. In their attempt to obtain highly transparent AlON ceramics, they used CRN method to synthesize aluminum oxynitride. A mixture of  $\gamma$ -Al<sub>2</sub>O<sub>3</sub> and carbon black underwent a 12h ball milling in presence of ethyl alcohol after which it was dried and sieved. Following a first calcining at 1550°C under Nitrogen atmosphere for 1h to achieve  $\gamma$ -Al<sub>2</sub>O<sub>3</sub> – AlN composite followed by heat treatment at 1750°C for 2h, a single phase AlON powders were obtained after a subsequent firing at 700°C for 4h in air to remove any residual carbon. The size was found to be reduced with the increase of milling time (3.36  $\mu$ m after 12h and 1.38 after 24h  $\mu$ m) [19]. The same method was reported in the synthesis of AlON powders with similar results with a difference in size reduction method via freeze drying for 24h at –80°C of AlON powders dispersed in deionized water, ultrasonic dispersion with absolute ethanol for 2h and liquid nitrogen ball milling for 6h. The last was found to give the best result in matters of size (3.08  $\mu$ m) [99].

#### **2.4.2.2. Other synthesis methods**

Beside the two-step CRN, there exists other methods to synthesize AlON. Direct nitridation is one step method used to produce AlON. Unlike CRN, direct nitridation eliminates the problem of carbon, which is a the main disadvantage of the reduction nitridation method as a further processing is needed for its elimination. Mingyi et. al. [100] obtained AlON powders via direct nitridation of Al-Al<sub>2</sub>O<sub>3</sub> mixture. The reactants were dispersed in alcohol and magnetically stirred, then dried at 80°C for 3h. The mixture was later treated at 1750°C for 3h under nitrogen. The obtained powder, which varied between 10 – 30  $\mu$ m, was reduced using ball milling with sintering additives (MgO, Y<sub>2</sub>O<sub>3</sub> and La<sub>2</sub>O<sub>3</sub>) for 24h to less than 1  $\mu$ m.

Although this method is advantageous as it eliminates the problem of carbon, its cost is considerably high with further milling needed as the as-synthesized powders are quite large.

Lysenkov et. al. [10] synthesized AlON from AlN and Al(OH)<sub>3</sub> powders synthesized via self-propagating high temperature synthesis (SHS). The mixture of AlN-Al(OH)<sub>3</sub> was nitrided at 1850°C for 15 min. the as-synthesized powder was reduced after milling to 1 – 3  $\mu$ m. Comparing to the previously mentioned methods, this last was the fastest, however in regard to the cost, it is not any better than the direct nitridation

method.  $\text{Al}(\text{OH})_3$  was also used beside Al powders, to synthesize AlON via direct nitridation process using ammonia instead of nitrogen [101]. AlON was obtained by first nitriding Al/ $\text{Al}(\text{OH})_3$  mixture with a molar ration of 1:4 at  $1100^\circ\text{C}$  for 4h to give AlN/ $\text{Al}_2\text{O}_3$  mixture, followed by calcination at  $1750^\circ\text{C}$  for 1h in flowing nitrogen. Ammonia was also used to obtain AlON by nitriding a precursor derived from aluminum-glycine gel [102]. As stated earlier, the use of ammonia in nitridation is due to its better reactivity in forming AlN [93].

There is also another solid-state reaction method in which previously prepared AlN and  $\text{Al}_2\text{O}_3$  powders are directly sintered into AlON. Hiroyuki et. al. [103] fabricated AlON powders in an early study from AlN and  $\alpha\text{-Al}_2\text{O}_3$  as starting materials. A mixture of powder was prepared in ethanol then dried and uniaxially pressed into a cylindrical pellet. The pellet was later placed in an arc-melting furnace under nitrogen atmosphere. Jianqi et. al. [14] prepared aluminum oxynitride powders from nano-sized AlN and  $\gamma\text{-Al}_2\text{O}_3$  powders. A mixture of powders was ball milled for 24h in alcohol, then dried in air for 24h at  $80^\circ\text{C}$ . The obtained mixture was calcined at  $1750^\circ\text{C}$  for 4h under nitrogen flow.

This route gave powders of particle size varying between 2 – 10  $\mu\text{m}$ . Naderi-Beni et. al. [104] tried to synthesize AlON via a sol-gel method using aluminum tri-sec-butoxide as an aluminum precursor, acetonitrile and chloroform were used as solvents while hydrazinium hydroxide was adapted as a catalyst. The obtained results revealed an AlON nano-powders obtained at  $1500^\circ\text{C}$  which after sintering at  $1600^\circ\text{C}$  results in a 54% transparency.

#### **2.4.2.3. Forming mechanism**

The mechanism following which AlON is formed varies from solid-solid (SS), to solid-gas (SG) and gas (G) reaction, depending on the existing parameters in the system (temperature and partial pressures).

A model, which shows the stability regions of AlON following different types of reactions, was presented by Xie et. al. [17]. According to this model, nitride layers form on aluminum oxide. These layers contain cracks from which an exchange of atoms takes place resulting in an oxynitride phase forming at the  $\text{Al}_2\text{O}_3\text{-AlN}$  contact region. This oxynitride phase keeps growing as long as  $\text{Al}_2\text{O}_3$  and AlN are in existence. However, when AlN is completely consumed, an aluminum oxide phase in the form

of  $\alpha$ - $\text{Al}_2\text{O}_3$  remains within the oxynitride making its possibility of elimination very low. Figure 2.12 illustrates AION forming mechanism.

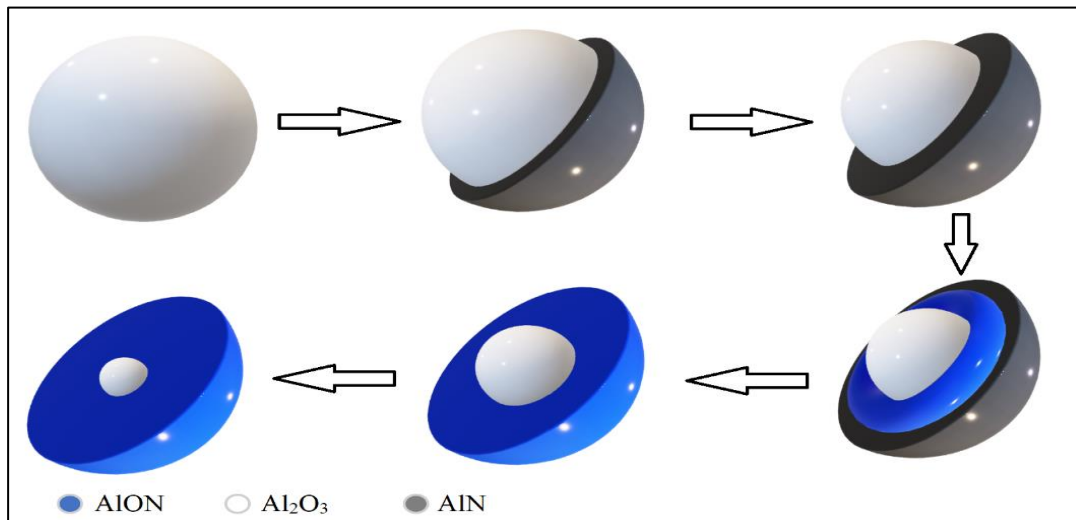


**Figure 2.12.** AION forming mechanism. [17]

### 2.4.3. MgAION

The possible existence of MgAION phase, dates back to 1993, when AION was reported to be made stable using MgO [34]. In the years that followed, different attempts to obtain a highly transparent MgAION phase were made. Being a magnesium stabilized AION, the synthesis methods of magnesium aluminum oxynitride do not by far differ from those used to fabricate AION powders. The conventional approach to synthesize magnesium aluminum oxynitride is the reaction sintering of  $\text{Al}_2\text{O}_3$ , AlN and MgO. Nonetheless, MgAION powder can be obtained via synthesis of Mg and Al bearing precursors in nitrating atmosphere.

Despite transparency being the main application for magnesium aluminum oxynitride, it is considered as a good candidate for high-performance refractories [105]. Similar to MAS and AION, the consideration of MgAION for refractory usage does not require meticulously controlled processes as those needed for powders destined for optical properties for which high purity precursors as well as advanced synthesis techniques are needed. This is due to the negative effect that the slightest defect or impurity can have on transparency. MgAION can be obtained directly via reaction sintering as well as in particulate form via synthesis. For powder synthesis, the widely used synthesis technique is carbothermal reduction nitridation.

MgAlON has been widely investigated in the last 20 years for both transparent and optical applications. Granon et. al. reported limited transparency of MgAlON (65% in the visible and 83% in the mid-IR [106]) obtained via reaction sintering of  $\text{Al}_2\text{O}_3$ , AlN and MgO, followed by hot isostatic pressing (HIP) [53]. Highly transparent MgAlON ceramic (80% in the visible and 84% in the mid-IR [106]) was prepared for the first time in 2014, via sintering of submicron MgO, AlN and  $\text{Al}_2\text{O}_3$  at  $1875^\circ\text{C}$  for 24h under  $\text{N}_2$  atmosphere [66]. Ma et. al. synthesized MgAlON from nanosized  $\gamma\text{-Al}_2\text{O}_3$  and MgO, mixed with carbon black at  $1600^\circ\text{C}$  for 2h under flowing  $\text{N}_2$  [106]. Bandyopadhyay et. al. [107] studied the effect of controlling parameters on the reaction sequence of MgAlON. Nevertheless, it has been found that the fabrication of highly transparent MgAlON requires high temperatures exceeding  $1800^\circ\text{C}$  [66]. The influence of reaction parameters was also studied by Dai et. al. [108] demonstrating that the CRN reaction rate increases with the rising temperature.

Despite the absence of need for meticulously controlled process, the synthesis of MgAlON for refractory usage, obeys to certain conditions. Studying the production of MgAlON bonded refractory material, Pichlbauer et. al. [109] found that the use of  $\text{MgAl}_2\text{O}_4$  as magnesium source results in less amount of secondary phase than the usage of MgO. The effect of impurities was also investigated by Ye et. al. [105] who found an accelerated oxidation takes place when natural raw materials are used comparing to the use of synthetic ones.

#### 2.4.3.1. Formation mechanism

The formation mechanism of MgAlON destined for refractory use was investigated by Cheng et. al. [110] when metallic Al is used.

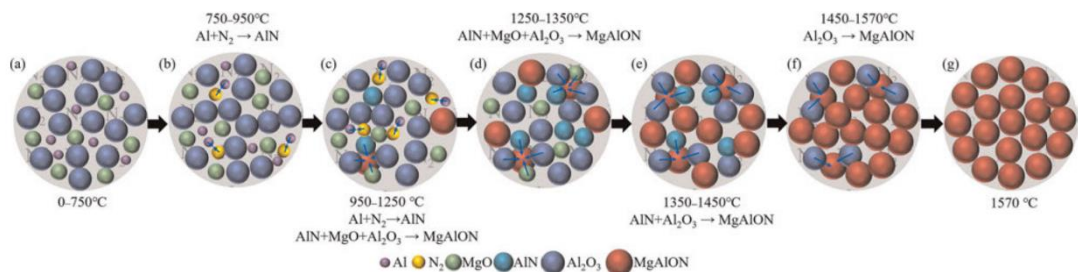


**Figure 2.13.** MgAlON evolution in Al- $\text{Al}_2\text{O}_3$ -MgO- $\text{N}_2$  system. [110]

It has been found that after a melting of Al at 660°C then its nitridation to form AlN at 1250°C, the nitride reacts with MgO and Al<sub>2</sub>O<sub>3</sub> to form MgAlON at 950°C with a continues dissolution until 1570°C. Figure 2.13 summarizes the reaction process.

The reaction mechanism of MgAlON for transparent window application has been investigated by Chen et. al. [16] in the C- MgO-Al<sub>2</sub>O<sub>3</sub> system. It has been found that an intermediate spinel phase, from which MgAlON in formed, takes place at low temperature, giving an MgAl<sub>2</sub>O<sub>4</sub>-Al<sub>2</sub>O<sub>3</sub>-AlN before the final stage in which a full MgAlON is obtained (Figure 2.13).

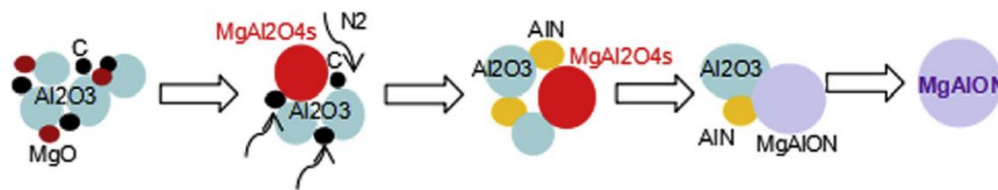


**Figure 2.14.** MgAlON formation mechanism in the C-Al<sub>2</sub>O<sub>3</sub>-MgO system. [16]

## 2.5. Densification of MAS, AlON and MgAlON for Transparent Windows

The densification of ceramics traditionally takes place via firing through which fine particles bond with each other to form a single strong body. The densification process allows the material to gain density as well as strength with a simultaneous decrease of porosity whose existence in the product causes a stress concentration at pores lowering the quality of the product.

Densification processes vary based on the expected properties which are tailored according to the product's area of application. Firstly, it is well known that a thorough elimination of porosity to achieve theoretical density is a very hard task, and thus, a certain percentage of porosity is allowed for specific applications of ceramic, since the elimination of porosity requires expensive sintering techniques coupled with the use of sintering additives [111]. In the case of traditional ceramics, a firing at moderate temperatures is sufficient to provide the needed densification. However, when technical ceramics are in question, and specifically, optical ceramics, sintering must be carefully controlled to avoid defects due to their detrimental effect, not only on mechanical properties, but also since they are a source of scattering which results in a lower transmission [1].

It is always better to obtain a pore-free bodies following sintering, yet an amount of porosity can be tolerated depending on the type of application as the techniques that allow a densification close to that of theoretical density are highly expensive in matters of cost. For optical applications, however, advanced sintering techniques such as hot pressing, hot pressing and spark plasma sintering, which guarantee the maximum densification, are generally used. Additives varying based on the type of ceramic powder to be used for the fabrication of transparent bodies, are also required to achieve fully densified bodies as their absence has been linked to low transmission [10,91,100].

### **2.5.1. Factors controlling densification**

Sintering can be subject to many factors which can differently affect the final properties of the densified body. These factors vary from the quality of the starting materials to powders processing, sintering temperature, the type and amount of sintering additives used as well as further processing if necessary (size reduction via milling, residual carbon burning...etc.).

#### **2.5.1.1. Ball milling**

A pre-sintering mechanical treatment was demonstrated to be important in obtaining a homogenization of the mixture of powders and sintering additives, as well as, reducing the powder size. For example, in the case of AlON, ball milling was performed before syntheses and/or sintering in many of the reviewed literature [10,14,19,88,100,102]. It has been reported that longer milling reduces the powder size giving better size distribution and lightening the degree of agglomeration through 12h and 24h ball milling of the as-synthesized AlON powders, mixed with both MgO and Y<sub>2</sub>O<sub>3</sub> as additives [19]. A highly transmitting AlON body was obtain after such process via pressureless sintering of an isostatically cold-pressed body at 1850°C for 6h.

In the case of MAS, milling can be used as a synthesis process allowing the production of spinel powders without any further heating. The powders obtained via milling has been shown to exhibit a better sinterability provided that the optimal milling time is determined since shorter time was linked to incomplete reaction where excessive milling results in impurities deriving from milling tools [112]. MgAl<sub>2</sub>O<sub>4</sub> powder for electroceramic applications has been investigated via different milling to identify optimum results for sintering behavior. After sintering at 1650°C for 2h in air, 99.22%

and 99.49% of the theoretical density were obtained from high energy horizontal attrition milling and solution combustion route using urea as fuel, respectively [113]. Powders processed via high energy ball milling has also been shown to exhibit lower densification activation energy, which remains constant throughout the sintering process comparing to non-milled samples whose energy is constantly increasing [114]. Obradovic et. al. [115] demonstrated that a milling of the starting powders for homogenization followed by mechanical activation results in an initiation of MAS sintering at much lower temperature in comparison to non-milled samples. The crystallization temperature as well, has been shown to be subject to milling as planetary micro-milling allows its reduction in addition to a reduced crystallites size of 25nm [116].

Not dissimilar to AlON and MAS, a full densification of MgAlON requires milling to provide a good mixing of starting materials, especially in the case of optical windows production in which full densification is needed. Cheng et. al. [110] mixed the starting materials in absolute alcohol for 3h. Ma et. al. [106,117] used ball milling to provide dispersion of the reactants in the densification of MgAlON. Chen et. al. [16] explained that milling allows the obtention of well-dispersed narrow-sized reactants.

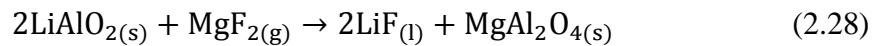
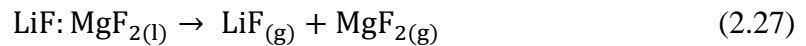
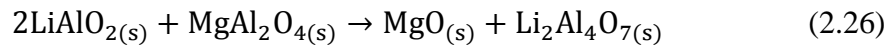
#### **2.5.1.2. Sintering additives**

The elimination of porosity is a crucial phase in the densification which aims to eliminate pores that are considered as a stress concentration area lowering the mechanical properties of the final product. Moreover, being considered as a source of scattering, porosity is a problem that must be avoided in the production of transparent windows. However, a complete elimination of porosity is a very hard task to achieve, and thus, sintering additives are used to provide full densification of the sintered bodies, which results in an enhancement of the properties.

Sintering additives for spinel structure can be in the form of solid solutions such as MgO and/or Al<sub>2</sub>O<sub>3</sub>, which dissolve in the structure without changing it, or liquid additives that allow a sintering of bodies without forming grain boundaries or introducing colors of the transparent body [7]. In order to obtain the optimum properties, additives must be homogeneously distributed within the powder prior to sintering.

In the case of MAS for transparent windows, the most commonly used additive is lithium fluoride (LiF). As mentioned earlier a poor distribution of additives causes lower transparency and properties following densification [6]. Thus, the distribution has been reported to be enhanced with a coating of powder prior to densification allowing the obtention of full densified transparent bodies [9].

LiF has been reported to be a liquid phase sintering additives which reacts following melting with  $MgAl_2O_4$  to form  $LiAlO_2$  or  $LiAl_4FO_6$  together with a fluoride melt (LiF:MgF<sub>2</sub>) which simplifies the rearrangement of spinel particles and enhances the diffusion of its atoms, whereas spinel with impurities in matters of Li, which contain oxygen vacancies, promotes the diffusion of  $MgAl_2O_4$  atomic components. Above 1000°C, LiF starts leaving the compact while MgF<sub>2</sub> reacts with  $LiAlO_2$  to reform spinel [7]. Reactions 2.25 to 2.28 explain the process by which LiF additives enhance the densification of spinel. It is important to mention that the failure to completely remove LiF from the sintered body, results in bad optical and mechanical properties.



In the case of AlON, sintering aids has an important impact. It is well established that additives enhance sintering, lower its temperature, and helps control grain growth [118]. On the other hand, not completely dissolved within AlON grains, sintering additives can cause secondary phases which can be found at grain boundaries, triple points and/or within the grains [100]. The presence of such defects can be a source of scattering, and by consequence, transmittance will be decreased [1].

Many studies investigated the effects of additives on the sintering of AlON. Lysenkov. et. al. [10] obtained an open porosity of 2,6% after a hot-pressing treatment. It has been suggested that the absence of sintering aids was the cause of those results. Qi et. al. [91] demonstrated that the insufficiency of sintering additives, as well as high temperature and holding time during sintering affect the microstructure of AlON in the sintering of powders obtained from AlN-Al<sub>2</sub>O<sub>3</sub> mixture, at 1880°C for 5h, 10h and 20h with Y<sub>2</sub>O<sub>3</sub> as sintering additive. The obtained results showed an increase of

transmittance with holding time, however, the maximum transmittance reached was low (54,55%), which was interpreted as the residual porosity caused by the lack of additives. The positive effect of sintering aids on AlON densification has also been investigated by Su. et. al. [100] who obtained a density of  $3,68 \text{ g/cm}^{-3}$ , which represent 99,2% of the theoretical value, by additives mixture of MgO,  $\text{Y}_2\text{O}_3$  and  $\text{La}_2\text{O}_3$ . The use of sintering aids mixture has been found to give better transmittance results than the use of one single additive [102]. Feng et. al. [119] investigated the use of different weight percentages of highly reactive nano sized  $\gamma\text{-Al}_2\text{O}_3$  as sintering additive in the consolidation of AlON obtaining an optimum of 81% transmission with the addition of 2.5wt% of gamma alumina.  $\text{SiO}_2$  has also been suggested as an effective additive in the densification of AlON with a transmittance exceeding 86% at an addition of 0.15wt% to 0.55wt% of  $\text{SiO}_2$  [120].

For magnesium aluminum oxynitride, the use of sintering has not been widely reported. Highly transmitting MgAlON (transmittance exceeding 80%) has been fabricated without sintering additives, mainly using advanced sintering techniques such as hot pressing and hot isostatic pressing [55,17,121]. Ma et. al. [106] used 0.5wt% LiF as sintering additive in the densification of MgAlON obtaining a maximum transmittance of 86%, however, no special positive effect on sintering has been attributed to the use of additives.

### **3. EXPERIMENTAL PROCEDURE**

As stated in the introduction, this research aims to investigate the efficacy of the novel ceramic powder synthesis method; dynamic thermochemical method (DTM) in the fabrication of three spinel powders,  $\text{MgAl}_2\text{O}_4$ , AlON and MgAlON. Intending to achieve that, a focus was placed on the effect of three main factors. The first is the selection of the starting powders and the effect of their characteristics on the final product. The second main factor was the effect of process parameters, such as temperature and holding time, on the synthesis. Finally, the examination of the effect between whether the system is dynamic or static (conventional). After synthesizing, powder products were later characterized via different methods to identify the obtained phases and their powder characteristics. It is important to highlight that this research focuses on the production of powders, not the fabrication of a ceramic body. Instead, this work aims to bring to light the effect of a novel approach on three technological ceramics of a great importance for their optical and mechanical characteristics. Hence, the sinterability of the synthesized powders was not investigated in this work, and instead, the effect of the powder properties on sintering was considered from a theoretical perspective.

#### **3.1. Powder and Reaction Temperature Selection**

It is a well-known fact that the selection of the right raw materials plays an important role in syntheses, specifically, that of technical ceramics powders due to their sensitivity to morphological feature and chemical contents. However, the effect of the right choice of the starting powders extends beyond their effects on the final product, as the financial factor becomes as important when mass production as that for commercial use, is in question. Thus, it is crucial that a compromise between the purity of the obtained product and cost of the starting powders should be achieved.

In addition, not only does the cost of the raw materials matter, but also their suitability for the intended process, whether they require further processing or not (prior or post synthesis), and their aptitude to deliver a product with characteristics that allow their

use in their as-synthesized form. All these facts play a crucial role in determining the overall cost of the synthesis and its efficiency.

Traditionally, nanosized powders of high purity and homogeneous morphology are selected for the synthesis of optical ceramics. When the product is destined to use for their mechanical and/or their refractory properties, characteristics of the raw materials are as important yet not as strictly controlled, tolerating a minor percentage of impurities and/or an irregularity of morphology. Consequently, the choices of starting materials for optical ceramics are limited whereas for other uses such as that for refractories provide a certain flexibility.

It has been stated earlier that different mixtures of  $\text{Al}_2\text{O}_3$ ,  $\text{AlN}$  and  $\text{MgO}$  are used for the synthesis of  $\text{MgAl}_2\text{O}_4$ ,  $\text{AlON}$  and  $\text{MgAlON}$ . Nevertheless, in our studies we chose to investigate precursors that have the ability to provide those starting powders as an intermediate phase from which the targeted ceramics can be obtained. In what follows, the starting materials for each of studied ceramics are discussed.

### 3.1.1. Magnesium aluminate

Normally, for the production of MAS,  $\text{MgO}$  and  $\text{Al}_2\text{O}_3$  powders are used as starting raw materials. However, in this study for synthesizing MAS,  $\text{Mg}(\text{OH})_2$  and  $\text{Al}(\text{OH})_3$  obtained from Alfa Aesar were as a starting materials. They are readily available and low cost to start with. The chemical compositions of the as-received powders are given in Tables 3.1 and 3.2 for  $\text{Al}(\text{OH})_3$  and  $\text{Mg}(\text{OH})_2$ , respectively.

**Table 3.1.** The chemical composition of  $\text{Al}(\text{OH})_3$  used, as obtained from the producing company.

Material	Size	Elements					
		Al	Fe	Na	Cl	$\text{SO}_4$	Other
$\text{Al}(\text{OH})_3$	<150 $\mu\text{m}$	Balance	0.01	0.30	0.01	0.05	-

Both powders were characterized via XRD (Rigaku, model D/Max-2200/PC, Japan) and SEM (JEOL, model 6060 LV, USA). The obtained results are given in Figures 3.1 and 3.2.

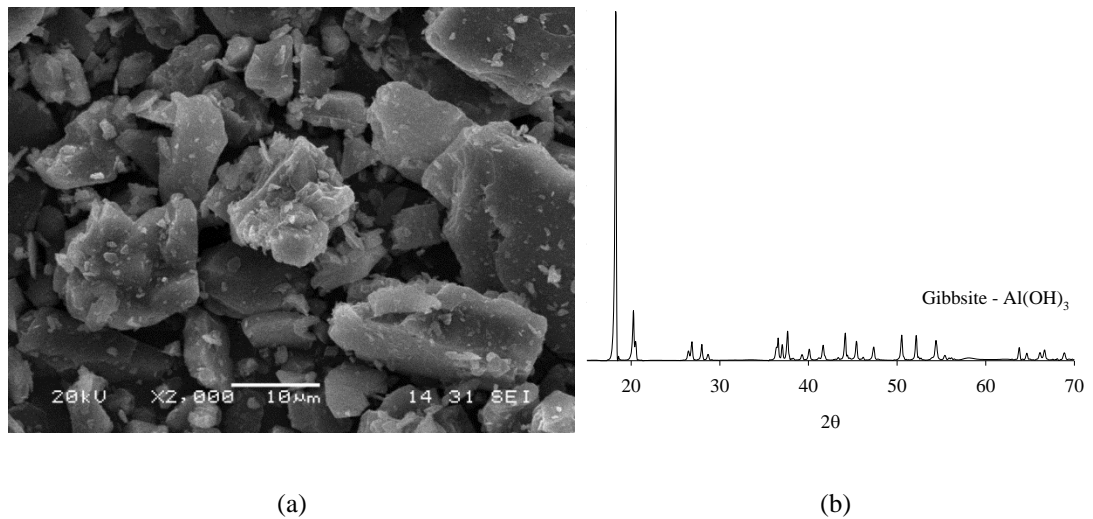


**Figure 3.1.** SEM analysis (a) and XRD pattern (b) of  $\text{Al(OH)}_3$  raw material.

**Table 3.2.** The chemical composition of  $\text{Mg(OH)}_2$  used as obtained from the producing company.

Material	Size	Elements	
		Mg	Other
$\text{Mg(OH)}_2$	< 2.4 $\mu\text{m}$	Balance	0.5%

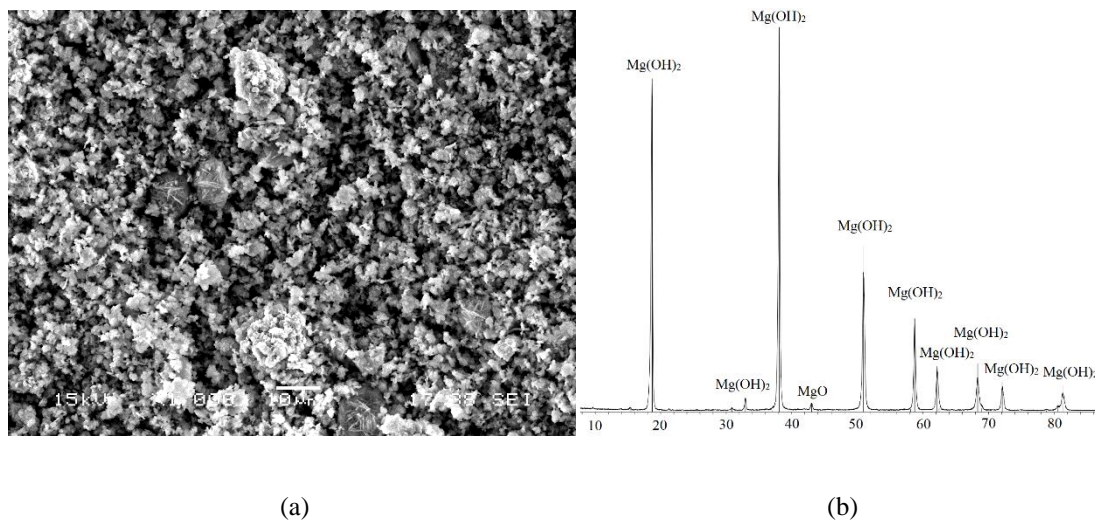


**Figure 3.2.** SEM analysis (a) and XRD pattern (b) of  $\text{Mg(OH)}_2$  material.

In the preparation process, two moles of aluminum hydroxide were mixed with one mole of magnesium hydroxide. Prior to mixing, a thermodynamic modal of the experiment was simulated using FactSage 7.0 to determine the resulting phases from

the reaction of aluminum and magnesium hydroxide. FactSage has been used successfully in many experiments providing insights about experiments prior to their occurrence. The program delivers information about the test parameters (such as temperature and free energy for the formation) and resulting phases that needed to complete the test to obtain the desired compound [122].

Figure 3.3 illustrates the simulation modal of the reaction of two moles of aluminum hydroxide with one mole of magnesium hydroxide under Ar atmosphere between 100°C and 1500°C. It can be seen from the simulation modal that one mole of spinel emerges earlier in the reaction confirming that MAS is thermodynamically possible to achieve under the given conditions and thus, that reaction was selected.

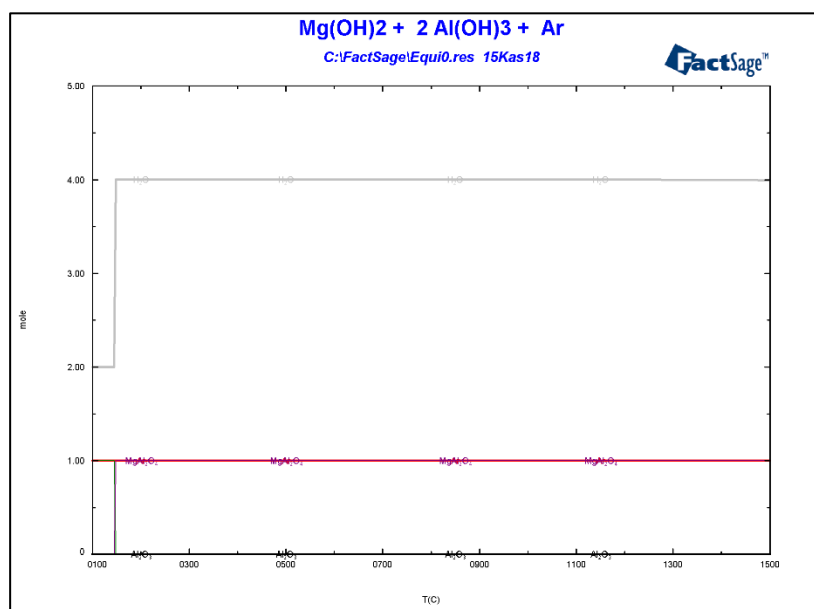


**Figure 3.3.** Thermodynamic modal of the reaction of 2 moles of  $\text{Al(OH)}_3$  with 1 mole of  $\text{Mg(OH)}_2$  under Ar atmosphere between 100°C and 1500°C.

Before proceeding thermochemical reactions raw materials / powders were mixed following two different techniques, manual and automatic. Manual mixing took place via an agate mortar with pestle followed by granulation in which ethanol with an added 5% glycerol was used as a binder. The granulation was performed via a wood spatula in a flat plastic cup to provide regular-shaped granules. Automatic mixing on the other hand was carried out using EIRICH EL1 laboratory mixer, in a stainless-steel container at 300rpm for 5 minutes (no balls were involved in the process) with ethanol as binder via spraying it on the raw powder during mixing. The granules were later sieved to 1-

3 mm size range due to their reported optimum of efficiency observed in previous studies [22-23,122-123,125]. Granules are given in Figure 3.4.



**Figure 3.4.** A photograph showing the prepared granules before charging into the reactor.

In a different approach, alumina balls (made of 99.9% pure alumina from Alfa Aesar) were charged into the reactor alongside the raw materials to investigate the possibility of an activation and/or size reduction of the obtained powders. This technique has been deemed effective in the synthesis allowing the formation of AlN nano powders below 100nm [126]. The alumina balls were added charged together with the raw powders at a ratio of balls to powder of 10 and 20.

### 3.1.2. AION

In order to synthesize aluminum oxynitride (AlON), aluminum hydroxide ( $\text{Al}(\text{OH})_3$ ) was chosen as a starting powder. Its chemical composition as well as the SEM and XRD pattern were previously given in Table 3.1 and Figure 3.1, respectively. The use of  $\text{Al}(\text{OH})_3$  is based on the fact that AlON can be obtained from a mixture of  $\text{Al}_2\text{O}_3/\text{AlN}$ , which can both be obtained from aluminum hydroxide. Kroke et. al. [92] studied the synthesis of AlN powders from  $\text{Al}(\text{OH})_3$  between  $1000^\circ\text{C}$  and  $1400^\circ\text{C}$ , using ammonia ( $\text{NH}_3$ ) as a nitriding source. It has been found that aluminum hydroxide converts to  $\gamma\text{-Al}_2\text{O}_3$ , from which AlN is formed gradually with the increasing temperature. Thus, before a full conversion to aluminum nitride, the existence of  $\gamma\text{-Al}_2\text{O}_3/\text{AlN}$  mixture is possible. Additionally, it has been found that the use of 0.5 vol%

propone ( $C_3H_8$ ) together with  $NH_3$ , allows an early nitridation of transition alumina, starting from  $1100^\circ C$ , with a full conversion possible to achieve at  $1200^\circ C$  [93,97]. Hence, we thought of the idea of a two-steps synthesis, with a first holding at  $1100^\circ C$  to obtain an  $Al_2O_3/AlN$  mixture, followed by a continuous heating and holding at a higher temperature to possibly fabricate AlON.

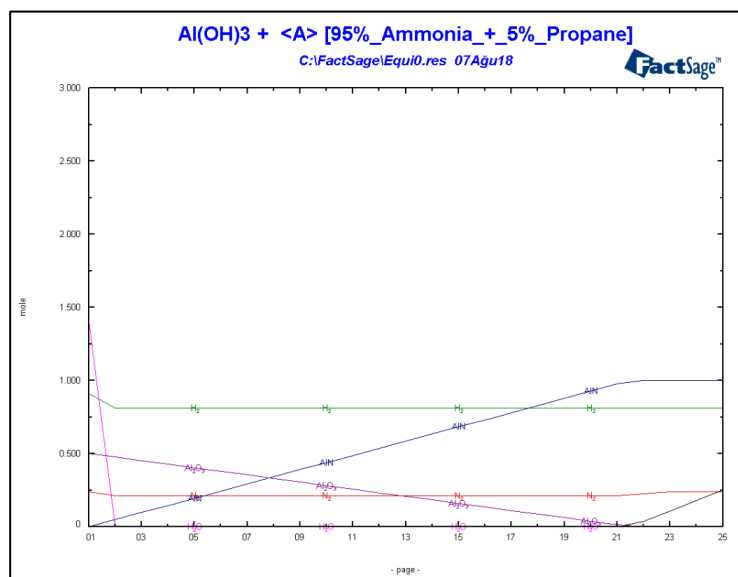


**Figure 3.5.** Thermodynamic modal of the reaction of  $Al(OH)_3$  at  $1450^\circ C$  under  $NH_3 + 5\% C_3H_8$ .

$Al(OH)_3$  was granulated both manually and automatically to a range of 1 to 3mm granules. It can be argued that the absence of a mixture waves the necessity for granulation or an automated mixing at high velocity. Nevertheless, it is crucial to understand that granulation does not only serve in offering a merge of reactants, but also, it facilitates the rotation of powders inside the dynamic furnace, which is the mainly investigated feature in this research.

In a different approach to synthesize AlON, the size of  $Al(OH)_3$  powder was reduced using a high energy ball milling device (Fritsch Pulverisette Model 6), in which the powders were milled for 15 min at 600rpm in the presence of stainless-steel balls with balls to powder ratio of 20:1. This operation, i.e. reducing raw materials` particle size was effective in reducing the final powder / product particle size after DTM to a submicron scale as reported in a previous work [25]. The obtained powders were later granulated manually as previously explained and isolated to 1 to 3 mm size range before being charged for synthesis.

FactSage 7.0 was used in determining the temperature range of the experiment with different simulations in which different gases combinations were verified. Figures 3.5 illustrates the thermodynamic modal of the adapted temperature and mole fraction for the gas mixture of  $N_2 + 5\% C_3H_8$ , whereas Figures 3.6 and 3.7 demonstrate other alternatives. The second two models are meant to explain the choice of the former over the latter modals.

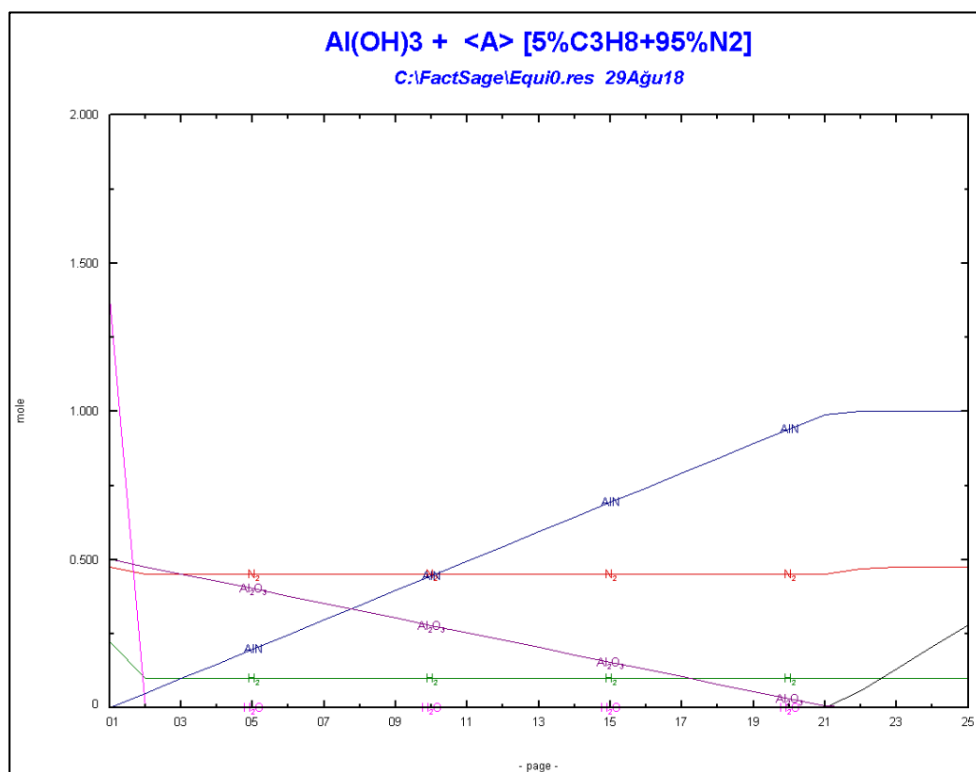


**Figure 3.6.** Thermodynamic modal of the reaction of  $Al(OH)_3$  under  $N_2 + 5\% C_3H_8$  at  $1450^\circ C$ .

It can be seen from the graphical representation given in Figure 3.5, in which the X and Y axes represent the formed molar fraction and the reaction steps with the increasing temperatures, respectively, that a simultaneous increase of AlN accompanied with a depletion of  $Al_2O_3$  takes place resulting in a formation of one mole of AlN after the total consumption of alumina. In Figures 3.6 and 3.7, corresponding to the use of nitrogen and propane gas mixture and carbon black as a reducing agent following the conventional synthesis method of aluminum nitride, respectively, an AlN formation takes place similarly to that of Figure 3.5. Nonetheless, ammonia has been reported to be more reactive than nitrogen promoting the formation of oxynitrides rather than nitrides, and thus, it has been chosen of nitrogen as a nitriding agent [127].

On the other hand, the use of carbon black as a reducing source requires an excess of carbon to allow a full synthesis resulting in a residual carbon following after the reaction. This excess of carbon would later necessitate a carbon burning process to removing it from the product [94]. Hence, it was preferable to investigate the synthesis using gas such as propene as a carbon source. The use of nitrogen as nitriding source in the conventional method elicits the necessity of an elevated temperature and/or an extended holding time. Consequently, the modal initially given in Figure 3.5 was adapted.

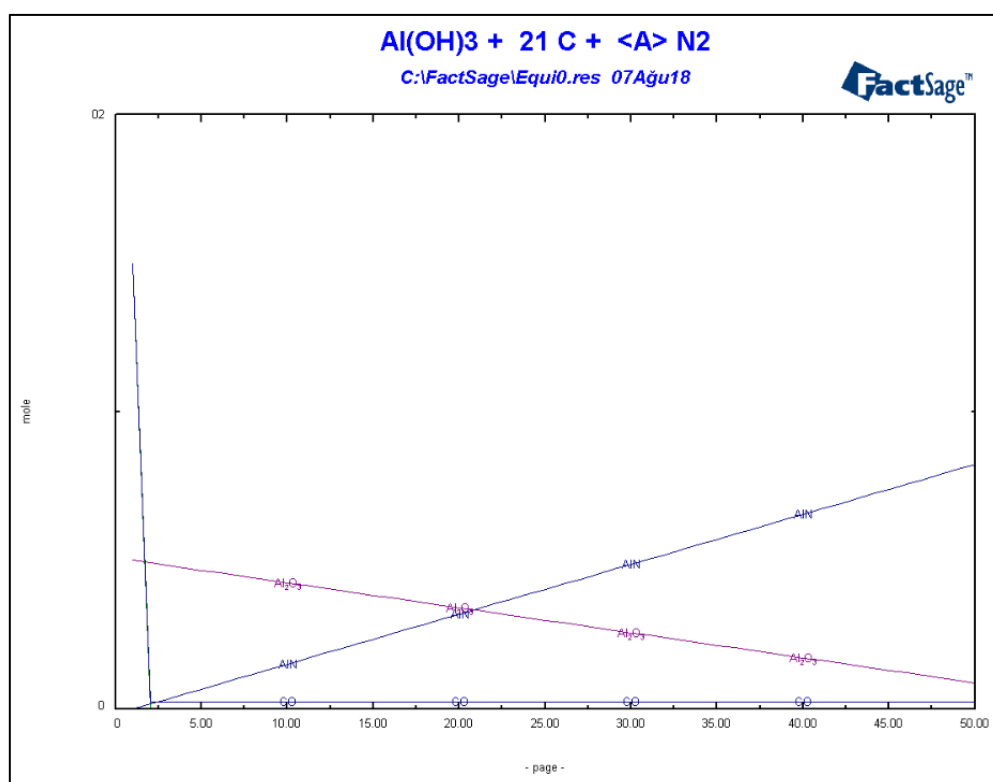


**Figure 3.7.** Thermodynamic modal of the reaction of  $\text{Al}(\text{OH})_3 + 21\text{C}$  under  $\text{N}_2$  with  $1500^\circ\text{C}$  as a completion temperature.

### 3.1.3. MgAlON

In order to produce MgAlON magnesium and aluminum hydroxides mixture was selected.  $\text{Mg}(\text{OH})_2$  has been reported to be a source for both MgO and  $\text{MgAl}_2\text{O}_4$  (when combined with  $\text{Al}(\text{OH})_3$ ).

As stated earlier in the previous chapter, the mixture of AlN, MgO and  $\text{Al}_2\text{O}_3$  has been reported to be the starting powders for the synthesis of MgAlON [16,53,105-106,110]. Since  $\text{Mg}(\text{OH})_2$  decomposes to MgO and  $\text{H}_2\text{O}$  above  $360^\circ\text{C}$  [105] and both AlN and  $\text{Al}_2\text{O}_3$  can be obtained from  $\text{Al}(\text{OH})_3$  in the reduction nitridation process [92], It was

thought that the synthesis of MgAlON from  $\text{Al}(\text{OH})_3$  and  $\text{Mg}(\text{OH})_2$  mixture is possible. In addition, it has been reported that a spinel phase ( $\text{MgAl}_2\text{O}_4$ ) formation takes place at lower temperature before the reduction nitridation from the reaction of  $\gamma\text{-Al}_2\text{O}_3$  with MgO in the presence of a reducing agent, giving rise to its reacting with AlN and  $\text{Al}_2\text{O}_3$  to form MgAlON [16]. Thus, we aimed to test these assumptions using  $\text{Mg}(\text{OH})_2$  and  $\text{Al}(\text{OH})_3$  as starting powders, under a nitriding atmosphere.

The molar fraction of the reactants, which was adapted in synthesis, was similar to that for MAS synthesis due to the fact that the latter is considered as a starting powder from which MgAlON can be obtained. The powders were granulated under the same conditions of the previous spinel powders. Figure 3.8 demonstrates an image of the granules used in the synthesis of magnesium aluminum oxynitride.

### **3.2. Experimental Design**

The process used in the study, is an original patented method that was based on the conventional carbothermal reduction nitridation [23] and has been deemed effective in the synthesis of many technical ceramics such as TiN, ZrN,  $\text{Si}_3\text{N}_4$ ,  $\text{B}_4\text{C}$ , BN,  $\text{TiB}_2$ ...etc [22-23,123,125]. In what follows, the process as well as the experimental parameters selected are discussed.

#### **3.2.1. The DTM furnace**

As explained earlier, the dynamic thermochemical method (DTM) is a modified carbothermal reduction process, in which the synthesizing takes place in a rotary kiln, allowing the reaction to take place in a relatively shorter time, offering fine powders that can be readily used in their as-synthesized form [122].

The rotary furnace used for DTM is a modified Protherm brand regular tube furnace, operating at up to  $1600^\circ\text{C}$ , with both heating and cooling rate control capability. A 3-volt DC servo motor and gear system were used to provide rotation. The refractory ceramic tube was aligned horizontally on to the bearing that are assembled on plate to allow a smooth rotation. The gas inlet system (between the rotating tube and the stationary gas hose) was made of predesigned stainless steel and brass conical sleeve type sealing. A reactor, specially designed in a cylindrical shape, was located in the middle of the refractory ceramic tube (Figure 8.3).

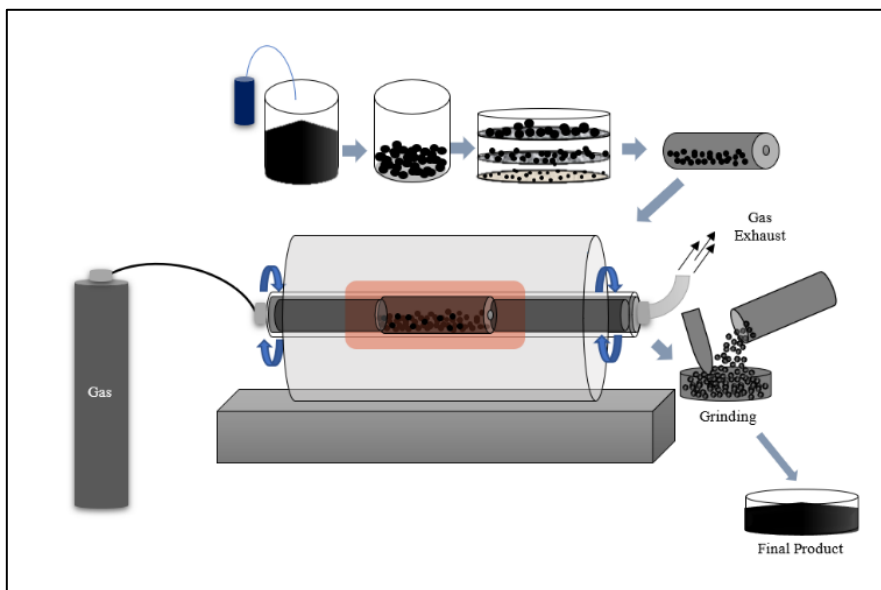


**Figure 3.8.** Schematic representation of the DTM process.

To prevent the reactor from moving inside the tube and assure its stability in the heat center of the furnace, alumina pipes were placed on both sides of the reactor. Figure 3.8 and Figure 3.9 show a schematic representation and a real photo of the DTM system, respectively. MFC system and gas mixing units are given in Figure 3.10.



**Figure 3.9.** The DTM modified rotary furnace.

Before charging into the DTM furnace, all the granules were dried at 80°C for 24 hours in a BINDER 2017 model oven. Then dried granules were charged into a cylindrical alumina reactor ( $\phi$  45 mm, L 192 mm) having centered vents on both sides, allowing gas flow in the reaction zone.

### 3.2.2. Gas use

Aiming to synthesize the desired ceramics, different test parameters were selected based on a thermodynamic simulation study (previously explained in in Section 3.1.).

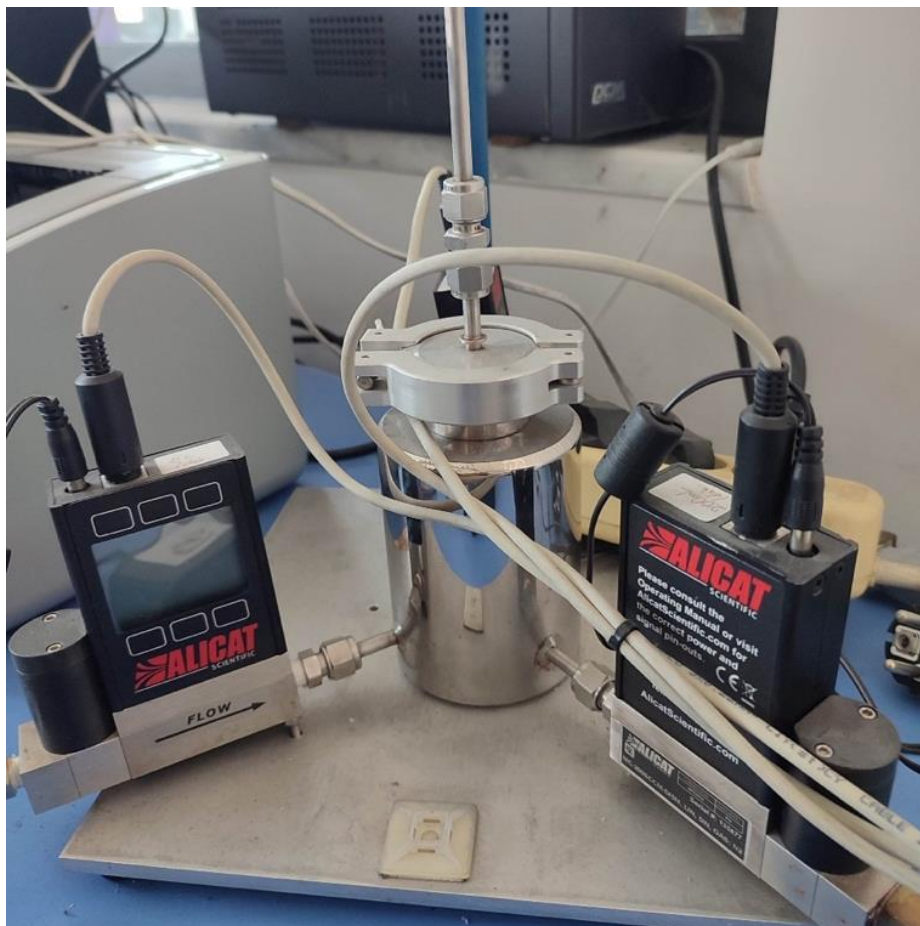


**Figure 3.10.** ALICAT brand MFCs for gas mixing used in the synthesis process.

To enable the mixing of gases, a gas mixing apparatus with MFCs from ALICAT Scientific Flo was setup allowing the merging of up to three gases. This apparatus provides the ability to control the gas flow rate as well as the proportion of the mixed gases which is required to perform a carbothermic reduction without using carbon black. Argon was used in the synthesis of spinel whereas a mixture of ammonia and propene was adapted for AlON synthesis, and finally, nitrogen and ammonia were used to synthesize MgAlON. Gas flow rate was adjusted and controlled using a software with PC.

In AlON experiments, a constant flow of nitrogen was provided up to 700°C. later, the mixture of ammonia and propene was allowed to flow within the system for the first step between 700°C until the end of the first holding. After the first holding / plateau

temperature, a switch to nitrogen flow took place lasting until cooling of the synthesized powders including the second holding. The general gas flow plan is given in Table 3.3. Heating and cooling rates were kept constants for all tests as 5 °C/ min, though cooling rate was not being able to keep constant after reaching approximately 550°C after which cooling rate reduced well below to 3°C/min since there is no cooling medium attached to the furnace. However, the change in cooling rate after 550°C have no adverse effects on the final product properties.

**Table 3.3.** The general gas flow plan in AlON synthesis.

25°	600°	1 <sup>st</sup> Step Holding	2 <sup>nd</sup> Step Holding	25°
100% N <sub>2</sub>		96% NH <sub>3</sub> + 4% C <sub>3</sub> H <sub>8</sub>		100% N <sub>2</sub>

### 3.2.3. Heating plan

In the case of spinel and MgAlON, no emphasis was placed on the heating plan. Aside from a couple of experiments in the synthesis of MgAlON, a single step heating was performed. For AlON synthesis, both single step and two-step heating plans were investigated due to the reported efficiency of the latter in the fabrication of aluminum oxynitride. A graphical representation of the heating plan is given in Figure 3.11.

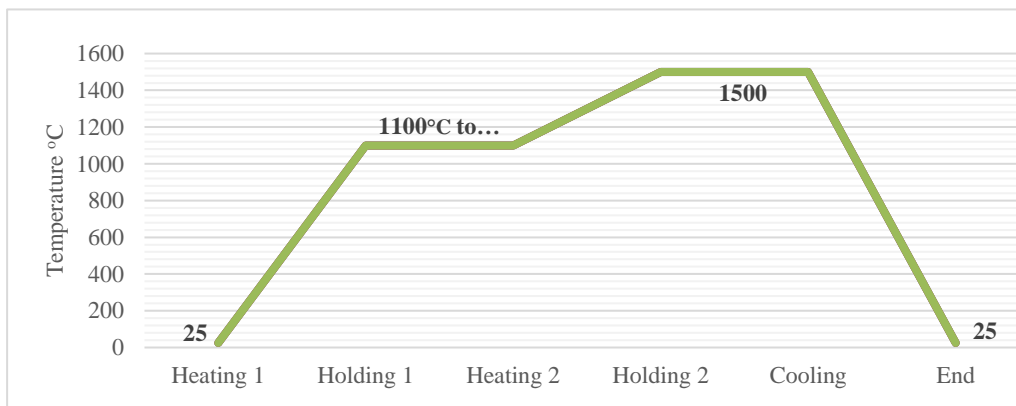


**Figure 3.11.** Graphical representation of the AlON heating plan.

To determine the ideal parameters for the first step holding in the synthesis of AlON, different temperatures as well as holding times were investigated. The biggest challenge of this approach is to determine both the optimum temperature and holding time at which an AlN/Al<sub>2</sub>O<sub>3</sub> mixture that allows the synthesis of AlON, is reached. The temperature range was selected between 1100°C and 1200°C. As stated earlier, in the gas synthesis process, AlN has been reported to start forming at 1100°C and can be fully obtained at 1200°C [92,97].

All the performed experiments on MgAl<sub>2</sub>O<sub>4</sub>, AlON and MgAlON are summarized in Tables 3.4, 3.5 and 3.6, respectively.

**Table 3.4.** The heating plans investigated in the synthesis of MgAl<sub>2</sub>O<sub>4</sub>

Sample	Experimental Procedures
D001S	1h at 1300°C (Static)
D002S	1h at 1400°C (Static)
D003S	1h at 1500°C (Static)
D004S	1.5h at 1500°C (Static)
D005S	1.5h at 1500°C (Static)
D006S	2h at 1500°C (Static)
D007S	1.5h at 1500°C (2rpm)
D008S	1.5h at 1400°C (10 Balls/2rpm)
D009S	1.5h at 1500°C (4rpm)
D010S	1.5h at 1500°C (20 Balls/2rpm)

**Table 3.5.** The heating plans investigated in the synthesis of AlON

Sample	Experimental Procedures
D001A	1h at 1450°C in 96% NH <sub>3</sub> + 4% C <sub>3</sub> H <sub>8</sub> (St)
D002A	1h at 1450°C in 96% NH <sub>3</sub> + 4% C <sub>3</sub> H <sub>8</sub> (4rpm)
D003A	1h at 1350°C in 96% NH <sub>3</sub> + 4% C <sub>3</sub> H <sub>8</sub> (4rpm)
D004A	1h at 1450°C in 96% NH <sub>3</sub> + 4% C <sub>3</sub> H <sub>8</sub> (St)
D005A	2h at 1500°C in 99% NH <sub>3</sub> + 1% C <sub>3</sub> H <sub>8</sub> (4rpm)

**Table 3.5. (Continued)** The heating plans investigated in the synthesis of AlON

Sample	Experimental Procedures
D006A	0.5h at 1100°C + 2h at 1500°C in 99% NH <sub>3</sub> + 1% C <sub>3</sub> H <sub>8</sub> (4rpm)
D007A	1h at 1100°C + 2h at 1500°C in 96% NH <sub>3</sub> + 4% C <sub>3</sub> H <sub>8</sub> (4rpm)
D008A	1.5h at 1100°C + 2h at 1500°C in 96% NH <sub>3</sub> + 4% C <sub>3</sub> H <sub>8</sub> (4rpm)
D009A	1.5h at 1100°C + 2h at 1500°C in 96% NH <sub>3</sub> + 4% C <sub>3</sub> H <sub>8</sub> (4rpm)
D010A	1.5h at 1100°C + 2h at 1500°C in 96% NH <sub>3</sub> + 4% C <sub>3</sub> H <sub>8</sub> (4rpm)
D011A	1.5h at 1100°C + 2h at 1500°C in 96% NH <sub>3</sub> + 4% C <sub>3</sub> H <sub>8</sub> (4rpm)
D012A	1h at 1200°C + 2h at 1500°C in 96% NH <sub>3</sub> + 4% C <sub>3</sub> H <sub>8</sub> (4rpm)
D013A	1.25h at 1200°C + 2h at 1500°C in 96% NH <sub>3</sub> + 4% C <sub>3</sub> H <sub>8</sub> (4rpm)
D014A	1.25h at 1100°C + 4h at 1500°C in 96% NH <sub>3</sub> + 4% C <sub>3</sub> H <sub>8</sub> (4rpm)
D015A	1h at 1150°C + 2h at 1500°C in 96% NH <sub>3</sub> + 4% C <sub>3</sub> H <sub>8</sub> (4rpm)
D016A	1h at 1150°C + 2h at 1500°C in 96% NH <sub>3</sub> + 4% C <sub>3</sub> H <sub>8</sub> (St)
D017A	1h at 1100°C + 2h at 1500°C in 96% NH <sub>3</sub> + 4% C <sub>3</sub> H <sub>8</sub> (4rpm)
D018A	1.25h at 1100°C + 2h at 1500°C in 96% NH <sub>3</sub> + 4% C <sub>3</sub> H <sub>8</sub> (4rpm)
D019A	1.25h at 1100°C + 2h at 1500°C in 96% NH <sub>3</sub> + 4% C <sub>3</sub> H <sub>8</sub> (4rpm)
D020A	1.25h at 1100°C + 2h at 1500°C in 96% NH <sub>3</sub> + 4% C <sub>3</sub> H <sub>8</sub> (4rpm)
D021A	1.h at 1100°C + 2h at 1500°C in 96% NH <sub>3</sub> + 4% C <sub>3</sub> H <sub>8</sub> (4rpm)
D022A	1.25h at 1100°C + 2h at 1500°C in 96% NH <sub>3</sub> + 4% C <sub>3</sub> H <sub>8</sub> (4rpm)
D023A	1h at 1100°C + 2h at 1500°C in 96% NH <sub>3</sub> + 4% C <sub>3</sub> H <sub>8</sub> (4rpm)
D024A	1.25h at 1100°C in 46% NH <sub>3</sub> + 4% C <sub>3</sub> H <sub>8</sub> + 50% N <sub>2</sub> (4rpm)
D025A	1h at 1100°C + 2h at 1500°C in 96% NH <sub>3</sub> + 4% C <sub>3</sub> H <sub>8</sub> (St)
D026A	1.25h at 1100°C + 2h at 1500°C in 46% NH <sub>3</sub> + 4% C <sub>3</sub> H <sub>8</sub> + 50% N <sub>2</sub> (St)
D027A	1.25h at 1100° + 2h at 1500°C in 96% NH <sub>3</sub> + 4% C <sub>3</sub> H <sub>8</sub> (4rpm)

**Table 3.5. (Continued)** The heating plans investigated in the synthesis of AlON.

Sample	Experimental Procedures
D028A	2h at 1500°C in 100% N <sub>2</sub> (St)
D029A	1.25h at 1100°C + 2h at 1500°C in 71% NH <sub>3</sub> + 4% C <sub>3</sub> H <sub>8</sub> + 25% N <sub>2</sub> (4rpm)
D030A	1.25h at 1100°C + 2h at 1500°C in 96% NH <sub>3</sub> + 4% C <sub>3</sub> H <sub>8</sub> (1rpm)

**Table 3.6.** The heating plans investigated in the synthesis of MgAlON

Sample	Experimental Procedures
D001M	1h at 1500°C in 100% N <sub>2</sub>
D002M	1.5h at 1500°C in 100% N <sub>2</sub>
D003M	1h at 1400°C in 100% N <sub>2</sub>
D004M	1.5h at 1400°C in 100% N <sub>2</sub>
D005M	1h at 1450°C in 100% N <sub>2</sub>
D006M	1.5h at 1450°C in 100% N <sub>2</sub>
D007M	1h at 1500°C in 100% N <sub>2</sub>
D008M	1h at 1500°C in 100% N <sub>2</sub>
D009M	1h at 1450°C in 100% Ar
D010M	1h at 1450°C in 100% N <sub>2</sub>
D011M	2h at 1500°C in 100% N <sub>2</sub>
D012M	2h at 1500°C in 99% NH <sub>3</sub> + 1% C <sub>3</sub> H <sub>8</sub> (St)
D013M	2h at 1500°C in 99% NH <sub>3</sub> + 1% C <sub>3</sub> H <sub>8</sub> (2rpm)
D014M	1h at 1100°C + 1h at 1500°C in 99% NH <sub>3</sub> + 1% C <sub>3</sub> H <sub>8</sub> (St)
D015M	1h at 1100°C + 1h at 1500°C in 99% NH <sub>3</sub> + 1% C <sub>3</sub> H <sub>8</sub> (2rpm)
D016M	2h at 1500°C in NH <sub>3</sub> (2rpm)
D017M	2h at 1500°C in NH <sub>3</sub> (St)

**Table 3.6. (Continued)** The heating plans investigated in the synthesis of MgAlON.

Sample	Experimental Procedures
D018M	2h at 1500°C 100% N <sub>2</sub> (2rpm)
D019M	2h at 1500°C in % N <sub>2</sub> (St)

### 3.3. Characterization methods

Following synthesizing process each product i.e., obtained powder was characterized with XRD, SEM and FESEM to determine the phases exist. Particle size distribution has also been used for some results that were thought to be good in matters of morphology. In what follows, the characterization techniques are described, and the equipment used are also given:



**Figure 3.12.** Rigaku D/MAX/2200-PC device used in the characterization of powders

### 3.3.1. X-ray diffraction (XRD)

XRD was used to determine the obtained phases via detecting the atomic and molecular structure of crystalline materials. A Rigaku, model D/Max-2200/PC, Japan, XRD diffractometer was used in all our experiments to determine the existing phases including that of the raw materials used in the synthesis of the different powders studied in this work (Figure 3.12).

The samples were prepared by placing a small amount of the powder on a pre-designed sample holder, then placed into the diffractometer at controlled working level. The collected data were later analyzed using the XRD data analysis software Jade 6.5 with an up-to-date database.

### 3.3.2. Scanning electron microscopy (SEM)

SEM analyses were performed using a JEOL, model 6060 LV, USA, scanning electron microscope to determine the morphology of the synthesized powders, via the detection of the current leaving the object after a focused electron beam that had been placed on a small spot. Prior to observation, the samples were prepared via placing a little amount of powders on the standard sample holder followed by a gold coating to allow transmission. Figure 3.13 illustrates the used SEM device.



**Figure 3.13.** JEOL, model 6060 LV, USA scanning electron microscope used in the characterization.



**Figure 3.14.** FESEM used in the characterization of the synthesized powders.

### **3.3.3. Field emission scanning electron microscope (FESEM)**

Field emission scanning electron microscopy due to its high resolution was used to allow a clearer observation of the synthesized submicron or nano sized powders. This can be attained via the field emission that emits an extremely focused electron beam allowing the improvement of the spatial resolution which provides as a result a clearer observation of the samples. FESEM - FEI Quanta FEG-450 from Japan was used in our experiments on the samples that showed a very fine particle size. The samples were prepared for observation in the same way that the other samples were prepared for SEM observations. An image demonstrating the used FESEM device is given in Figure 3.13.

### **3.3.4. Particle distribution analyses**

Particle size distribution is a characterization technique that is used to determine the variety in size range and the homogeneity of the synthesized powders. This is performed via allowing a given amount of powder to flow through a size distribution measurement device, which detects and records the size range of powders followed by

its translation to a graphical representation that summarizes the size distribution of the characterized powders.

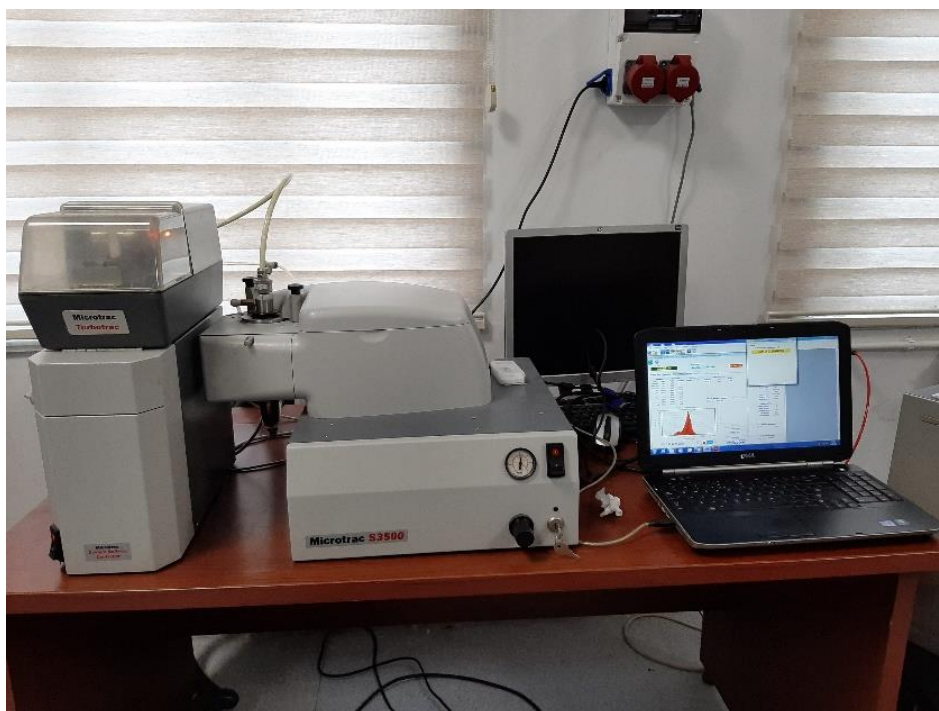


**Figure 3.15.** MICROTRAC S3500 size characterization device used in the determination of the size distribution.

MICROTRAC S3500 size characterization device was used in our experiments (Figure 3.14). The sample did not undergo a special preparation procedure. The powder to be characterized was placed in a sufficient amount inside the device then allowed to flow inside the apparatus.



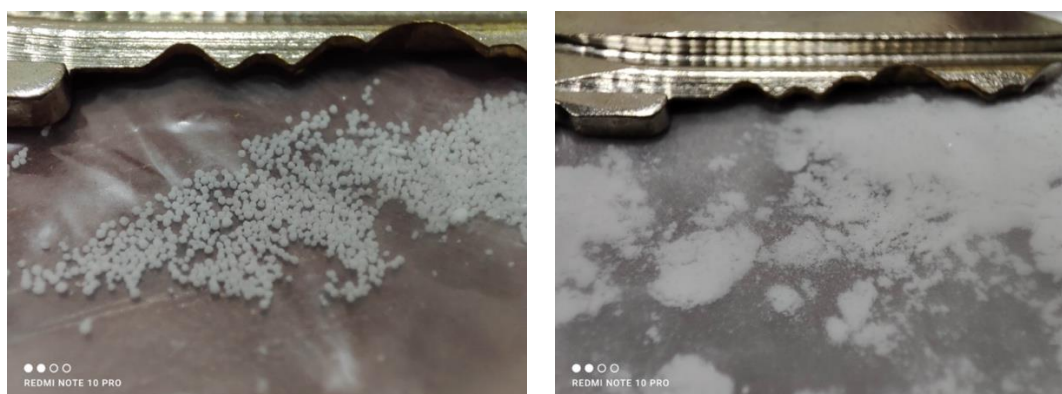
## 4. RESULTS AND DISCUSSIONS

After DTM for powder synthesis, powders remained in granulated form though it was so easy to powder them with light grinding using agate mortar. This is also need for accurate observation as well as the detection of the obtained phases in the XRD analysis.

### 4.1. Characterization Results

#### 4.1.1. Magnesium aluminate spinel

The obtained powder after the synthesis of MAS had no major difference than that charged into the reactor. Apart from the case powder synthesis in which alumina balls were used, the granules kept their form with no shrinkage nor agglomeration observed. In matters of color, the obtained powders were characterized by a white color similar to their initial one. When the powders were grinded using an agate mortar, the granules were easily crashed by hand into powders and no need for extensive force.



(a)

(b)

**Figure 4.1.** A photograph showing the obtained powder after the synthesis (a) using alumina balls and (b) without balls.

In the case of using alumina balls in DTM, however, the granules were crashed into a powder form a spherical shape with some deposition above the balls. Figures 4.1

illustrate the obtained powder in both cases where alumina balls were used (a) and that obtained without balls (a).

#### 4.1.1.1. Results of XRD analyses

A series of three experiments (D001S, D002S and D003S in Table 3.4) was performed first that focusing on the synthesis of MAS ( $\text{MgAl}_2\text{O}_4$ ) to verify the efficiency of the recipe adapted from the thermodynamic simulation obtained from FactSage 7.0. The obtained XRD results are given in Figure 4.2.

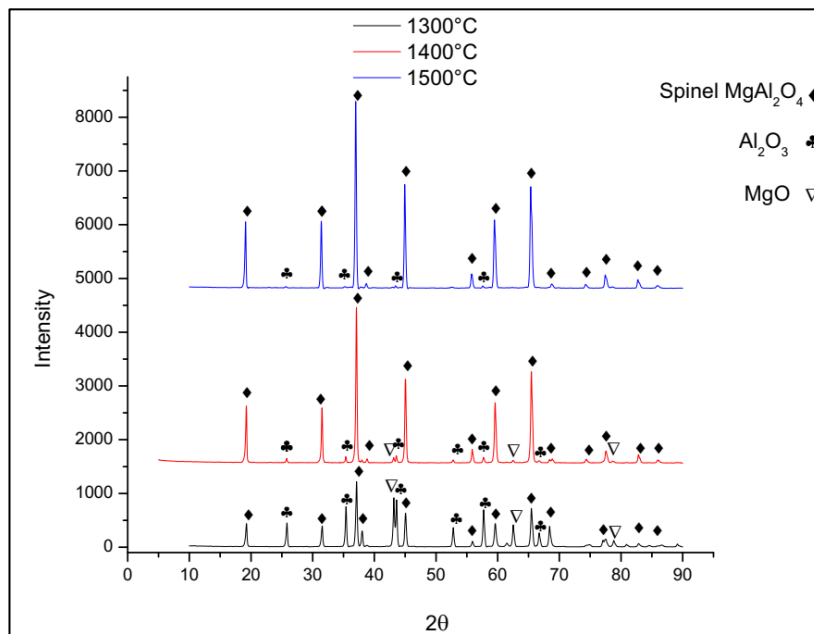


**Figure 4.2.** XRD patterns of powders synthesized for 1h at 1300°C, 1400°C and 1500°C.

As seen from the XRD results (Figure 4.2), at a temperature of 1300°C, peaks corresponding to spinel powders were recorded along with a considerable amount of  $\text{Al}_2\text{O}_3$  and  $\text{MgO}$ . This shows that reaction was incomplete in such temperature for a given time for synthesizing spinel phase. Prior to the transformation to spinel powders, aluminum and magnesium hydroxides give a mixture of alumina and magnesia from which  $\text{MgAl}_2\text{O}_4$  is synthesized subsequently. Therefore, insufficiency of both temperature and holding time results in an unreacted phase of both  $\text{Al}_2\text{O}_3$  and  $\text{MgO}$  at the end of the process.

Raising the temperature of the reaction to 1400°C peak intensity for  $\text{MgAl}_2\text{O}_4$  rises significantly becoming a major phase though unreacted alumina and magnesia still remains (Figure 4.2). In addition, the intensity of peaks was higher and sharper

comparing to that of powders obtained at 1300°C, which can be explained with a higher crystallinity. It is known that a higher temperature serves in providing a thermodynamic activation to the reaction. Consequently, more Al<sub>2</sub>O<sub>3</sub> and MgO were consumed in the synthesis of MAS.

Further increasing in temperature at 1500°C, it was almost completion occurred i.e., the product was almost MAS however there still remain very little of alumina phase. This was obvious that the temperature was well enough however holding time may be extended for full conversion. That was achieved after 1.5 h holding at 1500°C as seen in Figure 4.3.

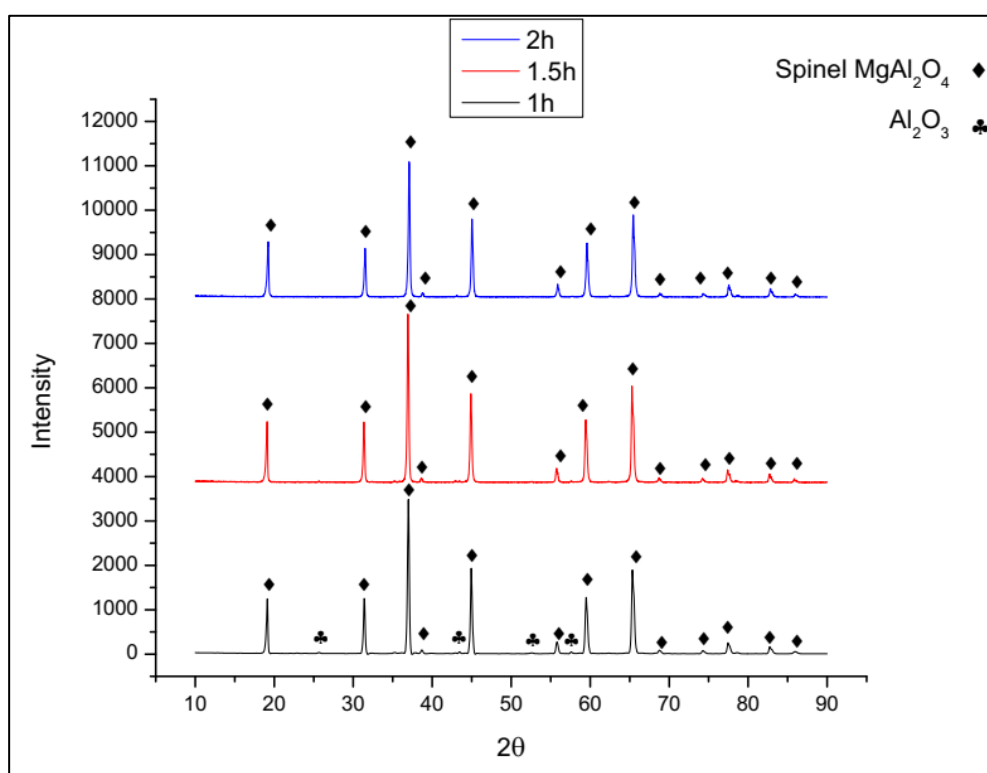


**Figure 4.3.** XRD patterns of spinel powder synthesized at 1500°C for 1h 1,5h and 2h.

In the case of the sample maintained for 1.5h at 1500°C, only peaks corresponding to MgAl<sub>2</sub>O<sub>4</sub> were recorded. This is explained with a complete transformation of the reactants to MAS after the extension of the holding time allowing the reactants to be fully consumed the reaction to be accomplished. This results in a full transformation to spinel phase. An extension of the holding time to 2h did not provide a major difference in matters of purity with similar pattern to that of 1.5h holding observed. A reenactment of the synthesis experiment at 1500°C for 1.5h was performed to verify our choice of those parameters as the optimum. A full conversion was achieved again

making 1.5h at 1500°C the optimum parameters for the static synthesis of magnesium aluminate spinel.

In matters of purity, MAUD program was used to verify the phase composition of the resulting powders from the obtained XRD result. This is accomplished via a refinement of the obtained XRD pattern followed by countifying the peaks associated to each phase to provide an idea about the purity of the synthesized powder. An example of the refinement of phases using MAUD is given in Figure 4.4. The amount of the present phases is provided in the window at bottom left.

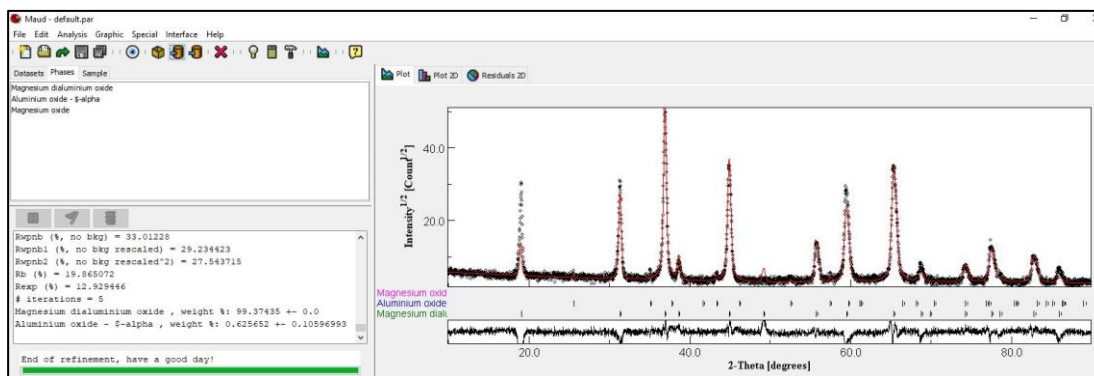


**Figure 4.4.** A computer screenshot of MAUD program used to countify the proportion of phases in the synthesis of magnesium aluminate.

As seen in Figure 4.4 (corresponding to best obtained result at 1500°C for 1.5h) about 99.4% magnesium aluminate spinel was obtained with an impurity proportion in matters of alfa alumina of around 0.6%. As explained earlier, in order to obtain spinel powder suitable for the synthesis of highly transparent optical ceramics, a high purity powder must be fabricated making the powder obtained via static synthesis of aluminum and magnesium hydroxide not suitable. Instead, it can be used to fabricate refractory ceramic.

The next series of experiments incorporated the investigation of the dynamic system in the synthesis of spinel powders from Al and Mg hydroxides mixture. The performed experiments included dynamic synthesis of the reactant at 2 and 4 rpm and then the dynamic synthesis of the raw powders in the presence of 10 and 20 balls to powders ratio (B/P) using alumina balls at 2rpm. Figure 4.5 illustrates the obtained XRD results following the dynamic synthesis of MAS at 1500°C for 1.5 h at 2 rpm without using balls.

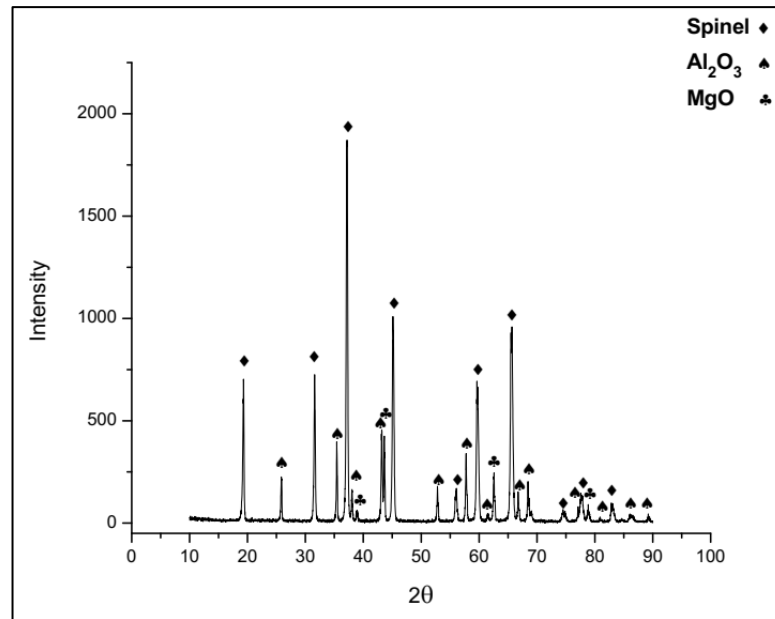


**Figure 4.5.** XRD pattern corresponding to powders synthesized at 1500°C for 1.5h at 2rpm tube rotation (no balls used).

As seen from Figure 4.5, a considerable presence of unreacted Al<sub>2</sub>O<sub>3</sub> and MgO took place. This result is similar to that obtained in the static system at 1300°C for 1h raising many questions regarding the reaction that occurred, and the reasons behind the synthesis failure. Knowing that the only difference between this experiment and the best result obtained in a static system at 1500°C for 1.5h, is the rotation of the alumina tube, the incomplete reaction can be explained with the shrinkage of some granules. This results in the separation of the raw powders whose insufficient contact prevents the completion of the reaction. As the temperature rises aluminum and magnesium hydroxides transform to alumina and magnesia, respectively.

In another attempt to investigate the effect of the dynamic system in the synthesis of spinel powders, we increased the tube rotation speed to 4 rpm while maintaining all the other parameters as those deemed as the optimum in the static synthesis. A considerable decrease in the amount of the unreacted alumina and magnesia took place. MAUD refinement revealed a 98.7% purity spinel. This could be considered as a good result. However, the ability of the static system to deliver a higher purity of spinel powders is an argument against the dynamic synthesis of spinel powders.

In a different approach, alumina balls were introduced into the system, mainly to verify their effect in reducing the powder size during the synthesis. Initially, balls to powder ratio (B/P) was chosen as 10, we decreased the temperature of the synthesis to 1400°C instead of 1500°C to avoid a deposition of the alumina powders on the balls whereas

the other parameters were maintained similar to the initial dynamic synthesis experiment (i.e., 1.5 h holding time at 2 rpm tube rotation). The obtained results are given in Figure 4.6 in comparing to the previous result in which no balls were used.

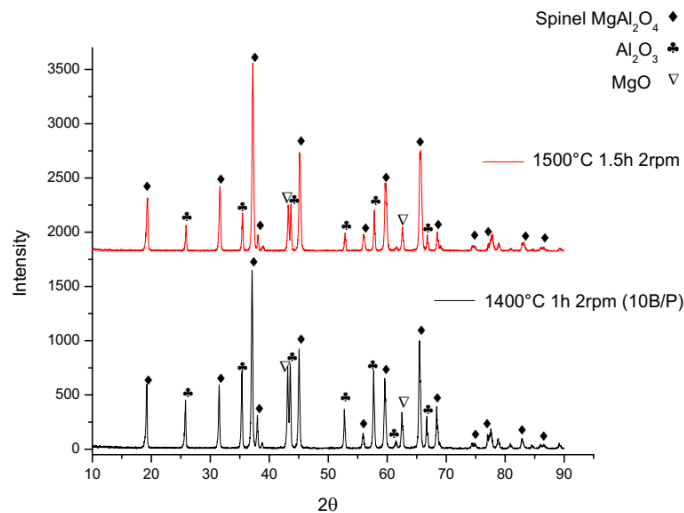


**Figure 4.6.** XRD pattern of powders synthesized at 1400°C for 1.5h in presence of 10B/P using alumina balls comparing to that obtained at 1500°C for 1.5h. Reactor speed in each test was 2 rpm.

It can be seen from the pattern that no significant difference took place. On the contrary, impurities seem to have increased in the test where balls were used. This could be explained with the insufficiency of temperature which does not provide the proper condition for a full synthesis.

Given the fact that the use of balls aims to investigate their effect on the morphology of product powders. In order to obtain a full conversion to magnesium aluminate spinel, another experiment was performed raising the temperature as 1500°C using alumina balls (since a test run at 1400°C failed). The obtained XRD result is given in Figure 4.7.

It can be seen from figure 4.7 that more spinel powder was obtained in comparison to the previous experiment in which alumina balls were used. Nevertheless, this could be associated with the deposition of alumina on the balls as the visual observation revealed their existence as shown in Figure 4.8.

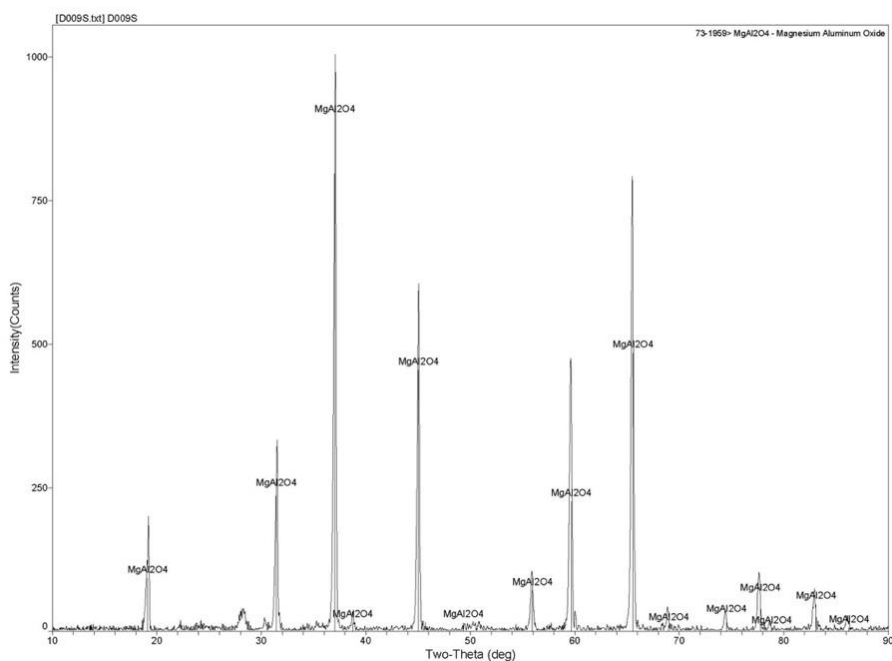


**Figure 4.7.** XRD results of powder synthesized at 1500°C for 1.5h at 2rpm.



**Figure 4.8.** Alumina balls after being used in the synthesis of spinel powder at 1500°C for 1.5h with at 2rpm. (B/P was 20.) Satellite formation clearly visible on the balls indicates alumina deposition.

Further experiments with varying parameters were carried out that yielded similar results. Therefore, it was concluded that the dynamic thermochemical method is not suitable for the synthesizing of spinel powders.

#### 4.1.1.2. Scanning electron microscopy results

As explained earlier, the SEM and FESEM analyses has the purpose of observing the synthesized powders' morphology. SEM micrographs of spinel powders obtained statically at 1500°C for 1.5h and 2h are given in Figure 4.9 and Figure 4.10, respectively.

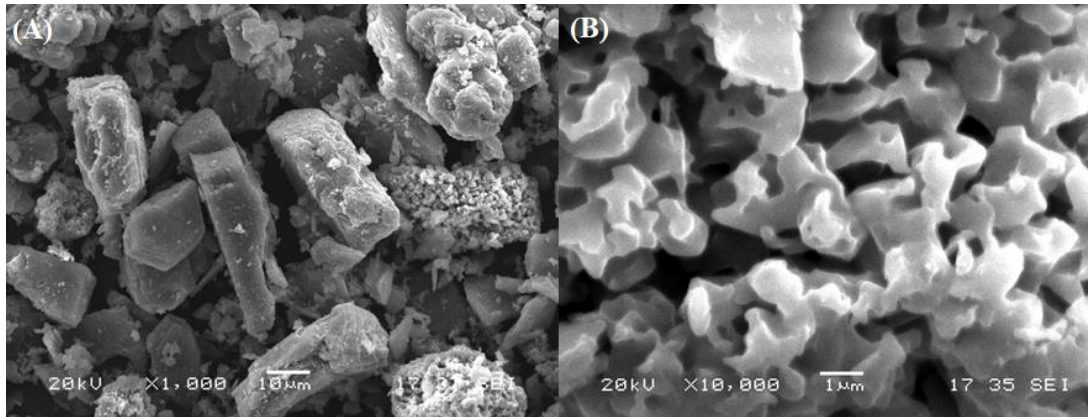


**Figure 4.9.** SEM micrograph illustrating the powder morphology of spinel powder synthesized at 1500°C for 1.5h.

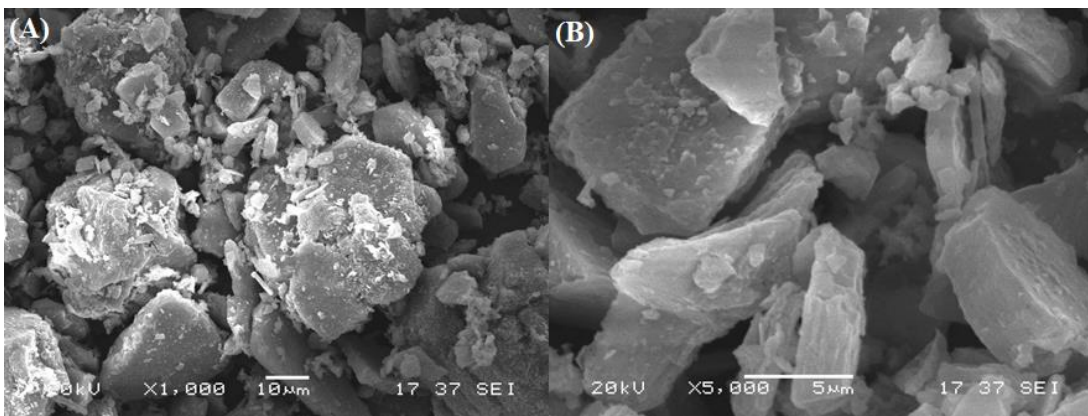


**Figure 4.10.** SEM micrograph illustration the powder morphology of spinel powder synthesized at 1500°C for 2h.

As seen in Figures 4.9 and 4.10, coarse powders with an irregularity of morphology were obtained. In addition, the size difference is considerable given the fact that some particles are in the order of 30 μm whereas others are below 1 μm. This can be attributed to initial powder morphology of the raw powders used in the synthesis. In a static system, the conversion to spinel occurs via an initial dehydration of powders to form both transition alumina phase and magnesia followed with reaction between the two oxides to form magnesium aluminate. Given the fact that both powders are in a granulated form the reaction is allowed to proceed without shrinkage of the granules

which explains their conservation of form after the synthesis. At the end of the reaction, and after a soft grinding by hand of the granules, spinel powders were obtained almost similar morphology compared to the initial raw materials.

In the magnified micrograph of Figure 4.9 (b), spinel particles are formed of smaller crystallites which is in accordance with previous results. In such powders synthesized from hydroxide are found to be particles on the order of micron size contains submicron satellite particles [126]. Attempts to reduce the powder size via separation of the crystallites were carried out in previous research and were deemed unsuccessful. Similarly, in this work, the powder products were grinded to separate particles, however no obvious size reduction achieved i.e., the morphology was exactly similar to that before grinding. Figures 4.11 illustrate the morphologies of powders synthesized dynamically at 1500°C for 1.5h at 2 rpm.

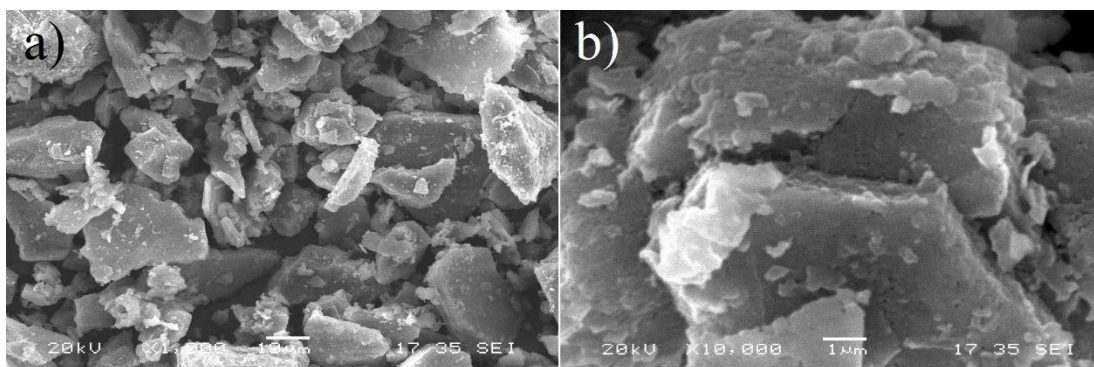


**Figure 4.11.** SEM micrograph of spinel powder synthesized at 1500°C for 1.5h at 2rpm. Figure “b” is the enlargement of image “a”.

It can be seen in the SEM results of Figures 4.11 that the powder morphology is relatively similar to that of Figure 4.9 where powders were synthesized following the same test parameters except rotation was not used. Therefore, it can be concluded that the DTM process does not help improve the powder morphology in the case of spinel powders.

This is added to its inability to provide pure spinel powders preventing the consideration of a positive effect of the dynamic synthesis under the above-mentioned parameters for spinel. It is possible to assume that the rotation of the tube in the case of spinel results in a decomposition of the granules preventing them from reacting, and thus, causing them to convert to MgO and alumina separately.

In the case of 10B/P, a significant change in morphology took place with submicron crystallites obtained at 1400°C. However, and similar to the previous results in the case of dynamic synthesis of spinel in no presence of alumina balls, the absence of a pure MAS phase does not allow the claim of a positive effect of the tube rotation on the conversion to magnesium aluminate spinel. No considerable amount of powders were obtained due to their deposition on the balls when 20B/P was used. Therefore, the characterization processes of the product obtained as a result of this test could not be performed.

When the rotation speed was raised to 4rpm, a deposition of powders on the alumina balls was visible (as shown in Figure 4.8). It is believed that this deposition originated from the alumina particles present in the powders. Given the nature of the rotating system, these particles exchange atoms via a diffusion mechanism at 1500°C, giving rise to the shape observed in Figure 4.8.

#### **4.1.2. Aluminum oxynitride**

Prior to AlON synthesis, an investigation of the efficacy of the dynamic system in the gas synthesis of aluminum nitride was carried out first, then compared with the static gas synthesis. Thus, the obtained results will be discussed first.

##### **4.1.2.1. XRD analyses results**

###### **AlN Synthesis**

Due to the crucial role that AlN plays in the attempt to obtain AlON, the synthesis of the former was studied as to understand the effect of the tube rotation on the gas synthesis of aluminum nitride. Initially, a static synthesis experiment was carried out under ammonia with 4% propene at 1450°C. The obtained XRD result is given in Figure 4.12.

As seen in Figure 4.12, pure AlN phase could be obtained without any existence of contaminants. This result is in accordance with the results reported in the literature [92-95].

To compare this result with that of dynamic synthesis, a reenactment of the synthesis under the same parameters took place with the difference of introducing a 2rpm tube rotation. The obtained XRD result (given in Figure 4.13) revealed an incomplete

reaction unlike the static synthesis in which pure AlN phase was obtained. Instead, a conversion to  $\alpha$ -Al<sub>2</sub>O<sub>3</sub> took place with an appearance of AlON peaks.

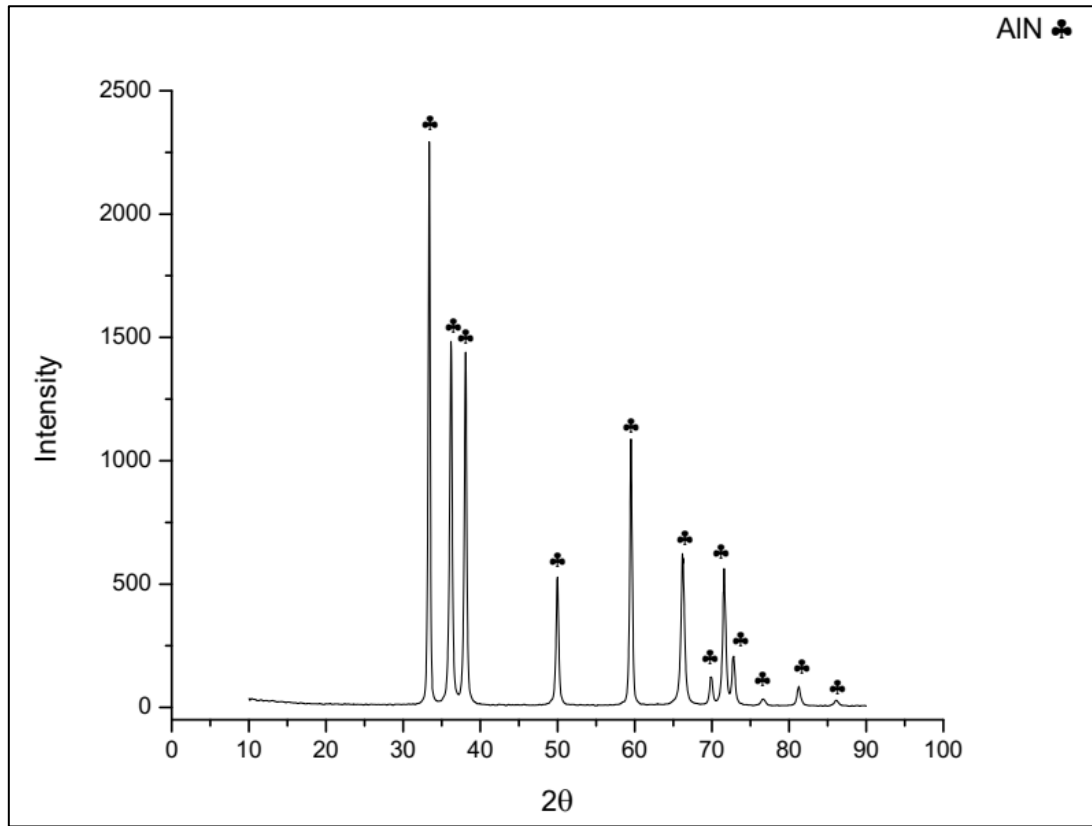


**Figure 4.12.** XRD pattern of AlN powders synthesized via gas reduction nitridation at 1450°C for 1h.

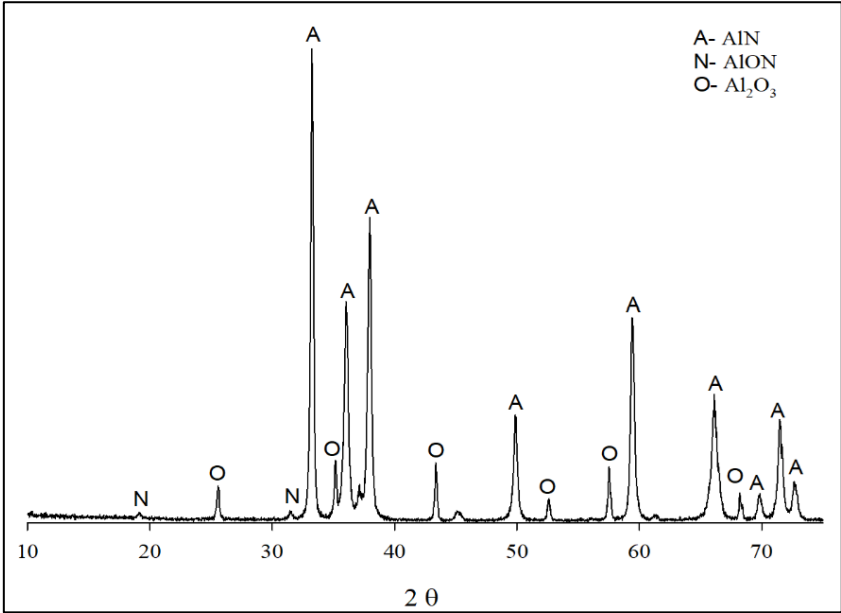
AlON is known to be synthesized from a mixture of  $\gamma$ -Al<sub>2</sub>O<sub>3</sub> and AlN [17,19-20,33-34,100,106] with  $\gamma$ -Al<sub>2</sub>O<sub>3</sub> as an intermediate phase from which aluminum nitride is obtained [97].

Other investigations have shown that a mixture of  $\gamma$ -Al<sub>2</sub>O<sub>3</sub> and AlN take place below 1200°C in the gas synthesis of aluminum nitride [93,97]. Thus, we assumed that an early nitridation taking place in the dynamic system which prevents a full conversion to AlN. This explains the obtained result in matters of  $\alpha$ -Al<sub>2</sub>O<sub>3</sub> and AlN mixture with AlON traces [17].

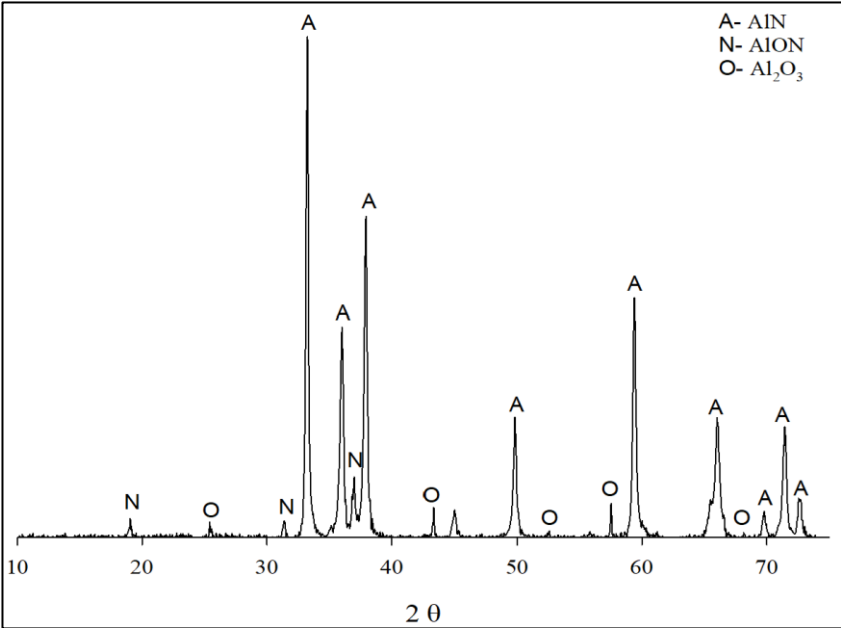
Aiming to verify our assumptions, an investigation of the dynamic synthesis of AlN was carried out under different parameters in which the reaction temperature, holding time and kiln rotation were all taken a step further.

Figure 4.14 illustrates the XRD results of powders maintained for 2h at 1500°C and 4rpm tube rotation. As seen in Figure 4.14, AlON peaks are higher in comparison with

those of Figure 4.16, whereas both AlN and Al<sub>2</sub>O<sub>3</sub> peaks are lower. The difference is clearly seen in Al<sub>2</sub>O<sub>3</sub> peaks while AlN can be said to be relatively lower.



**Figure 4.13.** XRD pattern of powders synthesized at 1450°C for 1h at 2rpm.



**Figure 4.14.** XRD patterns of powders synthesized at 1500°C for 2h at 4rpm.

Consequently, it can be said that the DTM process promotes the synthesis of aluminum oxynitride rather than AlN due to an early nitridation occurring at a lower temperature than that of synthesis.

Further experiments were conducted to investigate whether higher AION peaks could be obtained in a single step synthesis via varying different parameters. However, the highest peaks were those obtained in Figure 4.14.

### Aluminum oxynitride synthesis results

As explained previously, AION synthesis has been observed not to be possible in the DTM process via a single step synthesis. Hence, an investigation of the two-step synthesis reported to be the ideal process to fabricate AION. In our system however, a continuous heating was chosen rather than the conventional two-step synthesis reported in the literature in which the calcinated powders are cooled to room temperature then heated again to the predetermined synthesis temperature. Figure 4.15 illustrates XRD patterns of powders obtained via two-steps synthesis.

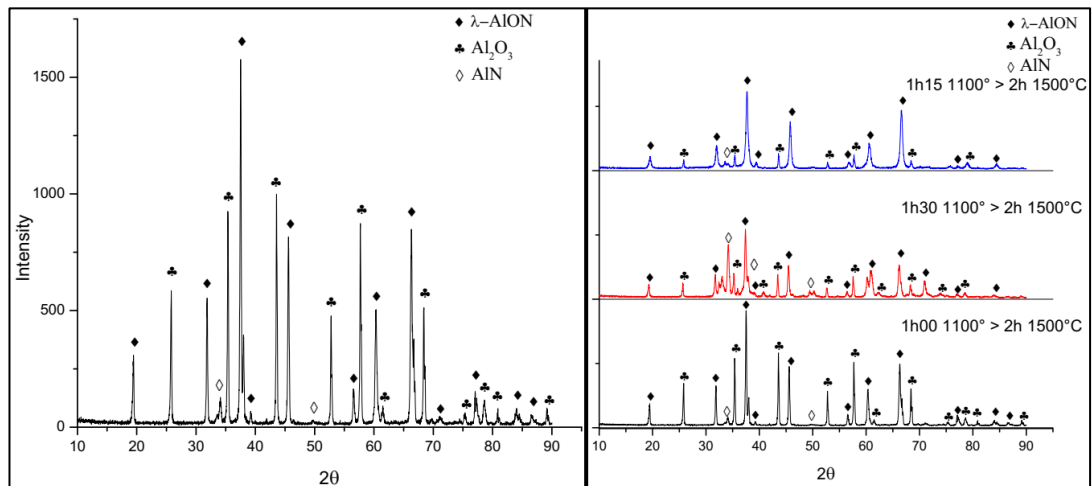


**Figure 4.15.** XRD pattern for two-steps synthesis performed at 1100°C followed by continuous heating and holding at 1500°C with varying holding time of the first step.

It can be seen that in the case of an intermediate holding for 1h at 1100°C given in Figure 4.15 (the left pattern),  $\gamma$ -AION is present as the dominant phase which confirms the efficacy of the DTM system in promoting the synthesis of the oxynitride of aluminum over AlN.

The mechanism following which AION is formed varies from solid-solid (SS) to solid-gas (SG) and gas (G) reaction depending on the existing parameters in the system (temperature and partial pressures) [17]. The model presented by Xie et al. from the last reference, who studied the stability regions of AION according to different reactions, explains that AlN layers containing cracks forms on alumina during the

nitridation phase. In the contact region, an exchange of atoms takes place resulting in an oxynitride phase which keeps growing provided that  $\text{Al}_2\text{O}_3$  and  $\text{AlN}$  are in existence. However, if  $\text{AlN}$  runs out, an oxide phase in form of  $\alpha\text{-Al}_2\text{O}_3$  remains within the aluminum oxynitride phase, making its possibilities of elimination very low. Figure 4.16 illustrates the forming mechanism of AION.

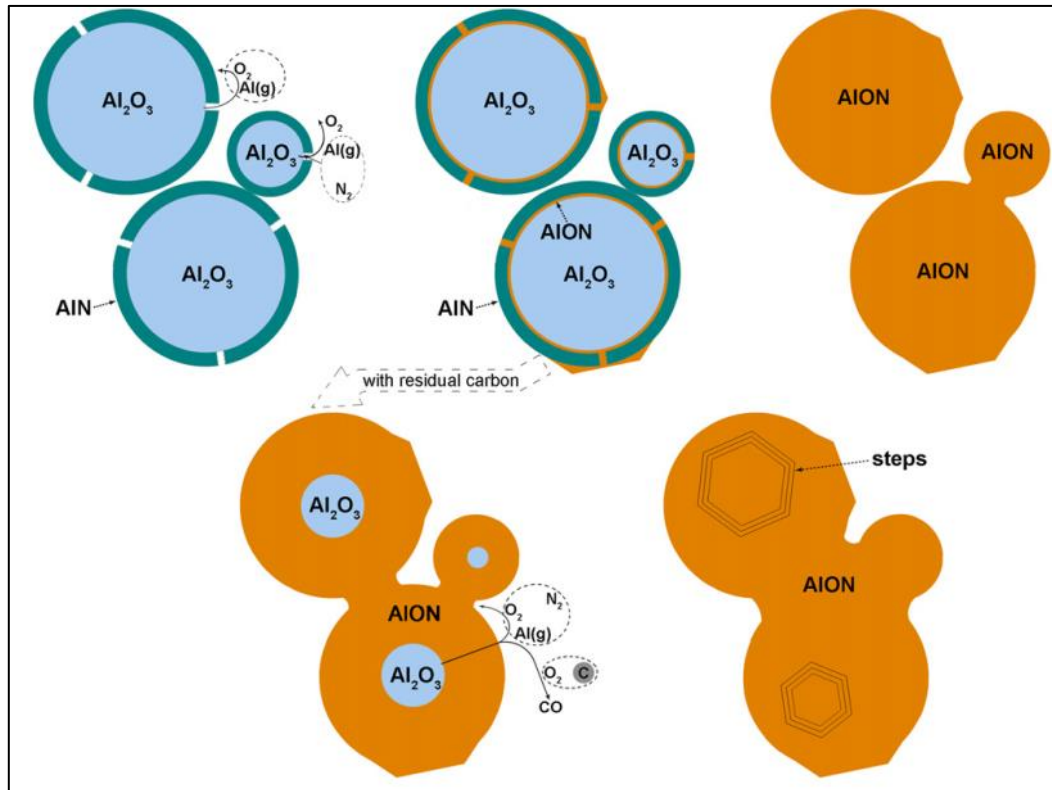


**Figure 4.16.** AION forming mechanism as given by Xie et al. [17]

In our study, there exist multiple suggestion to explain the fact that the performed experiments, have not given a full conversion to AION. For a starter, it is believed that the  $\text{AlN}$  phase forming over the oxide was not enough to allow the obtention of a pure oxynitride phase. Moreover, due to the narrow stability region of aluminum oxynitride, it is more likely to be the temperature not being enough to maintain AION stable. This suggestion is supported with the fact that  $\text{AlN}$  polytypoids in form of  $\text{Al}_8\text{O}_3\text{N}_6$ ,  $\text{Al}_9\text{O}_3\text{N}_7$ ,  $\text{Al}_{10}\text{O}_3\text{N}_8$ ...etc. were present in the XRD patterns of Figure 4.15 (the uncategorized peaks at 1.5 h and 1.15). Another possibility is the dynamic nature of the system in which a possible shrinkage of granules may take place. This shrinkage causes a separation of the oxide and nitride phases, and when this occurs, a conversion to aluminum oxynitride is less likely to happen. Thus, aluminum nitride and alumina are obtained separately.

In a different series of experiments, the holding time of the intermediate phase was maintained stable (1.25h corresponding to the optimum result obtained in the previous series of experiments) while the second holding duration and gas mixtures were changed. The parameters used in the synthesis process are summarized in Table 4.1 with the changing parameters in bold.

**Table 4.1.** Heating plans of experiments with varying parameters comparing to that of the optimum result.

Experiments	Parameters
1	1.25h at 1100°C then 2h at 1500°C in 96% NH <sub>3</sub> + 4% C <sub>3</sub> H <sub>8</sub>
2	1.25h at 1100°C then 4h at 1500°C in 96% NH <sub>3</sub> + 4% C <sub>3</sub> H <sub>8</sub>
3	1.25h at 1100°C then 2h at 1500°C in 100% NH <sub>3</sub>

In the case of the optimum obtained result (Experiment 1 in Table 4.1) the heating plan comprised a first holding at 1100°C for 1.25h followed by a second holding at 1500°C for 2h in flowing mixture of ammonia and propene. Nitrogen gas was used up to 700°C due to its reported positive effect of eliminate oxygen in the heating phase [93,95].

Experiments listed in Table 4.1, different parameters were used to observe their effect on the synthesis of AlON via DTM. In the first one the use of gas mixture was extended until the end of the second holding, whereas in the second one, the holding time was extended to 4h instead of 2h. The third experiment is similar to the first one with the difference of not using propene during the second holding. The obtained XRD results are given in Figure 4.17.

It can be seen in Figure 4.17 that the 1<sup>st</sup> pattern corresponding to the first experiment in Table 4.1, aluminum nitride synthesis was favored. This is believed to be due the fact that the gas mixture atmosphere promotes the synthesis of AlN as a result of the reducing effect of propene. That is propene enhanced a full conversion of the existing oxide preventing the existence of AlN/Al<sub>2</sub>O<sub>3</sub> mixture which is essential for the formation of aluminum oxynitride. This is supported with the result shown in the 3<sup>rd</sup> pattern corresponding to the third experiment in Table 4.1 in which pure ammonia gas was used.

As seen, a dominant existence of alumina is apparent due to the absence of a reducing effect of propene. This means that the elimination of propane caused a conversion to

alumina with small amount of AlN and less  $\gamma$ -AlON. In the 2<sup>nd</sup> pattern in Figure 4.17, which corresponds to a 4h holding time at 1500°C,  $\alpha$ -Al<sub>2</sub>O<sub>3</sub> appeared again as a dominant phase, suggesting that a conversion to corundum ( $\alpha$ -Al<sub>2</sub>O<sub>3</sub>) took place prior to the second step. Being a stable phase, it is less likely for  $\alpha$ -Al<sub>2</sub>O<sub>3</sub> to lose oxygen in order to form a nitride phase, and thus, less amount of both aluminum nitride and oxynitride formed. On the other hand, aluminum oxynitride has been reported to be thermodynamically unstable under 1640°C causing its quick decomposition if formed below that temperature, especially in the case of an extended holding time below its stability region [21]. However, this is less likely the case in the second experiment of Table 4.1, as a decomposition of the oxynitride means the existent of its reactants in matters of alumina and aluminum nitride.

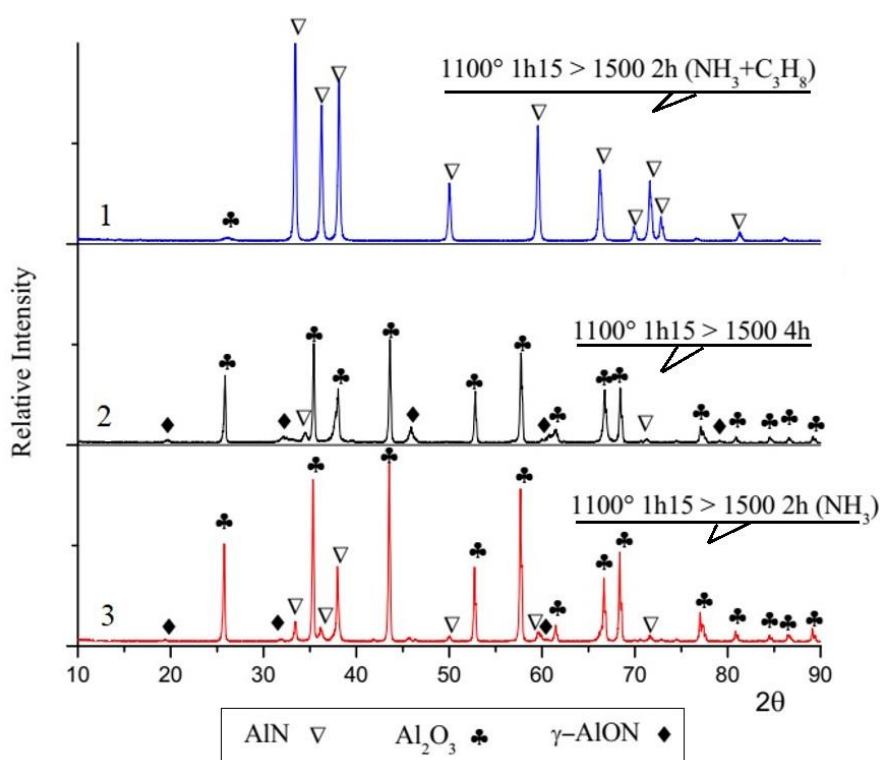


**Figure 4.17.** XRD patterns of powder obtained with a two steps synthesis at 1100°C for 1.25h followed by a second holding at 1500°C under different conditions.

The instability of AlON below 1640°C has been observed however, in different experiments. Figure 4.18 illustrates the XRD pattern of powders obtained via a two-steps synthesis under similar conditions as that of the optimum result (an intermediate holding at 1100°C for 1.25h under 1 l/m flow of ammonia and propene followed with a 2h holding at 1500°C).

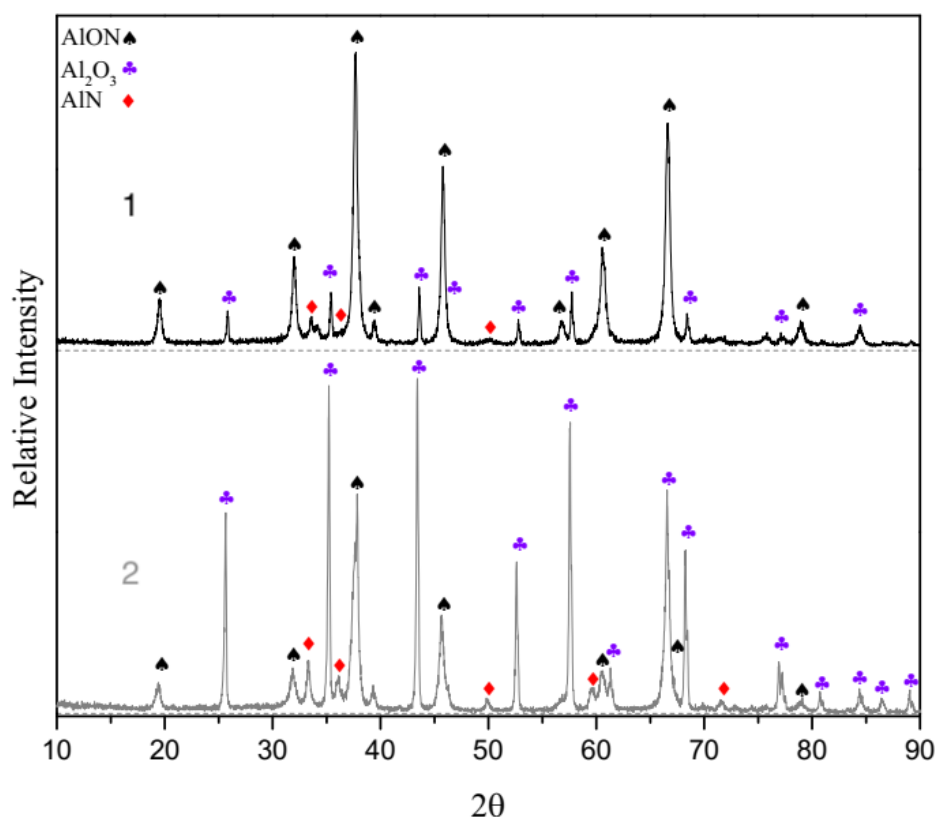


**Figure 4.18.** Powders synthesized under the same conditions (two-steps continuous heating at 1100 °C for 1.25h then 2h at 1500 °C).

It can be observed that despite being obtained under the exact same parameters, AION peaks in the second pattern (grey) are lower than that of the first (black) in which alumina was not the dominant phase unlike the result of the second experiment where alumina was dominant. This can be explained with the thermodynamic study of Willems et al. [21] who explained that although an AION phase is possible to be obtained at 1500°C under limited conditions, the phase is less likely to be stable and decomposes to aluminum nitride and alumina upon cooling. Similar results to that of Figure 4.18 have been observed repeatedly in the different experiments which had been performed where despite the reenactment of the experiments under the exact same conditions, different results of AION peaks were recorded with the one previously given in Figure 4.18 being the optimum to be ever achieved.

Aiming to investigate the effect of gas mixture on the synthesis and whether varying gas proportions would promote an optimization of the synthesis, other experiments were performed in which different gas mixtures were used. Figure 4.19 illustrates XRD results of powders synthesized via the two-holding method (1.25h at 1100°C then continued 2h at 1500°C) under different gas mixture proportions.

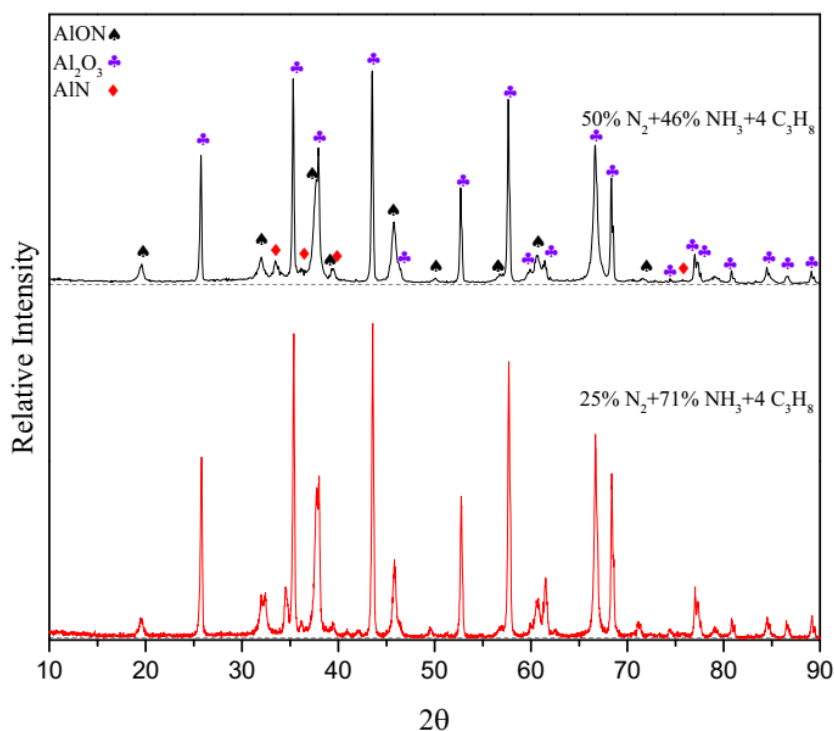


**Figure 4.19.** XRD patterns of powders synthesized at 1500°C for 2 h, after holding at 1100 °C for 1.25h under different atmospheres.

It can be observed from the patterns that the amount of AION was very low, and no optimization of the results took place with the introduction of nitrogen to the gas mixture. It is also seen that both nitrides (AION and AlN) increased with the decreasing N<sub>2</sub> proportion. This can be explained with the better reactivity of NH<sub>3</sub> which is more efficient in nitration than using pure N<sub>2</sub> gas [98].

In a different approach, a mixture of Al(OH)<sub>3</sub> and AlN was prepared. This mixture has been reported to be a good possible starting powder to obtain  $\gamma$ -AION [10]. The used aluminum nitride was synthesized via static synthesis with a 99.9% purity via gas synthesis. The corresponding XRD result is given in Figure 4.20. As seen from the pattern, a very low conversion to AION took place, whereas AlN and  $\alpha$ -Al<sub>2</sub>O<sub>3</sub> were the dominant phases. This can be explained with the insufficient temperature to allow a conversion to AION if compared to the finding of Lysinov et al. [10] who obtained AION at 1850°C using a similar mixture. In our investigation Al(OH)<sub>3</sub> was believed to convert to alumina without any reaction with the existing AlN.

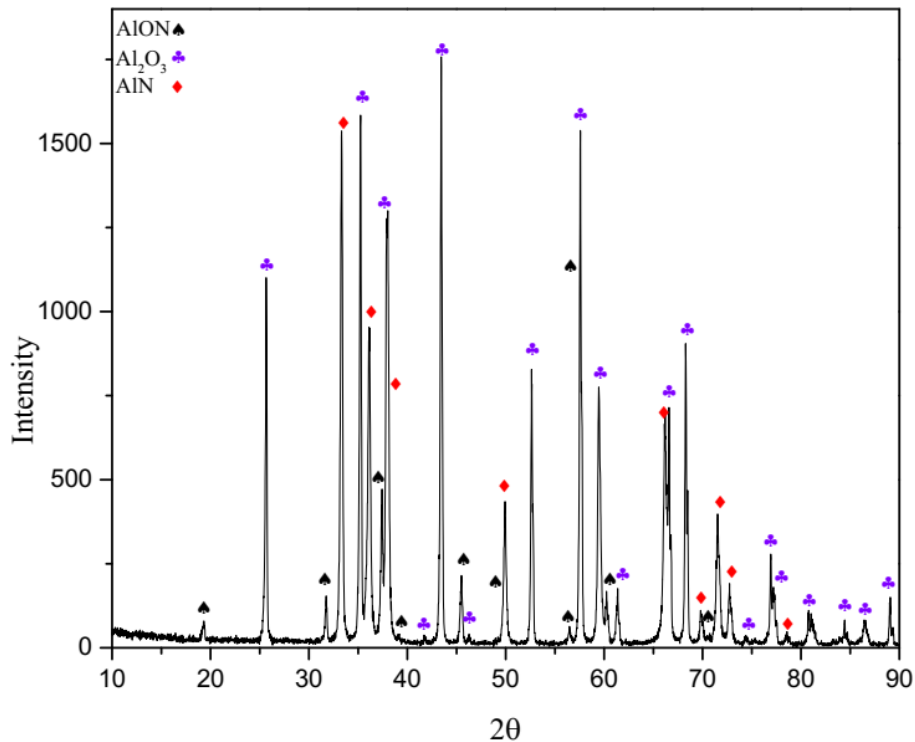


**Figure 4.20.** Powder synthesized from AlN and Al(OH)<sub>3</sub> mixture at 1500 °C for 2h under 1 liter per minute N<sub>2</sub> gas flow.

In order to investigate the effect of the dynamic system on both steps of the synthesis, two experiments were performed under the optimum conditions (experiment 1 in Table 4.1). In the first experiment, the static system was maintained throughout the first stage of heating (25 °C to 1100 °C), followed by a dynamic in the second step. In the second experiment, the opposite was investigated (dynamic from 25 °C to 1100 °C the static between 1100 °C and 1500 °C).

Both experiments were held under a 1 l/m steady flow of NH<sub>3</sub> and C<sub>3</sub>H<sub>8</sub> atmosphere with 96% and 4% proportion, respectively. XRD patterns of the obtained results are given in Figure 4.21.

When the system was dynamic in the first stage then static in the second,  $\alpha$ -Al<sub>2</sub>O<sub>3</sub> was obtained beside a very low amount of AlN and traces of AlON. This is explained with a non-conversion to AlN in the first step due to the absence of the activation provided by the dynamic system, and thus, the powders convert to  $\alpha$ -Al<sub>2</sub>O<sub>3</sub> in absence of an effective reducing/nitriding mixture due to N<sub>2</sub> being supplied in the second step.

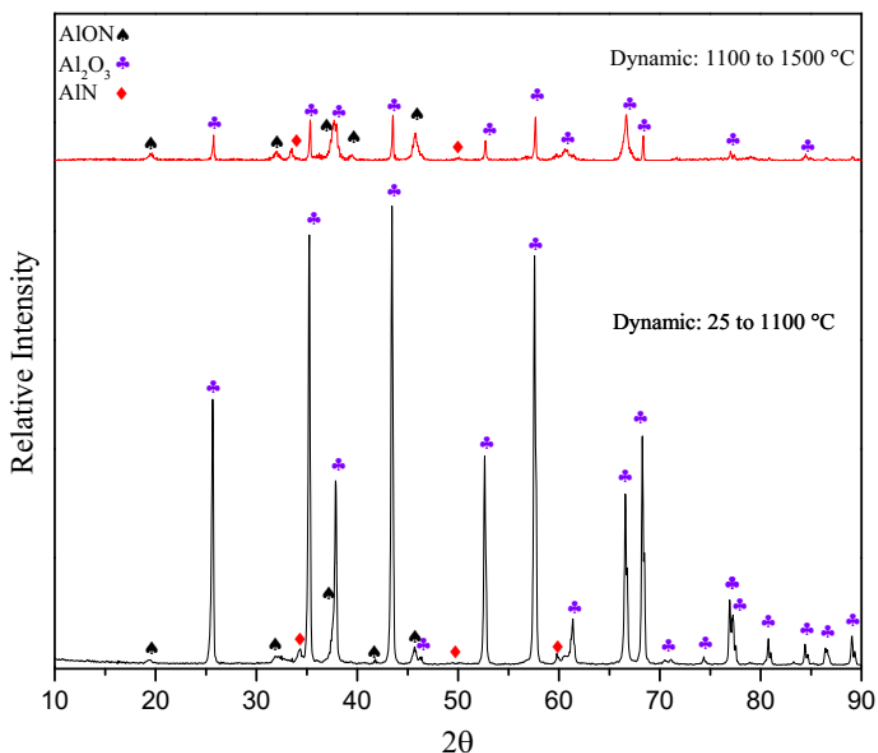


**Figure 4.21.** Powder synthesized at 1500°C for 2h with an intermediate holding at 1100°C for 1.25h under flow of NH<sub>3</sub> + 4% C<sub>3</sub>H<sub>8</sub> gas mixture with different conditions.

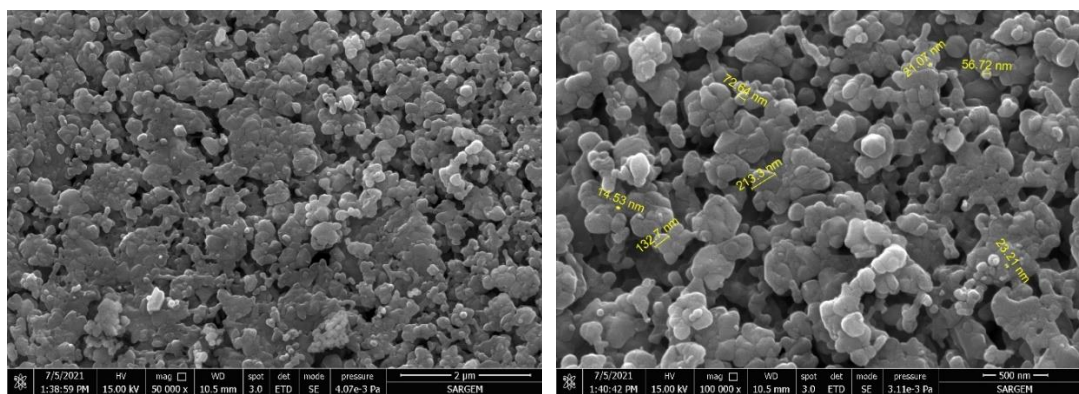
In the opposite case in which the system was first dynamic then static in the second step, less amount of corundum was obtained with low peaks in comparison to the first experiment. It is believed that the absence of AlN coupled with the insufficiency of temperature prevent the formation of AION phase. Comparatively, a full dynamic system provides better condition for the formation of AION at a moderate temperature.

#### 4.1.2.2. Scanning electron microscopy

An initial visual observation of all the synthesized powders revealed fine powders that were thought to be of a nanoscale. SEM analyses were first performed on all samples whereas FESEM was chosen in the case of fine powders that were difficult to observe clearly via SEM. The obtained results are given and discussed in the following sections.

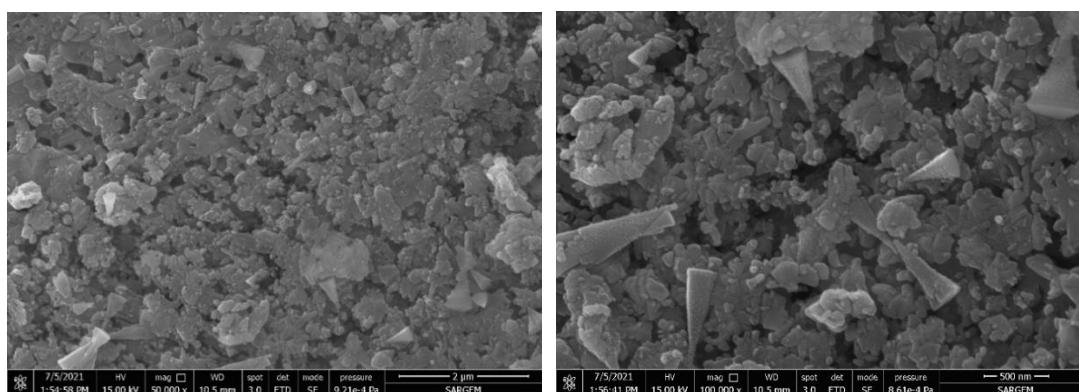
#### Aluminum Nitride:

Figure 4.22 (a) and (b) illustrate FESEM images of powders synthesized at 1450°C for 1h statically and the one obtained in DTM process after 2 rpm rotating speed, respectively.



(a)1

(a)2



(b)1

(b)2

**Figure 4.22.** FESEM images of powders obtained under  $\text{NH}_3 + 4\% \text{C}_3\text{H}_8$  atmosphere at  $1450^\circ\text{C}$  for 1h, statically (a) versus that obtained via DTM at 2rpm (b).

As mentioned earlier, a full conversion of  $\text{Al}(\text{OH})_3$  to  $\text{AlN}$  took place in the static system where the DTM process gave a mixture of  $\text{AlN}$  and  $\text{Al}_2\text{O}_3$  with traces of  $\text{AlON}$ . In Figure 4.22 (a),  $\text{AlN}$  homogeneous nano powders with a relatively spherical shape and an average particle size of 70nm can be observed. This is in accordance with the literature in which gas synthesis has been linked to nano-sized aluminum nitride powders [92-93,96,97]. In contrast, DTM synthesis did not provide similar results as seen in Figure 4.22 (b), where a con-shaped structure, which appears in a closed look as made of much smaller nano particles, emerged. Additionally, an agglomeration of powders seems to have taken place with some blocks of powder unevenly distributed causing an irregularity of morphology. It is believed that both phenomena are results of high surface energy of the nano-powders coupled with the dynamic nature of the DTM process. The con-like structure is thought to have emerged during the rotation of the tube which explains the fact that it is made of much smaller particles whereas the con shape is believed to be the resultant of the irregularity of the surface on which they rotate. That is, when the powders are rotating on each other, smaller particles with

high surface energy tend to for an agglomeration that takes the form of a con while the tube rotates.

For the samples synthesized at 1500°C for 2h at 4rpm, no SEM nor FESEM observation was believed to be necessary due to the similar XRD result to that of the dynamic synthesis at 1450°C for 1h at 2rpm.

#### **Aluminum oxynitride:**

In further experiments investigating the possibility of obtaining AlON via two-steps dynamic synthesis, both SEM and FESEM analyses were performed revealing fine particles of a relatively uniform morphology.

Figure 4.23 A and B illustrates SEM images of powders obtained from Al(OH)<sub>3</sub> via a two-steps synthesis at 1500°C for 2h at 4rpm having an intermediate stage with 1h and 1.5h at 1100°C, respectively. Figure 4.24 gives FESEM observation of the optimum result in AlON investigation obtained at 1500°C for 2h at 4rpm having an intermediate stage at 1100°C for 1.25h.

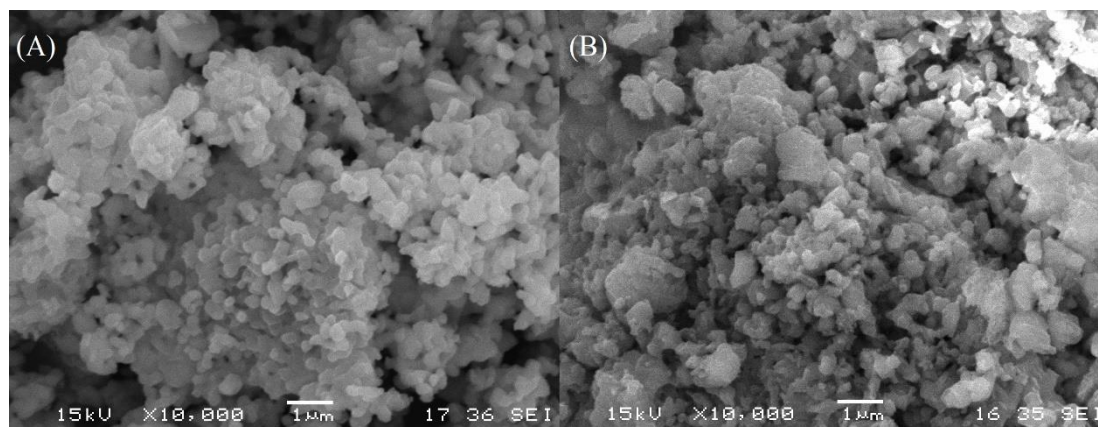


**Figure 4.23.** SEM micrographs illustrating morphologies of powder synthesized at 1500°C for 2h at 4rpm after holding at 1100°C for: A) 1h B) 1.5h.

It can be seen in Figure 4.23 (A) and (B) corresponding to partial synthesis of AlON with alumina and aluminum nitride impurities, that submicron particles are obtained. This is in accordance with our claim that the DTM process promotes the synthesis of submicron particles. In addition, the morphology of the obtained powders is relatively homogeneous with certain agglomeration taking place. This agglomeration can be attributed to the high surface energy that fine particles possess, especially since nano-sized particles are observed, causing certain agglomerates to form.

It is also observed in Figure 4.23 that the con-like structure previously seen in Figure 4.22 (b), disappeared. This is believed to be the result of the calcination performed in the two-steps synthesis in which a mixture of AlN and Al<sub>2</sub>O<sub>3</sub> is allowed to form first at 1100°C then at 1500°C reacts with each other to form AlON. This can be supported by the fact that the cone-like shape has only been observed in the single-step synthesis attempt and none of the two-steps synthesis experiments.

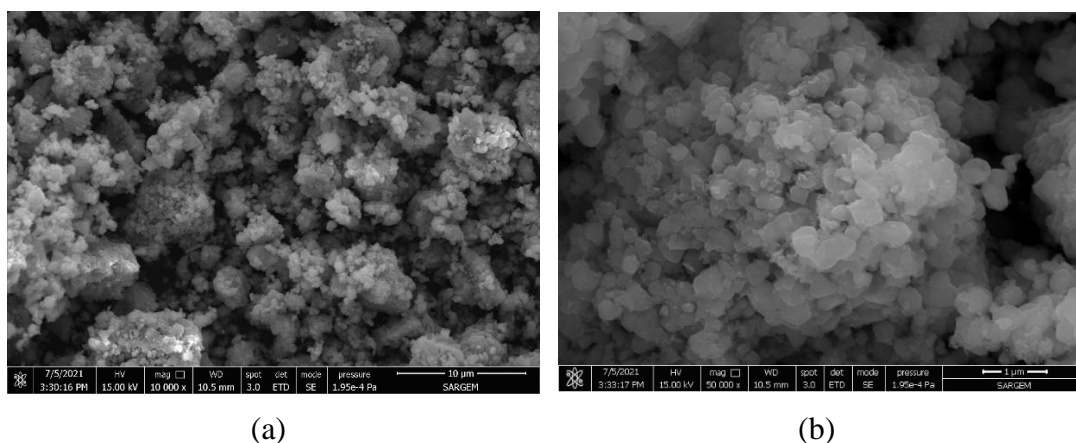


**Figure 4.24.** FESEM micrographs illustrating morphologies of powders synthesized at 1500°C for 2h at 4rpm after holding at 1100°C for 1.25h. Image b is the enlargement of image a.

In Figure 4.24, it can be seen that similar to powders given in Figure 4.23, submicron particles can be clearly seen. Additionally, the powders seem to have uniform spherical morphology with some agglomeration, which can be attributed to the high surface energy of the fine particles, taking place.

In case of further results in which no significant proportion of aluminum oxynitride was obtained, SEM and FESEM analyses were thought to be unnecessary and thus, no further observations were performed as no improvement of the result took place.

### 4.1.3. Magnesium aluminum oxynitride

The emergence of magnesium aluminum oxynitride (MgAlON) phase, which is a magnesium stabilized form of aluminum oxynitride (AlON), occurred as coincidence when a nitriding gas was used in the dynamic synthesis instead of argon. In XRD result, the obtained result revealed a shift of pattern towards the right when compared with that of magnesium aluminate. This shift has been observed in all the XRD results in which a nitriding source was used then disappears in the absence of a nitriding

atmosphere, which was an interesting phenomenon leading to a thorough investigation of the event.

#### 4.1.3.1. XRD analyses results

As mentioned earlier, the event leading to the investigation of a MgAlON was due to a shift taking place in XRD patterns of powders obtained in a nitriding atmosphere. XRD pattern of MgAlON thought to be spinel phase is given in Figure 4.25.

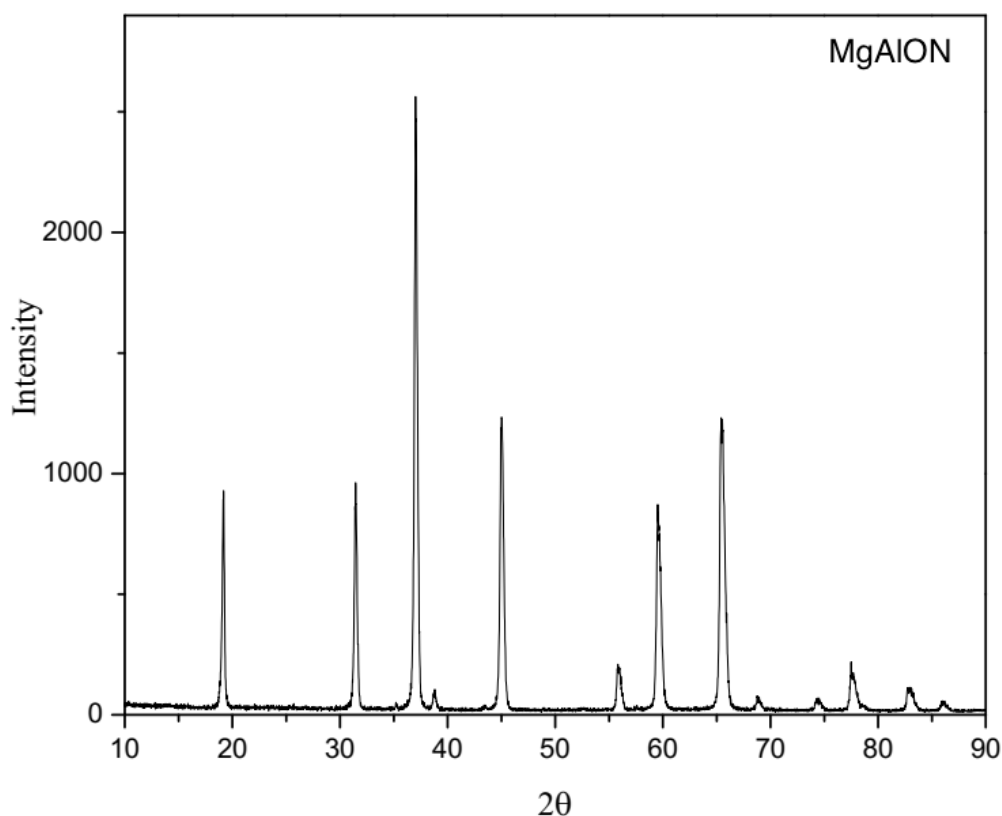


**Figure 4.25.** XRD pattern of powder synthesized at 1500°C for 2h under N<sub>2</sub>

The obtained powder, as shown in the XRD pattern of figure 4.25, was believed to be magnesium aluminate spinel phase. Nevertheless, the reenactment of the investigation under the exact same parameters with the difference of Ar atmosphere instead of nitrogen failed in providing a full conversion with impurities in terms of MgO and Al<sub>2</sub>O<sub>3</sub> existing beside spinel. The experiments were repeated multiple times with the same results which necessitated further investigation to understand the phenomenon, with an assumption of the obtained spinel being something different than MgAl<sub>2</sub>O<sub>4</sub>.

Figure 4.26 demonstrates an XRD pattern of powders synthesized under N<sub>2</sub> atmosphere compared to another obtained in a static system under Ar atmosphere. It

can be seen that a shifting towards higher angles took place when a different gas was used. That is to say that this is a sign of decreasing inter atomic distance in the crystal lattice of the product powders. This shifting has been observed in all the experiments in which the nitriding source was used.

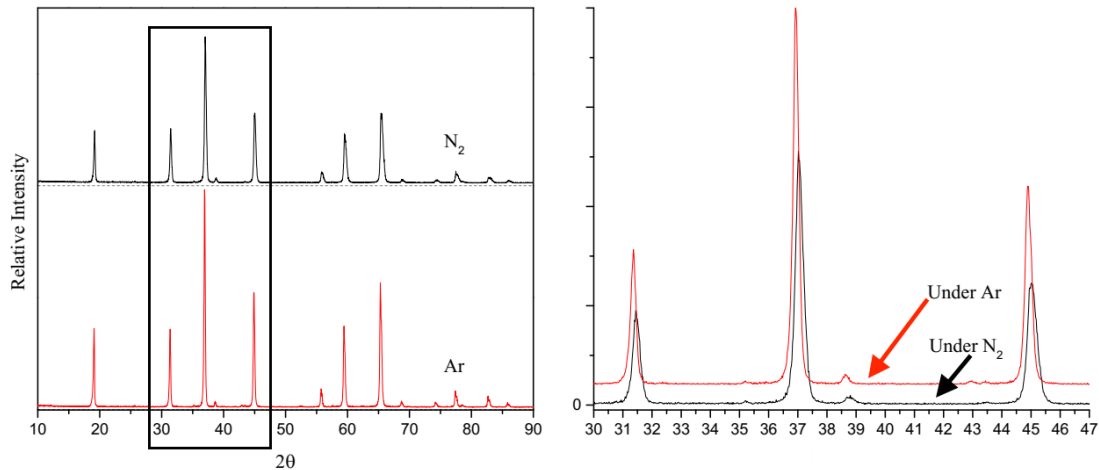


**Figure 4.26.** XRD pattern of powders synthesized dynamically under  $N_2$  atmosphere compared to  $MgAl_2O_4$  obtained in a static system under Ar.

It has been reported that a shifting of the XRD pattern of  $MgAlON$  towards the left in comparison with MAS takes place as  $MgAlON$  has smaller lattice parameter than that  $MgAl_2O_4$  [15,128]. In addition, it has been reported that  $MgAlON$  forms from a reaction of  $MgAl_2O_4$  with  $Al_2O_3$  and  $AlN$  [16]. The MAS that reacts with alumina and aluminum nitride has been reported to be the product of  $MgO$  reaction with alumina. Figure 4.27 illustrates a schematic representation of  $MgAlON$  formation following the model presented by Chen et al. [16]

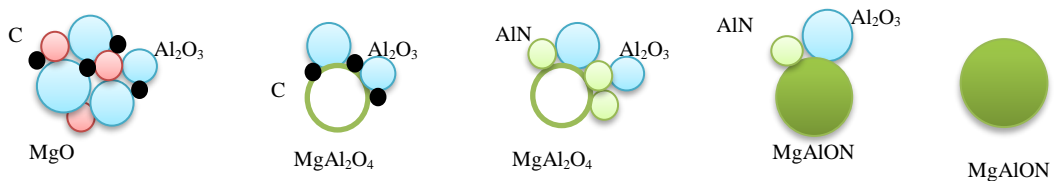


**Figure 4.27.** Representation of  $MgAlON$  formation as given by Chen et al. [16]

It can be seen that  $MgAlON$  is given as a product of the reaction of alumina with magnesium aluminate, which forms from  $MgO$  and  $Al_2O_3$ , and  $AlN$  obtained from the reduction of alumina in a nitriding atmosphere. In order to investigate with the presence of the  $MgAlON$  besides  $AlN$  and  $Al_2O_3$ , an experiment in which the holding

time was reduced to one hour was carried out. Figure 4.28 illustrates the obtained XRD results.

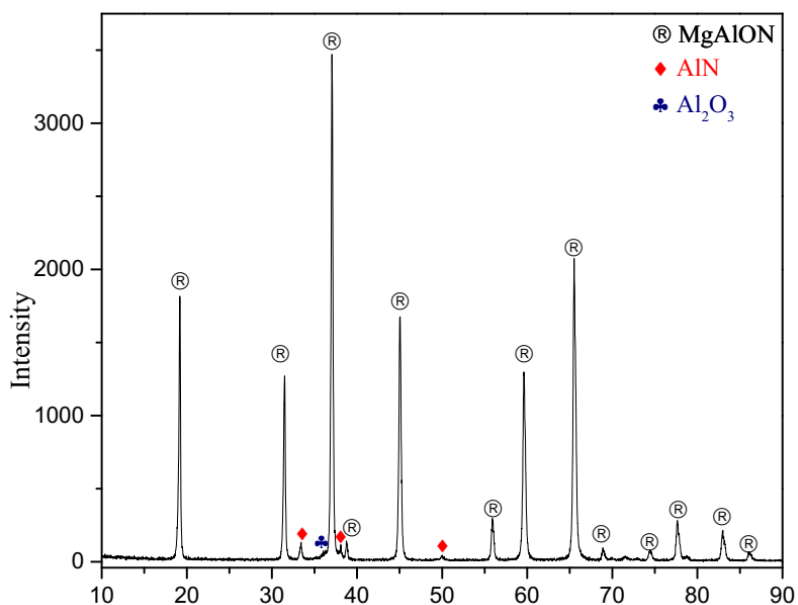


**Figure 4.28.** XRD patterns of powders synthesized at 1500°C for 1h in NH<sub>3</sub> + 1% C<sub>3</sub>H<sub>8</sub> at 2rpm.

It can be clearly seen in Figure 4.28 that the reduction of the holding time resulted in an incomplete conversion with AlN and Al<sub>2</sub>O<sub>3</sub> remains existing besides what is believed to be MgAlON. Based on this result and the comparison of the pattern with that of MAS revealing a shifting towards the left, the obtained powder was concluded to be MgAlON.

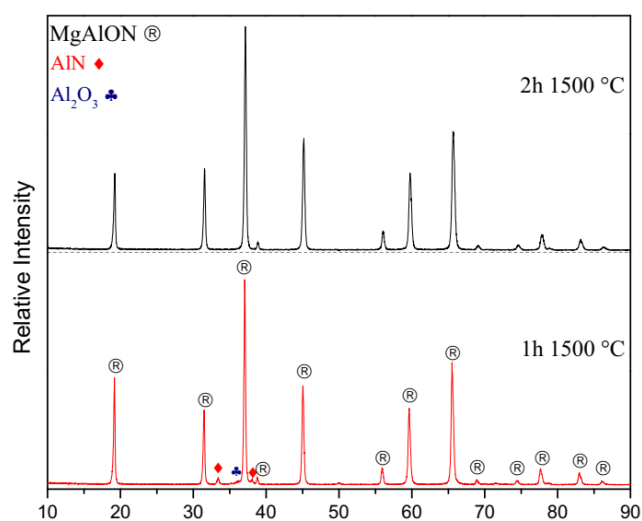


**Figure 4.29.** XRD patterns of powders obtained in DTM method under NH<sub>3</sub> + 1% C<sub>3</sub>H<sub>8</sub> at 1500°C for 1h and 2h.

In the case of raising the holding time to 2 hours instead of 1h as given in Figure 4.28, the AlN and Al<sub>2</sub>O<sub>3</sub> remains disappeared leaving a single phase which was concluded to be MgAlON seen in Figure 4.29. Product powders given in Figure 4.29 synthesized at 1500 °C for 1h and 2h under NH<sub>3</sub> gas having 1% of C<sub>3</sub>H<sub>8</sub>.

Figure 4.30 illustrates XRD patterns of powders synthesized in different nitriding atmospheres at 2rpm, comparing to magnesium aluminate spinel powder synthesized statically, under Ar flow. The reason of choosing the powder obtained in static system instead of that obtained dynamically is due to the inability to obtain pure spinel powders in the dynamic system under Ar.

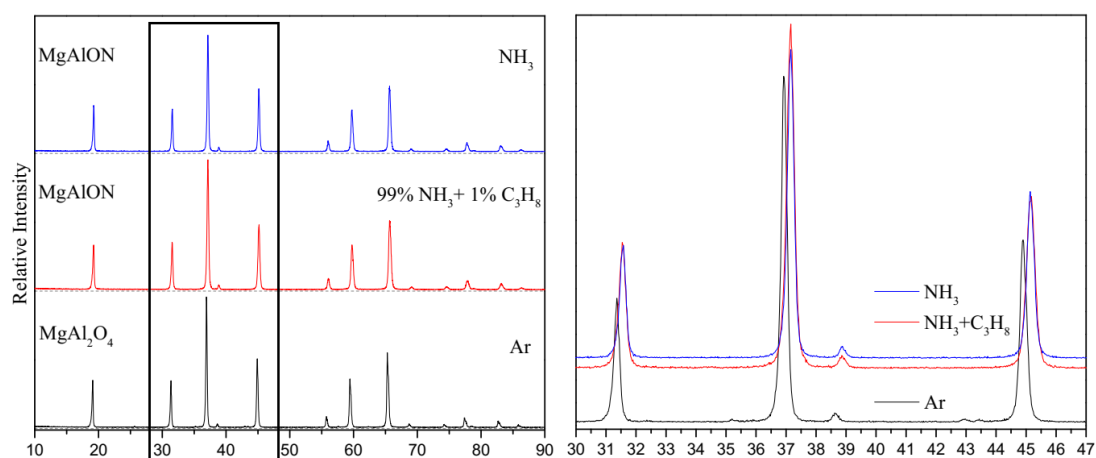


**Figure 4.30.** XRD patterns of powders synthesized using DTM method at 1500°C for 2h at 2 rpm comparing to MgAl<sub>2</sub>O<sub>4</sub> obtained statically at 1500°C for 2h.

It can be seen clearly in Figure 4.30 that the patterns of powders obtained under a nitriding atmosphere are similarly shifting towards the right in comparison to that synthesized under Ar. This shifting was reported to be associated with MgAlON phase as reported in the literature [15,128]. The differences among powders are not limited to the XRD patterns. Both powders obtained in NH<sub>3</sub> and NH<sub>3</sub>+C<sub>3</sub>H<sub>8</sub> had a grey color, while the one synthesized under Ar flow was white.

The effect of the dynamic system has been investigated to determine its efficiency in giving a full conversion to MgAlON phase. Corresponding XRD patterns are given in Figure 4.31.

When the powder was synthesized in a static system, an incompleteness of the conversion took place with remains in matters of aluminum nitride observed whereas Al<sub>2</sub>O<sub>3</sub> was absent. This can be explained with the existence of a reducing and nitriding gas mixture (NH<sub>3</sub>+C<sub>3</sub>H<sub>8</sub>) which may have resulted in the consumption of alumina in

the nitridation. Another possibility can be the complete consumption of alumina in the synthesis of MgAlON before AlN leaving the latter in the system. On the other hand, a dynamic synthesis (DTM method) enhanced the reaction through the homogenization provided by the rotating system which promotes a full conversion to MgAlON phase without any reactant left in the system following the synthesis.

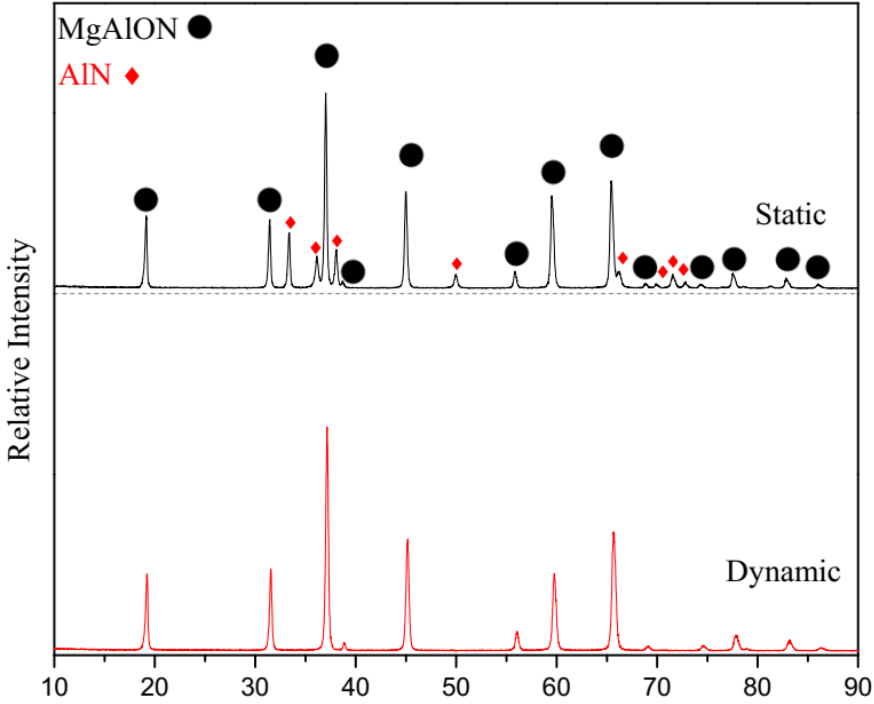


**Figure 4.31.** XRD patterns of powders obtained at 1500 °C for 2h under NH<sub>3</sub> + 1% C<sub>3</sub>H<sub>8</sub> in both static and dynamic system.

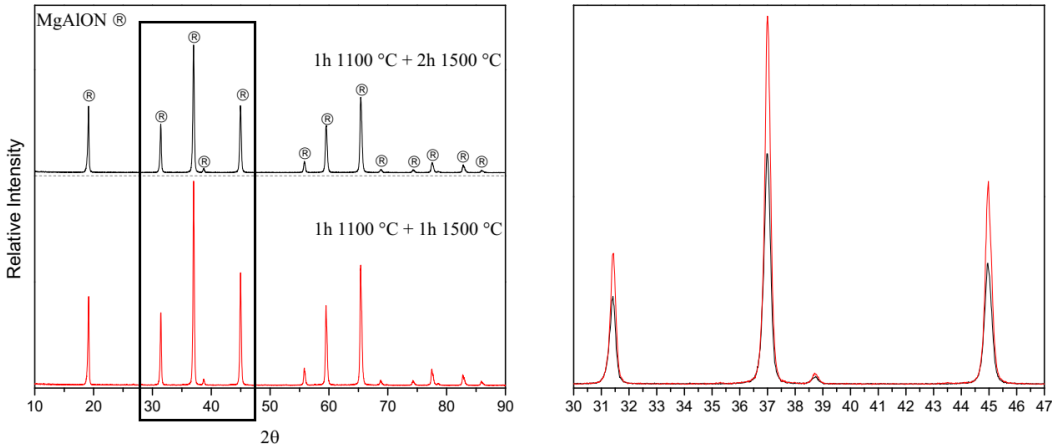


**Figure 4.32.** XRD patterns of powders synthesized under NH<sub>3</sub> + 1% C<sub>3</sub>H<sub>8</sub> atmosphere.

In another series of experiments investigating whether a two-steps synthesis gives an advantage over the single step one. XRD results of powders synthesis via a two-steps synthesis with a first holding at 1100°C followed by a second one at 1500°C for 1h

and 2h under  $\text{NH}_3 + 1\% \text{C}_3\text{H}_8$  atmosphere, are given in Figure 4.32. It can be seen that a pure  $\text{MgAlON}$  has been obtained in both cases. Nonetheless, when the powder was held for a longer time at  $1500^\circ\text{C}$ , the intensity of the peaks slightly decreased (can be clearly seen in the magnified pattern between  $30^\circ$  and  $47^\circ$  on the right). In addition, no difference in the XRD results of the two-steps synthesis was observed in comparison with that of the single step one. Thus, it is possible to say that the optimum condition of  $\text{MgAlON}$  synthesis is a single step dynamic synthesis at  $1500^\circ\text{C}$  for 1h at 2rpm under  $\text{NH}_3 + 1\% \text{C}_3\text{H}_8$  atmosphere. It can be stated that this method offers the best energy efficient conditions in which a full conversion to magnesium aluminum oxynitride, has ever been achieved.

Based on the obtained XRD results, it can be said that the two main factors of  $\text{MgAlON}$  synthesis are the atmosphere and the nature of the system whether dynamic or static. The former plays the key role in offering optimum conditions for a reduction and nitridation, whereas the latter, promotes a homogenization of the reactants throughout the reaction which results in a full conversion to  $\text{MgAlON}$ .

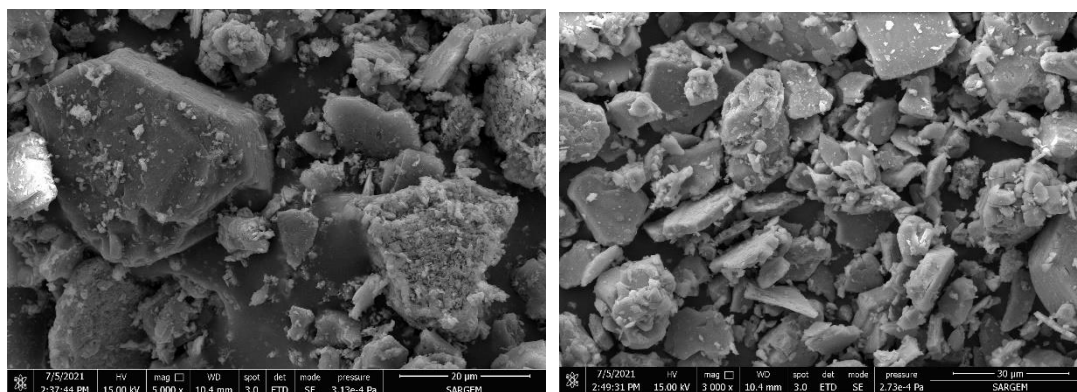
#### **4.1.3.2. Scanning electron microscopy results**

FESEM observations of the synthesized powders, revealed morphological results inconsistent with the good results obtained in the XRD analysis. The synthesized powders were characterized by an irregularity of morphology ranging from fine grains to coarse particles in the form of blocks or agglomerates. Additionally, the powders seemed to have a similar morphology to that of the initial state of reactants (seen in Figure 3.4). In what follows the obtained FESEM results are discussed.

Figure 4.33 illustrates FESEM image of powders synthesized at  $1500^\circ\text{C}$  for 2h under  $\text{NH}_3 + 1\% \text{C}_3\text{H}_8$  at 2rpm comparing to that obtained statically under the same conditions. It can be seen that no major difference between the powders whereas the XRD results (given in Figure 4.31) revealed full conversion to  $\text{MgAlON}$  in the case of the dynamic system and remains of aluminum nitride when the powder was synthesized statically. This result is also inconsistent with previous results in which the dynamic system has been shown to promote the synthesis of spherical powders with homogeneous morphology.

It is believed that the initial morphology of the powders played a detrimental role in the synthesis as the powder did not change their morphology. In other words, the

powders maintained their initial state while reduction and nitridation took place giving powders that are similar to the raw materials. Thus, despite the success in promoting the synthesis of a full MgAlON phase, the dynamic system was unable to give fine particles of a homogenous morphology.

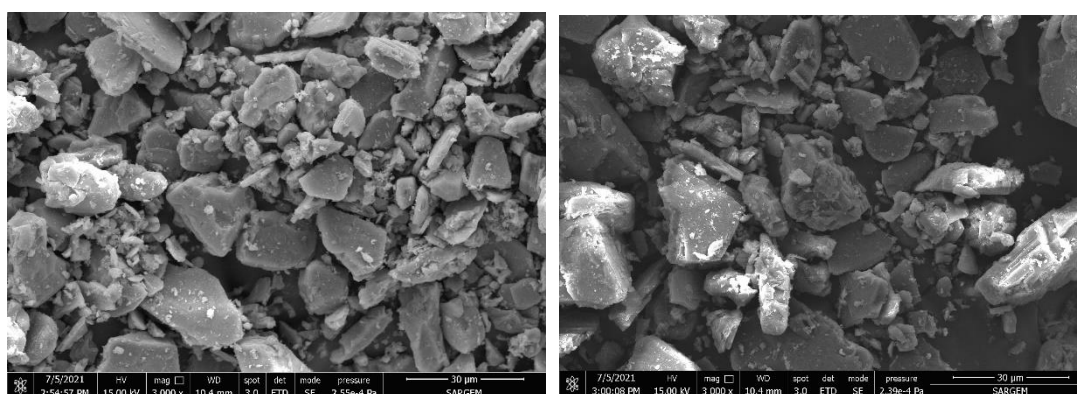


(a)

(b)

**Figure 4.33.** FESEM images of powders obtained after 2h at 1500°C under  $\text{NH}_3 + 1\% \text{C}_3\text{H}_8$  at (a) 2rpm and (b) statically.

Aiming to observe the effect of gases on the morphology, the experiment was repeated under  $\text{NH}_3$  as the sole gas. FESEM images of powders obtained at 1500°C for 2h under  $\text{NH}_3$  at 2rpm comparing to that obtained statically under the same conditions are given in Figure 4.34.



(a)

(b)

**Figure 4.34.** FESEM images of powders obtained after 2h at 1500°C under  $\text{NH}_3$  at (a) 2rpm and (b) statically.

Similarly, to the previous results of the gas mixture synthesis, the removal of propene did not promote any enhancement of the morphology of powders giving coarse particles with irregularity of grains. These powders are not different than the raw powder

mixture used in the synthesis of MgAlON. Consequently, propene can be said not to have any influence on the morphology of powders.

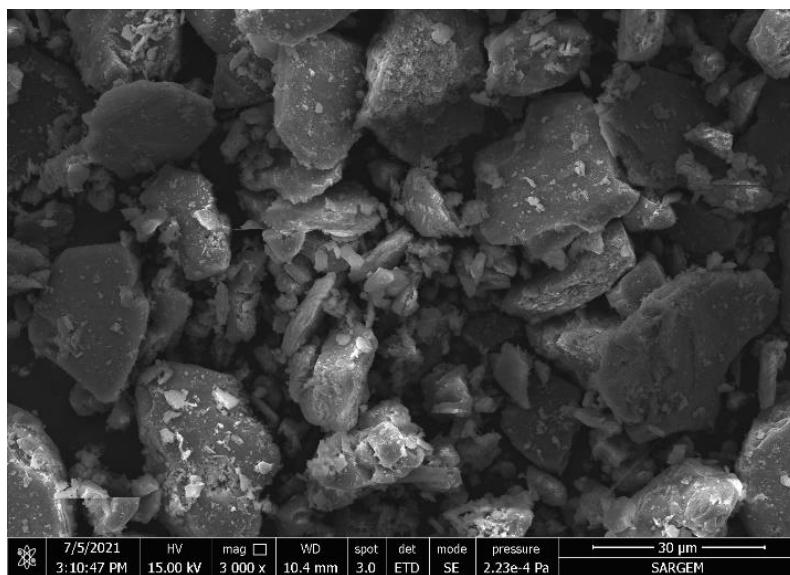


**Figure 4.35.** FESEM images of powders obtained after 1h at 1500°C under  $\text{NH}_3 + 1\% \text{C}_3\text{H}_8$  at 2rpm.

The holding time as well was not found to be of an influence on the morphology of powders as seen in Figure 4.35 corresponding to powders obtained at 1500°C under  $\text{NH}_3 + 1\% \text{C}_3\text{H}_8$  at 2rpm for 1h instead of 2h. It can be seen that the grains are similar to the previously shown FESEM results of MgAlON.

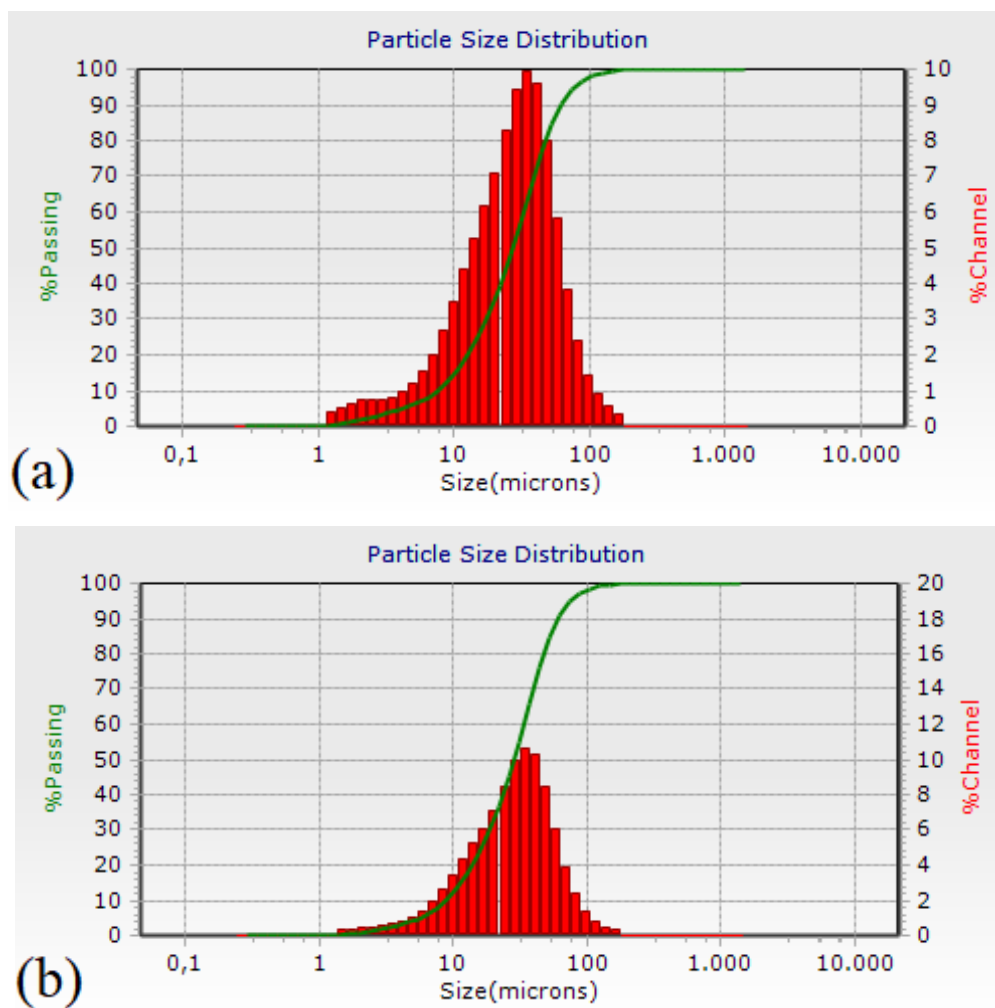
#### 4.1.3.3. Particle size distribution results

Due to the difference in the morphology of the obtained MgAlON powders, a particle size distribution analysis was performed to determine the size range of the synthesized powders. Figure 4.36 illustrates the obtained results for powders obtained at 1500°C for 2h under  $\text{NH}_3 + 1\% \text{C}_3\text{H}_8$  at 2rpm versus that obtained statically under the same conditions.

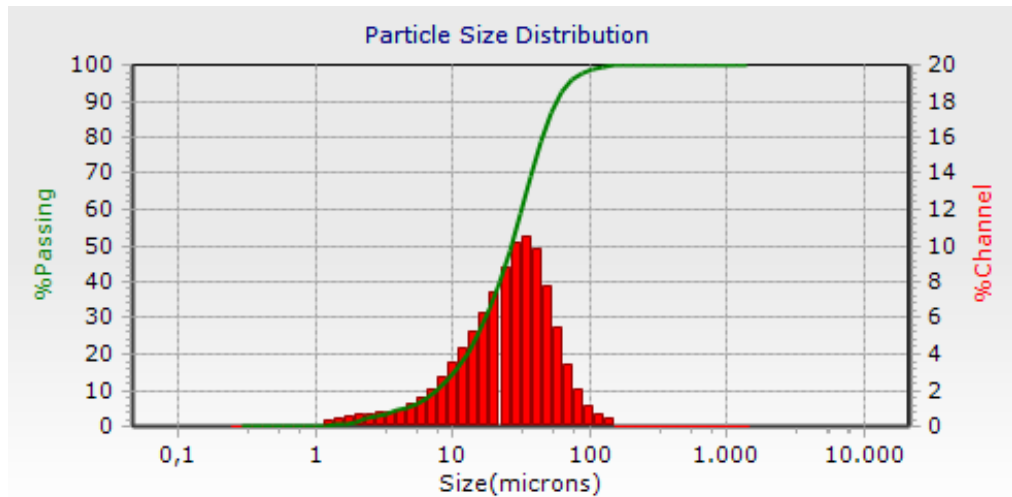
It can be seen that in both cases, the synthesized powders had similar distribution and an average particle size of around 30 $\mu\text{m}$  for both. Thus, it can be confirmed that the dynamic method did not promote the synthesis of fine powders in the case of MgAlON, as both powders obtained dynamically and statically showed similar results.

Figure 4.37 illustrates particle size distribution analysis results of powders obtained at 1500°C for 2h under  $\text{NH}_3$  instead of the gas mixture, synthesized at 2rpm. As seen in

Figure 4.38, the size distribution curve is similar to that of the gas mixture results confirming again that no enhancement of the particle size has taken place.



**Figure 4.36.** Particle size distribution of powders obtained at 1500°C for 2h under  $\text{NH}_3 + 1\% \text{C}_3\text{H}_8$  synthesized (a) statically versus (b) that obtained at 2rpm.



**Figure 4.37.** Particle size distribution of powders obtained at 1500°C for 2h under  $\text{NH}_3$  synthesized at 2rpm.

Aiming to investigate the effect of an intermediate holding on the powder morphology, an analysis of the size distribution of powders synthesized at 1500°C for 1h after holding at 1100°C for 1h under  $\text{NH}_3 + 1\% \text{C}_3\text{H}_8$  at 2rpm, has been performed. The obtained results are given in Figure 4.38.

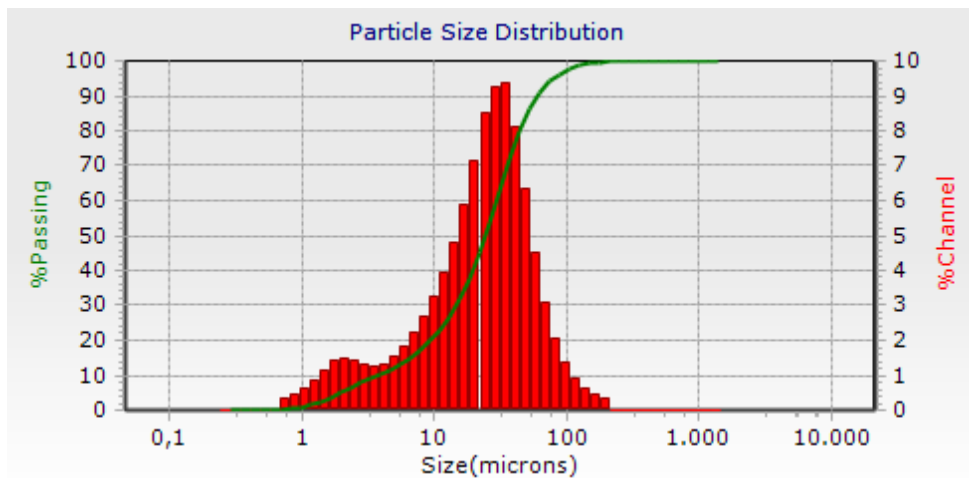


**Figure 4.38.** Particle size distribution of powders obtained at 1500°C for 1h after holding at 1100°C for 1h under  $\text{NH}_3 + 1\% \text{C}_3\text{H}_8$  synthesized at 2rpm.

It can be observed in Figure 4.38 that the curve is slightly different than that of the single step synthesis with more particles below 10 $\mu\text{m}$ . This can be associated with the intermediate holding which is thought to allow the formation of some spinel particles at a lower temperature promoting their nitridation without further grain growth. However, this enhancement is due to the insufficiency of the temperature to allow a full conversion to MAS, disallowing the synthesis of fine MgAlON particles.

## **4.2. Discussions**

The performed analyses revealed different results whose interpretation varies based on different factors ranging from the adapted method, the atmosphere of synthesis and test parameters. In what follows, the interpretation of the obtained results is given for each ceramic.

### **4.2.1. Magnesium aluminate spinel**

In the case of MAS, the static synthesis has been found to be the ideal condition for the synthesis of pure spinel powders. The purity of the obtained powder reached a maximum of around 98.7% disqualifying it from being a potential raw powder for transparent windows manufacturing and limiting its use to refractories.

When the dynamic method was used to investigate the possibility to obtain higher purity powders, the process failed in promoting a full conversion to spinel with the highest conversion limited to about 60%. There are many assumptions regarding the reason behind this failure in obtaining a full conversion to spinel. One reason is thought to be the rotating nature of the method, which in the case of granules formed from two or more reactants, a shrinkage may take place separating the reactants. This can engender the synthesis of the stable alfa alumina which is known to be hard to react once formed causing remains of alumina and magnesia. This can be confirmed with the existence of a certain amount of powder after the synthesis.

In previous investigations in which a full conversion to desirable compound was achieved [22,122,126], the powders were found to preserve their granulated form following the synthesis and thus, requiring a soft grinding by hand prior to characterization. However, in the case of the dynamic synthesis of spinel, a considerable amount of the synthesized powder was found to lose their granulated form. Consequently, a separation of the reactants may have taken place disallowing the formation of a full spinel phase.

When the rotation speed of the kiln was raised, an increase in the synthesized spinel has taken place leading to more than 98% conversion, yet the results obtained in the static system with a conversion of as close as 99.97% remained better than the results obtained in our modified dynamic system.

In matters of powder morphology, and with the failure of the dynamic system to provide purer powders than those obtained in the static system, the morphology was in question to determine whether there an advantage of rotation of the tube during the synthesis. However, it has been observed that both methods (static and dynamic) gave similarly close results with irregularity of shape and inhomogeneous particles. Furthermore, the shape of powder post-synthesis has been found to be similar to that of the starting raw materials.

It is believed that a reaction and conversion has taken place without a change in the morphology of the reactant which might have resulted in similar shapes of the reacting raw powders and the obtained compound.

Despite the fact that the obtained morphology is undesirable for sintering, the powders can still be used for applications other than transparency in which a full densification is needed to obtain high transparency. For example, a common use can be the field of refractories, which has already been reported to use spinel in the production, particularly, when high strength is needed.

#### **4.2.2. Aluminum oxynitride**

Unlike the case of spinel in which the dynamic method has been found ineffective under the investigated parameters, AlON synthesis via the dynamic thermochemical method has been a success despite the inability to acquire a full conversion. This is due to the fact that AlON has been widely reported to be thermodynamically unstable and not possible to form below 1640°C. Conversely, the dynamic process was the key to allow the obtention of more than 50% conversion to the oxynitride of aluminum after a two steps continuous synthesis with a first holding at 1100°C in an atmosphere of  $\text{NH}_3 + \text{C}_3\text{H}_8$ , for 75m followed by another holding at 1500°C, which is 140°C below the temperature reported to be the one at which AlON starts forming, under  $\text{N}_2$  for 2h. This conclusion has been made based on the fact that even having a single step of the two that allowed the conversion to AlON, performed in a static condition, fails to provide a considerable amount of aluminum oxynitride.

In the first investigation of AlN synthesis via the dynamic system, it has been found that the introduction of rotation to the synthesis causes a failure in obtaining AlN. Moreover, it was found that AlON makes its first appearance with switching to a dynamic synthesis under the same parameters. The appearance of AlON has been

explained with the rotation of the tube blocking the nitridation of alumina. When, they are kept in closeness at high temperature,  $\text{Al}_2\text{O}_3$  and  $\text{AlN}$  can form  $\text{AlON}$  [129].

The previously explained results were for synthesis that took place with a single heating and holding at  $1500^\circ\text{C}$  at 4rpm. However, the introduction of an intermediate holding at the  $\text{AlN}$  formation temperature followed by raising the temperature to  $1500^\circ\text{C}$  and a second holding at that temperature for 2h resulted in an increase of  $\text{AlON}$  making it the mostly dominant phase with a proportion of as high as 52%. The impurities were recorded as  $\text{Al}_2\text{O}_3$  and  $\text{AlN}$  which are the main reactant in the formation of the oxynitride. Hence, the dynamic nature of the process can only be the reason for this unprecedented formation of  $\text{AlON}$  at the temperature as other investigations carried out with same parameters in the static system failed in providing  $\text{AlON}$  powders.

Another important observation is that the gas mixture used in the first step to generate a mixture of  $\text{AlN}$  and  $\text{Al}_2\text{O}_3$ . It is crucial to note that the obtention of  $\text{AlON}$  at  $1500^\circ\text{C}$ . has always been considered not possible due to the thermodynamic limitations which results in the decomposition of  $\text{AlON}$  right after its formation as stated by Willems et. al. [33]. Our investigation on the other hand, confirmed the possibility of maintaining the stability of  $\text{AlON}$  below  $1640^\circ\text{C}$  via introducing an intermediate holding. Nevertheless, this is believed to be the first reason. The second is thought to be the gas mixture adapted instead of carbon black nitrogen, which in contrast to the former mixture, require higher temperatures to allow the formation of  $\text{AlON}$ .

The findings of previous investigations reporting the possibility of obtaining a mixture of  $\text{AlN}$  and  $\text{Al}_2\text{O}_3$  below  $1200^\circ\text{C}$  is another argument to explain  $\text{AlON}$  formation. Unlike the case of  $\alpha\text{-Al}_2\text{O}_3$  and  $\text{AlN}$  as a starting mixture, the formation of  $\text{AlN}$  from alumina within the system has the advantage of transition alumina. It is well known that below  $1200^\circ\text{C}$ , the stable  $\alpha$  alumina is less likely to form which leaves  $\text{AlN}$  with transition alumina in the system. As transition alumina has been found to be the favorite reactant in the formation of  $\text{AlON}$  together with  $\text{AlN}$ , the reaction of  $\text{AlON}$  formation is believed to be favored leading to the synthesis of  $\text{AlON}$ .

Additionally, regarding the incomplete conversion of  $\text{AlON}$ , the temperature limitation of our dynamic system is believed to be the main reason for which full, or at least higher conversion could not be obtained. While the formation of  $\text{AlON}$  was

made possible thanks to the introduction of atmosphere-controlled kiln rotation throughout the synthesis. This does not eliminate the thermodynamic limitations which remain the main reason for the incompleteness of the reaction. While AlON could be maintained stable following 2h holding at 1500°C, nor increasing the tube rotation neither extending the holding time beyond 2h appeared to help increase the rate of conversion. On the contrary, these attempts resulted in the decomposition of AlON to its main reactants, and therefore, only an increase of temperature is believed to be the key in allowing a full conversion to aluminum oxynitride.

Hence, although the partial conversion to AlON at 1500°C raises the chances of a full AlON synthesis below 1640°C, it does not revoke the statement of its instability below that temperature as the reenactment of experiments gave different conversion rates. Additionally, a temperature of 1500°C is believed to be low for a full conversion to the oxynitride. The limitation of our modified furnace to 1500°C unfortunately, prevents the investigation of whether a full conversion to aluminum oxynitride could be achieved at 1550°C or 1600°C. This remains a possibility for further investigations.

In matter of powder morphology, the three samples whose intermediate holding varied from 1h to 1.25h and 1.5h revealed submicron powders with that of 1.25h being relatively finer than others. The sample of 1.25h intermediate holding is also the one that exhibited the highest rate of conversion to AlON comparing to the two others, which leads to the conclusion of 1.25h at 1100°C being the ideal condition for the intermediate holding with regard to both conversion rate and powder morphology.

The starting powders given in Figure 3.1, reveals coarse Al(OH)<sub>3</sub> with an average size above 30μ. Nevertheless, in the resulting powders, we could clearly observe fine submicron particles which is explained by the reduction of aluminum hydroxide powder size to finer particles resulting in fine powder upon the completion of the synthesis. This result is in contrast with our previous studies [126] in which Al(OH)<sub>3</sub> was used, and unlike the current results, kept its initial form resulting in particles of 10μ average.

The use of gas mixture in the reduction nitridation can be the reason behind this reduction of size which is in accordance with literature in which gas mixture use in the synthesis of aluminum nitride has been linked with submicron particles. Another possible reason behind the reduction of size can be explained with AlON particles

which are known to be of fine particles if they are obtained from  $\gamma$ - $\text{Al}_2\text{O}_3$  and  $\text{AlN}$  mixture. It is possible that in our system, the intermediate holding resulted in the formation of transition alumina and  $\text{AlN}$  from which  $\text{AlON}$  was later obtained in the second holding at  $1500^\circ\text{C}$ . Hence, this can also support our assumption that the intermediate holding at  $1100^\circ\text{C}$  played a key role in the formation of aluminum oxynitride.

One final point to make regarding the obtained  $\text{AlON}$ , is the fact that even with achieving a full conversion, a possibility to use the powders for transparent windows would still be a challenge due to the limitation of optical ceramics. It is a well-known fact that fully transparent windows require highly pure  $\text{AlON}$  powders. However, with our aluminum hydroxide which contained some impurities prior to the synthesis, a highly pure powder is less likely to be achieved.

#### **4.2.3. Magnesium aluminum oxynitride**

In the case of  $\text{MgAlON}$ , the dynamic system has proven its efficacy as a full conversion to the oxynitride could only be obtained when the reaction was activated via tube rotation. Furthermore, it has been shown that the introduction of rotation during the synthesis allows a better reactivity of powders leading to impurity free product.

With this in hand, the dynamic system is believed to provide the condition for three different reactants to be fully consumed in producing  $\text{MgAlON}$ . This happens via a mechanism following which both reactants,  $\text{Mg}(\text{OH})_2$  and  $\text{Al}(\text{OH})_3$ , initially produce  $\text{MgO}$  and  $\text{Al}_2\text{O}_3$  via dehydration. In what followed, a nitridation of alumina took place giving rise to  $\text{AlN}$ , while another part reacted with  $\text{MgO}$  to produce  $\text{MgAl}_2\text{O}_4$ . When  $\text{MgAl}_2\text{O}_4$ ,  $\text{Al}_2\text{O}_3$  and  $\text{AlN}$  are present together,  $\text{MgAlON}$  is formed from the reaction of the two latter with the former. This mechanism is in accordance with the literature and our findings where the static synthesis (Figure 4.31) results failed in providing reaction conditions while an insufficient holding (Figure 4.29) resulted in an incomplete reaction. Hence, there are few points to make regarding the synthesis of  $\text{MgAlON}$  via the dynamic process:

First, as explained before, maintaining the rotation of the tube in the presence of a nitriding and a reducing source can allow the synthesis of  $\text{MgAlON}$ . Otherwise, the

result can be either an incomplete reaction with AlN and Al<sub>2</sub>O<sub>3</sub> as well as MgAl<sub>2</sub>O<sub>4</sub>, or a failure of the synthesis with unreacted starting powders.

Second, it is crucial to understand that the use of ammonia instead of nitrogen as nitriding source plays an important role in the formation of magnesium aluminum oxynitride. Similar to AlON synthesis, NH<sub>3</sub> seems to favor the formation of oxynitride since it allows an early nitridation in accordance with what has been reported in the literature. When N<sub>2</sub> is used this early nitridation does not take place and hence AlN formation is delayed leading to the transition of alumina to its stable  $\alpha$  form which is known to be harder to enter in reaction with nitrides at 1500°C to form an oxynitride compound.

A third point to make regarding the synthesis of MgAlON via the dynamic thermochemical method is the importance of holding time in allowing a full synthesis. Since the reduction of the holding time from 2h to 1h resulted in an incomplete conversion, 2h can be set as the minimum holding time to allow a full conversion of the reactants. An insufficient holding does not give the required time for the reactants to be fully consumed in the formation of MgAlON leading to impurities in matters of AlN and Al<sub>2</sub>O<sub>3</sub>.

Concerning the powder morphology, and unlike the case of AlON in which submicron powders were obtained, the resulting MgAlON powders had inhomogeneous round shape with an average particle size of 20 $\mu$ . This result was similar for the use of ammonia as well as that of powder mixture and that in which Ar was used. In fact, the obtained powders were similar to those of spinel in shape.

Unlike the case of AlON in which aluminum hydroxide powder size was reduced to the order of submicron, Al(OH)<sub>3</sub> seems to have kept its initial shape and size leading to the results observed in the scanning electron microscopy figures of MgAlON. It is well established that the difference between AlON and MgAlON is magnesium which plays the role of AlON stabilizer. Consequently, it can be concluded that the reason behind the rough morphology of AlON can be caused by Mg substitution.

Finally, regardless of the rough morphology of the obtained MgAlON, the results we achieved in this research are still positive for multiple factors. First, a full conversion to magnesium aluminum oxynitride has not been obtained at 1500°C. This means that energy is saved with the drop of synthesis temperature from 1600°C. Second, the

starting powders in our study are cheaper compared to high purity fine MgO, AlN and Al<sub>2</sub>O<sub>3</sub> used in many reported studies. This means that the cost of the production would drastically drop. Third, the possibilities to obtain better powder morphologies are always possible. A possible approach is the size reduction of Al(OH)<sub>3</sub> prior to the synthesis. Given the fact that Mg(OH)<sub>2</sub> powders are on the order of the submicron, reducing the particle size of Al(OH)<sub>3</sub> to submicron raises the chances of obtaining fine MgAlON particles.

It is also important to highlight that it is hard to claim that the obtained magnesium aluminum oxynitride can be used for transparent windows use given the fact that sintering must be carried out in prior to verify the transparency. Furthermore, transparency requires highly pure starting powders whereas our raw materials seemed to have some impurities. Therefore, sintering investigation may be carried out in further studies to determine both the sinterability of our powders and their potentials to deliver a certain level of transparency.

## 5. CONCLUSION AND RECOMMENDATIONS

In this study, the synthesis of three different technical ceramics has been investigated both using the conventional reduction (or reduction and nitridation) method and via our novel dynamic thermochemical method (DTM). A total of more than hundred experiments were carried out in varying conditions leading to different results. At the end of this research, it is possible to conclude a few points regarding the DTM process and the synthesis of spinel, AlON and MgAlON powders. These points can be given as follows:

In matters of conversion and purity of powders, DTM was successful in achieving two positive results whereas the synthesis of spinel via this method can be rather said “to be improved” and further investigated under different conditions other than those observed in this research. Our DTM was able to deliver a full conversion of  $\text{Al}(\text{OH})_3$  and  $\text{Mg}(\text{OH})_2$  to MgAlON using ammonia or a mixture of ammonia and propene as nitriding source, at an unprecedented temperature of  $1500^\circ\text{C}$ , while more than 50% conversion to AlON from  $\text{Al}(\text{OH})_3$  under a mixture of ammonia and propene was recorded at  $1500^\circ\text{C}$ , which is as well a first, since solid state synthesis of AlON has been reported to be unachievable below  $1640^\circ\text{C}$  due to aluminum oxynitride instability.

The synthesis of MgAlON at  $1500^\circ\text{C}$  from cheap raw materials can open the door to possible commercialization of the method as both the low cost of the starting powders and the intermediate synthesis temperature can help lower the production cost. Currently, MgAlON is not available in the market in form of ready to use windows like AlON. In contrast, magnesium aluminum oxynitride is only presented in studies as a possible substitute and a cheaper form of aluminum oxynitride whose production is limited by many difficulties.

As mentioned before, the partial conversion to AlON at  $1500^\circ\text{C}$  can be considered as a very positive result for two reasons: First,  $1640^\circ\text{C}$  has been given as the minimum temperature below which aluminum oxynitride cannot be obtained. Second, a 50% plus conversion to AlON at  $1500^\circ\text{C}$  can possibly mean that a further increase in

temperature with 100°C can lead to a full conversion. In addition, different ways of processing such as high energy ball milling of aluminum hydroxide prior to the synthesis can have the potential to deliver a full conversion to AlON as it may result in the transition of the hydroxide into transition alumina which has been reported to favor the synthesis of the oxynitride of aluminum in the presence of ammonia and propene mixture.

Unlike AlON and MgAlON, the dynamic thermochemical method was not as efficient in providing better results than those obtained in the static system. This was explained with one of the following explanations: The dynamic method preventing the formation of the compound, which is not thought to be a strong argument as our method has proven the opposite in almost all the previous studies. The second (and more logical explanation) is that the dynamic method favors the synthesis of oxynitride in that range of compounds. This is supported with the fact that AlN was similarly, unable to achieve in the dynamic system, but achievable in the static. Thus, in the absence of nitriding source, only a partial conversion to spinel could be achieved.

Regarding the powder morphology, while in our previous studies, DTM has been deemed effective in delivering a better morphology of powders, only one of the studied ceramic powders had a morphology that can be considered as positive for sintering. In contrast, both spinel and magnesium aluminum oxynitride have both had a coarse powder with inhomogeneous size. Since the dynamic system and almost all the parameters studied were the same, the reason of this morphology could only be narrowed to the involvement of magnesium which is the only difference between the two and AlON powders which had a very positive powder shape.

Nevertheless, and as mentioned previously, this morphological inhomogeneity does not make the obtained results negative, but rather subject to improvement. It can be argued that the results are negative in the case of spinel which was not possible to obtain at a 100% conversion rate via the dynamic method. However, in the case of MgAlON, whose XRD results revealed a full conversion at an unprecedented temperature of 1500°C, the morphology results can only be considered as an undesirable shape that can be improved. Thus, our results remain arguably better than what has been reported for oxynitride powders synthesis.

In this work, we tried to avoid the use of solid carbon as a reducing agent and instead we chose a gas mixture that gives carbon after decomposition, to avoid both the problem of carbon excess, which results in further processing, and the possibility of contamination of the obtained powders. The choice of ammonia over nitrogen, however, arose from the advantages of the former in allowing an early synthesis which was believed to be the key in our positive results regarding the synthesis of AlON.

Despite the failure of DTM to give better result in the case of spinel comparing to the static method, it did prove itself effective in both AlON and MgAlON synthesis. Therefore, it can only be considered an advantageous method and a promising choice in the synthesis of nitride and oxynitride based ceramics.

DTM process remains under investigation both in the ceramics studied in this thesis and other technical ceramic powders to optimize the method and determine possibly an approach to provide better morphology.

Finally, this thesis was built on the argument of optimizing the powder synthesis process of technical ceramic powders. In the end of this research, it was able to determine that the method proposed does optimize the synthesis of MgAlON allowing a full conversion at lower temperature than what has been ever reported. Furthermore, it has been shown that AlON can be obtained at 1500°C despite the previously reported results which dismissed the possibility of its synthesis below 1640°C whereas in our research, more than 50% conversion could be achieved at 1500°C with a submicron size of homogenous morphology.

## **5.1. Recommendations**

Regarding spinel synthesis, it is believed that the dynamic method should be further investigated using the conventional raw materials for spinel synthesis ( $\text{Al}_2\text{O}_3$  and MgO) to determine whether there is a difference when the main spinel forming compounds are used rather than obtained as intermediate conversion from hydroxides.

In the case of AlON, it is vital to highlight the importance of investigating its formation via the dynamic system at 1600°C. The fact that more than 50% conversion was achieved at a temperature at which AlON is considered unstable raises the chances of possible synthesis below the current stability temperature.

MgAlON was the ceramic we fully synthesized below the reported stability temperature. However, the powder morphology was not the best result to provide powders that can be used without further processing and therefore, it is important to investigate the effect of prior size reduction before mixing and charging into the DTM furnace.

It is also important to investigate the sinterability of the obtained powders and the properties of the products formed from the synthesized powders. This will provide a full understanding of the quality of the powders synthesized via this novel approach.

## REFERENCES

- [1] J. William D. Callister and D. G. Rethwisch, *Materials Science and Engineering, An Introduction*, 8th ed., USA: John Wiley & Sons, Inc, 2009, p. 844.
- [2] P. J. Patel, "Processing and characterization of aluminum oxynitride ceramics," PhD Thesis, Johns Hopkins University, 1999.
- [3] L. Lallemand, G. Fantozzi, V. Garnier and G. Bonnefont, "Transparent Polycrystalline Alumina Obtained by SPS: Green bodies processing effect," *Journal of the European Ceramic Society*, vol. 32, p. 2909–2915, 2012.
- [4] A. Golubovi, S. Nikoli and S. Djuri, "The Growth of Sapphire Single Crystals," *Journal of the Serbian Chemical Society*, vol. 66, no. 6, p. 411–418, 2001.
- [5] D. C. Harris, "A Century of Sapphire Crystal Growth," in *Proceedings of the 10th DoD Electromagnetic Windows Symposium*, Norfolk, Virginia, May 2004.
- [6] J. Sanghera, G. Villalobos, S. B. W. Kim and I. Aggarwal, "Transparent Spinel Ceramic," Naval Research Lab Washington DC Optical Sciences Division, Washington DC, 2009.
- [7] M. T. Vu, "PhD Dissertation: Densification and Characterization of Transparent Polycrystalline Spinel Produced by Spark Plasma Sintering," The State University of New Jersey, New Jersey, 2014.
- [8] L. R. Pinga, A.-M. Azadb and T. W. Dung, "Magnesium Aluminate (MgAl<sub>2</sub>O<sub>4</sub>) Spinel produced via Self-Heat-Sustained (SHS) Technique," *Materials Research Bulletin*, vol. 36, p. 1417–1430, 2001.
- [9] J. Sanghera, G. Villalobos, W. Kim, S. Bayya and I. Aggarwal, "Fluoride Salt Coated Magnesium Aluminate". USA Patent U.S. Patent 7,211,325, 1 5 2007.
- [10] A. S. Lysenkov, I. A. Timoshkin, Y. F. Kargin, D. D. Titov, A. Y. Fedotov, A. A. Ashmarin and A. E. Baranchikov, "Synthesis of Aluminum Oxynitride (AlON) and Study of the Properties of Ceramics Based on it," *Materialovedenie*, vol. 11, p. 54–56, 2015.
- [11] M. Ramisetty, S. Sastri, U. Kashalikar, L. M. Goldman and N. Nag, "Transparent Polycrystalline Spinel Protect and Defend," *American Ceramic Society Bulletin*, vol. 92, no. 2, pp. 20 - 25, 2013.

- [12] X.J.Zhao, H.Q.Ru, N.Zhang, X.Y.Wang and D.L.Chen, "Corrosion of Aluminum Oxynitride Based Ceramics by Molten Steel," *Ceramics International*, vol. 39, no. 3, pp. 3049-3054, 2013.
- [13] C.-F. Chen, P. Yang, G. King and a. E. L. Tegtmeier, "Processing of Transparent Polycrystalline AlON:Ce<sup>3+</sup> Scintillators," *Journal of the American Ceramic Society*, p. 1–7, 2015.
- [14] J. Qi, Y. Wang, T. Lu, Y. Yu, L. Pan, N. Wei and J. Wang, "Preparation and Light Transmission Properties of AlON from nanosized Al<sub>2</sub>O<sub>3</sub> and AlN," *The Minerals, Metals & Materials Society and ASM International*, vol. 24A, p. 4075–4079, 2011.
- [15] S. Tong, Y. Li, M. Yan, P. Jiang, J. Ma and D. Yue, "In situ reaction mechanism of MgAlON in Al–Al<sub>2</sub>O<sub>3</sub>–MgO composites at 1700°C under flowing N<sub>2</sub>," *International Journal of Minerals, Metallurgy and Materials*, vol. 24, no. 9, p. 1061, 2017.
- [16] Q. Chen, Y. Wang, J. Qi and H. Wang, "A contrast of carbothermal reduction synthesis of MgAlON and AlON powders for transparent ceramics," *Journal of Alloys and Compounds*, vol. 791, pp. 856-863, 2019.
- [17] X. Xie, Y. Wang, J. Qi, N. Wei, Q. Shi, S. Wang, H. Wu and T. Lu, "Gas-Phase and Solid-State Simultaneous Mechanism for Two-Step Carbothermal AlON Formation," *Journal of the American Ceramic Society*, vol. 98, no. 6, p. 1965–1973, 2015.
- [18] J. W. McCauley, "Structure and Properties of AlN and AlON," US Army Research Lab ARL-TR-2740, 2002.
- [19] Q. Liu, N. Jiang, J. Li, K. Sun, Y. Pan and J. Guo, "Highly Transparent AlON Ceramics Sintered from Powder Synthesized by Carbothermal Reduction Nitridation," *Ceramics International*, vol. 42, p. 8290–8295, 2016.
- [20] J. Zheng and B. Forslund, "Carbothermal Synthesis of Aluminium Oxynitride (AlON) Powder Influence of Starting Materials and Synthesis Parameters," *Journal of the European Ceramic Society*, vol. 15, pp. 1087-1100, 1995.
- [21] H. X. Willems, M. M. R. M. Hendrix, R. Metselaar and G. d. With, "Thermodynamics of Alon I: Stability at Lower Temperatures," *Journal of the European Ceramic Society*, vol. 10, pp. 327-337, 1992.
- [22] N. Canikoğlu, B. Özdemir, Y. Y. Özbek and A. O. Kurt, "Synthesis of TiN Powders Using Dynamic CRN Method," *SAU JOURNAL OF SCIENCE*, vol. 22, no. 5, pp. 1438-1443, 2018.
- [23] A.O. Kurt, «The method of producing the high-tech ceramics` raw materials in an atmosphere-controlled rotary furnace», Turkish Patent: TR 2011 02804 B, 2011.

- [24] A.O. Kurt and Y.G.Vardar, "Synthesis of  $\alpha$ -Si<sub>3</sub>N<sub>4</sub> ceramic powders via Dynamic CRN," *Afyon Kocatepe University Journal of Science*, pp. 125-130, 2003.
- [25] S. Bakan, A. B. Bila, H. Boussebha and A. O. Kurt, "A Technique for the Production of Submicron Boron Carbide Powder," *Afyon Kocatepe University Journal of Science and Engineering*, Vol.19, No.Special Issue, pp. 71-78, 2019.
- [26] R. J. Naumann, *Introduction to the Physics and Chemistry of Materials*, CRC Press, 2008.
- [27] M. Vu, R. Haber and H. Gocmez, "Preparation and Sintering of Al<sub>2</sub>O<sub>3</sub> - Doped Magnesium Aluminate Spinel," *Advances in Ceramic Armor; The American Ceramic Society*, vol. 8, pp. 93-103, 2013.
- [28] D. C. Harris, "History of Development of Polycrystalline Optical Spinel in the U.S.," in *SPIE Vol. 5786 Window and Dome Technologies and Materials IX*, Bellingham, Washington, 2005.
- [29] G. Yamaguchi, "On the Refractive power of the lower-valent aluminum ion (Al<sup>+</sup> or Al<sup>2+</sup>) in the crystal," *Bulletin of the Chemical Society of Japan*, vol. 23, pp. 89-90, 1950.
- [30] G. Yamaguchi and H. Yanagida, "Study on the Reductive Spinel-A New Spinel Formula AlN-Al<sub>2</sub>O<sub>3</sub> instead of the Previous One Al<sub>3</sub>O<sub>4</sub>," *Bulletin of the Chemical Society of Japan*, vol. 32, no. 11, pp. 1264-1265, 1959.
- [31] N. D. Corbin, "Aluminum Oxynitride Spinel: A Review," *Journal of the European Ceramic Society*, vol. 5, p. 143 154, 1989.
- [32] J. W. McCauley and N. D. Corbin, "Phase Relations and Reaction Sintering of Transparent Cubic Aluminum Oxynitride Spinel (ALON)," *Journal of the American Ceramic Society*, vol. 62, no. 9-10, pp. 476-479, 1979.
- [33] H. X. Willems, M. M. R. M. Hendrix, G. d. With and R. Metselaar, "Thermodynamics of Alon II: Phase Relation," *Journal of the European Ceramic Society*, vol. 10, pp. 339-346, 1992.
- [34] H. X. Willems, G. d. With and R. Metselaar, "Thermodynamics of AlON III: Stabilization of AlON with MgO," *Journal of the European Ceramic Society*, vol. 12, pp. 43-49, 1993.
- [35] I.-H. Jung, S. A. Decterov and A. D. Pelton, "Critical Thermodynamic Evaluation and Optimization of the MgO-Al<sub>2</sub>O<sub>3</sub>, CaO-MgO-Al<sub>2</sub>O<sub>3</sub> and MgO-Al<sub>2</sub>O<sub>3</sub>-SiO<sub>2</sub> Systems," *Journal of Phase Equilibria and Diffusion*, vol. 25, no. 4, pp. 329-345, 2004.
- [36] W. B. D.Sc.F.R.S., "The Structure of the Spinel Group of Crystals," *Philosophical Magazine Series 6*, vol. 30, no. 176, pp. 305-315, 1915.

- [37] G. Ibram, "A Review on Magnesium Aluminate (MgAl<sub>2</sub>O<sub>4</sub>) Spinel: Synthesis, Processing and Application," *International Materials Reviews*, vol. 58, no. 2, pp. 63-112, 2013.
- [38] S. Nishikawa, "Structure of Some Crystals of Spinel Group," in *Proceedings of the Tokyo Mathematico-Physical Society. 2nd Series*, 1915-1916.
- [39] B. Hallstedt, "Thermodynamic Assessment of the System MgO-Al<sub>2</sub>O<sub>3</sub>," *Journal of the American Ceramic Society*, vol. 75, no. 6, pp. 1497-1507, 1992.
- [40] V. P. Dravid, J. A. Sutliff, A. D. Westwood, M. R. Notis and C. E. Lyman, "On the Space Group of Aluminium Oxynitride Spinel," *Philosophical Magazine A*, vol. 61, no. 3, pp. 417-434, 1990.
- [41] J. Labbe and A. Jeanne, "Structural Modification of Aluminium Oxynitride Phases Under Stresses at High Temperatures, High Pressures and Under Irradiation by Fast Neutrons," *Materials Chemistry and Physics*, vol. 26, no. 1, pp. 47-55, 1990.
- [42] J. Evans and T. Grove, "MIT OpenCourseWare," Fall 2004. [Online]. Available: <https://ocw.mit.edu/courses/earth-atmospheric-and-planetary-sciences/12-108-structure-of-earth-materials-fall-2004/lecture-notes/lec4.pdf>. [Accessed 29 June 2020].
- [43] J. W. McCauley and N. D. Corbin, "High Temperature Reactions and Microstructure in The Al<sub>2</sub>O<sub>3</sub>-AlN System," *Progress in Nitrogen Ceramics*, vol. 65, pp. 111-118, 1983.
- [44] L. Hwang, A. H. Heuer and T. E. Mitchell, "On the Space Group of MgAl<sub>2</sub>O<sub>4</sub> Spinel," *Philosophical Magazine*, vol. 28, no. 1, pp. 241-243, 1973.
- [45] M. Tokonami and H. Horiuchi, "On the Space Group of Spinel, MgAl<sub>2</sub>O<sub>4</sub>," *Acta Crystallographica*, vol. 36, no. A, pp. 122-126, 1980.
- [46] J. W. McCauley, "A Simple Model for Aluminum Oxynitride Spinels," *Journal of The American Ceramic Society*, vol. 61, no. 7-8, pp. 372-373, 1989.
- [47] P. Tabary and C. Servant, "Crystalline and Microstructure Study of the AlN-Al<sub>2</sub>O<sub>3</sub> Section in the Al-N-O System. I. Polytypes and  $\gamma$ -AlON Phase," *Journal of Applied Crystallography*, vol. 32, p. 241-252, 1999.
- [48] L.-J. Yin, C. Cai, H. Wang, Y.-J. Zhao, H. V. Bui, X. Jian, H. Tang, X. Wang, L.-J. Deng, X. Xu and M.-H. Lee, "Luminescent properties and microstructure of SiC doped AlON: Eu<sup>2+</sup> Phosphorus," *Journal of Alloys and Compounds*, vol. 725, pp. 217-226, 2017.
- [49] R. M. H. H. G. d. W. C.M. Fang, "Structure Models for  $\gamma$ -Aluminum Oxynitride from ab initio Calculations," *Journal of the American Ceramic Society*, vol. 84, pp. 2633-2637, 2001.

- [50] H. W. X. L. W. W. Z. F. B. Tu, "First-Principles Insight into the Composition-Dependent Structure and Properties of  $\gamma$ -AlON," *Journal of the American Ceramic Society*, vol. 97, pp. 2996-3003, 2014.
- [51] D. T. G. G. J. M. I.G. Batyrev, "Density Functional Theory and Evolution Algorithm Calculations of Elastic Properties of AlON," *Journal of Applied Physics*, vol. 115, p. 6, 2014.
- [52] K. H. Jack, "Review: Sialons and related nitrogen ceramics," *Journal of Material Science*, vol. 11, pp. 1135-1158, 1976.
- [53] A. Granon, P. Goeuriot and F. Thevenot, "Reactivity in the Al<sub>2</sub>O<sub>3</sub>-AlN-MgO System. The MgAlON Spinel Phase," *Journal of the European Ceramic Society*, vol. 13, pp. 365-370, 1994.
- [54] L. Liu, C. Zhang, K. T. T. Nishimura and H. Segaw, "Uniform and Fine Mg- $\gamma$ -AlON Powders Prepared from MgAl<sub>2</sub>O<sub>4</sub>: A Promising Precursor Material for Highly-Transparent Mg- $\gamma$ -AlON Ceramics," *Journal of the European Ceramic Society*, vol. 39, p. 928–933, 2019.
- [55] X. Zong, H. Wang, H. Gu, L. Ren, S. Guo, B. Tu, W. Wang, S. Liu and Z. Fu, "Highly Transparent Mg<sub>0.27</sub>Al<sub>2.58</sub>O<sub>3.73</sub>N<sub>0.27</sub> Ceramic Fabricated by Aqueous Gelcasting, Pressureless Sintering, and Post-HIP," *Journal of the American Ceramic Society*, vol. 102, no. 11, pp. 6507-6516, 2019.
- [56] O. Morey, "PhD Thesis "Rôle de l'azote sur l'élaboration (synthèse de poudre-frittage) et les propriétés diélectriques de solutions solides spinelles de type MgAlON", " Ecole Nationale Supérieure des Mines de Saint Etienne, 2000.
- [57] O. Morey and P. Goeuriot, "'MgAlON' spinel structure: A new crystallographic model of solid solution as suggested by <sup>27</sup>Al solid state NMR," *Journal of the European Ceramic Society*, vol. 25, p. 501–507, 2005.
- [58] T. E. Mitchell, "Dislocations and Mechanical Properties of MgO–Al<sub>2</sub>O<sub>3</sub> Spinel Single Crystals," *Journal of the American Ceramic Society*, vol. 82, no. 12, p. 3305 –3316, 1999.
- [59] F. Y. Cui, A. Kundu, A. Krause, M. P. Harmer and R. P. Vinci, "Surface Energies, Segregation, and Fracture Behavior of Magnesium Aluminate Spinel Low-Index Grain Boundary Planes," *Acta Materialia*, vol. 148, pp. 320-329, 2018.
- [60] R. W. Rice, C. C. Wu and K. R. McKinney, "Fracture and Fracture Toughness of Stoichiometric MgAl<sub>2</sub>O<sub>4</sub> Crystals at Room Temperature," *Journal of Material Science*, vol. 31, pp. 1353-1360, 1996.
- [61] D. Viechnicki, F. Schmid and J. W. McCauley, "Growth of nearly stoichiometric MgAl<sub>2</sub>O<sub>4</sub> spinel single crystals by a gradient furnace technique," *Journal of Applied Physics*, vol. 43, no. 11, p. 4508–4512, 1972.

- [62] O. Tokariev, L. Schnetter, T. Beck and J. Malzbender, "Grain Size Effect on the Mechanical Properties of Transparent Spinel Ceramics," *Journal of the European Ceramic Society*, vol. 33, p. 749–757, 2013.
- [63] H. X. Willems, PhD Dissertation: Preparation and Properties of Translucent Gamma-Aluminium Oxynitride, Eindhoven: Eindhoven University of Technology, 1992.
- [64] T. Hartnett and R. Gentilman, "Optical and Mechanical Properties of Highly Transparent Spinel and AlON Domes," in *SPIE Advances in Optical Materials*, 1984.
- [65] B. Ma, W. Zhangb, Y. Wang, H. Song, X. Xie, Z. Zhang, C. Yao, H. Luo and R. Niu, "Fabrication and Nanoindentation Characterization of MgAlON Transparent Ceramics," *Optical Materials*, vol. 84, p. 714–721, 2018.
- [66] X. Liu, H. Wang, B. Tu, W. Wang and Z. Fu, "Highly Transparent Mg<sub>0.27</sub>Al<sub>2.58</sub>O<sub>3.73</sub>N<sub>0.27</sub> Ceramic Prepared by Pressureless Sintering," *Journal of the American Ceramic Society*, vol. 97, no. 1, pp. 63-66, 2014.
- [67] A. Krell, K. Waetzig and J. Klimke, "Effects and elimination of nanoporosity in transparent sintered spinel (MgAl<sub>2</sub>O<sub>4</sub>)," *Proc. of SPIE Vol. 801602-1*, vol. 8016, no. 801602, pp. 1-10, 2011.
- [68] D. Blodgett, D. Hahn and M. Thomas, "Optical Characterization of AlON and Spinel," *Proc. SPIE*, vol. 5786, no. Window and Dome Technologies and Materials IX, pp. 83-94, 2005.
- [69] T. Hartnett, S. Bernstein, E. Maguire and R. Tustison, "Optical properties of ALON (aluminum oxynitride)," *Infrared Physics & Technology*, vol. 39, no. 4, p. 203–211, 1998.
- [70] X. Liu, F. Chen, F. Zhang, H. Zhang, Z. Zhang, J. Wang, S. Wang and Z. Huang, "Hard transparent AlON ceramic for visible/IR windows," *Int. Journal of Refractory Metals and Hard Materials*, vol. 39, pp. 38-43, 2013.
- [71] A. Krell, K. Waetzig and J. Klimke, "Effects and elimination of nanoporosity in transparent sintered spinel (MgAl<sub>2</sub>O<sub>4</sub>)," *Proc. of SPIE*, vol. 8016, no. 02, pp. 1-10, 2013.
- [72] I. Ganesh, "A review on magnesium aluminate (MgAl<sub>2</sub>O<sub>4</sub>) spinel: synthesis, processing and applications," *International Materials Reviews*, vol. 58, no. 2, pp. 63-112, 2013.
- [73] F. Tavangarian and R. Emadi, "Synthesis and characterization of pure nanocrystalline magnesium aluminate spinel powder," *Journal of Alloys and Compounds*, vol. 489, no. 2, pp. 600-604, 2010.

- [74] C.-T. Wang, L.-S. Lin and S.-J. Yang, "Preparation of MgAl<sub>2</sub>O<sub>4</sub> Spinel Powders via Freeze-Drying of Alkoxide Precursors," *J. of the American Ceramic Society*, vol. 75, no. 8, pp. 2240-2243, 1992.
- [75] M. Amini, M. Mirzaee and N. Sepanj, "The effect of solution chemistry on the preparation of MgAl<sub>2</sub>O<sub>4</sub> by hydrothermal-assisted sol-gel processing," *Materials Research Bulletin*, vol. 42, no. 3, pp. 563-570, 2007.
- [76] C.Păcurariu, I.Lazău, Z.Ecsedi, R.Lazău, P.Barvinschi and G.Mărginean, "New synthesis methods of MgAl<sub>2</sub>O<sub>4</sub> spinel," *Journal of the European Ceramic Society*, vol. 27, no. 2-3, pp. 707-710, 2007.
- [77] A. Saberi, F. Golestani-Fard, H. Sarpoolaky, M. Willert-Porada, T. Gerdes and R. Simon, "Chemical synthesis of nanocrystalline magnesium aluminate spinel via nitrate-citrate combustion route," *Journal of Alloys and Compounds*, vol. 462, no. 1-2, pp. 142-146, 2008.
- [78] L. Schreyeck, A. Wlosik and H. Fuzellier, "Influence of the synthesis route on MgAl<sub>2</sub>O<sub>4</sub> spinel properties," *J. Mater. Chem.*, vol. 11, pp. 483-486, 2001.
- [79] S. Hashimoto, S. Zhang, W. Lee and A. Yamaguchi, "Synthesis of Magnesium Aluminate Spinel Platelets from  $\alpha$ -Alumina Platelet and Magnesium Sulfate Precursors," *J. of the American Ceramic Society*, vol. 86, no. 11, pp. 1959-1961, 2003.
- [80] C. Bickmore, K. Waldner, D. Treadwell and R. Laine, "Ultrafine spinel powders by flame spray pyrolysis of a magnesium aluminum double alkoxide," *J. Am. Cer. Soc.*, vol. 79, no. 5, pp. 1419-1423, 1998.
- [81] S. Sanjabi and A. Obeydavi, "Synthesis and characterization of nanocrystalline MgAl<sub>2</sub>O<sub>4</sub> spinel via modified sol-gel method," *Journal of Alloys and Compounds*, vol. 645, pp. 535-540, 2015.
- [82] J. McHale, A. Navrotsky and R. Kirkpatrick, "Nanocrystalline Spinel from Freeze-Dried Nitrates: Synthesis, Energetics of Product Formation, and Cation Distribution," *Chemistry of Materials*, vol. 10, no. 4, p. 1083-1090, 1998.
- [83] N. Radishevskaya, A. Y. Nazarova, O. Lvov, N. Kasatsky and V. Kitler, "Synthesis of magnesium aluminate spinel in the MgO-Al<sub>2</sub>O<sub>3</sub>-Al system using the SHS method," *Journal of Physics: Conf. Series*, vol. 1214, pp. 1-6, 2019.
- [84] V. Gorshkov, P. Miloserdov, V. Yukhvid, N. Sachkova and I. Kovalev, "Preparation of magnesium aluminate spinel by self-propagating high-temperature synthesis metallurgy methods," *Inorganic Materials*, vol. 53, no. 10, p. 1046-1052, 2017.
- [85] D. Domanski, G. Urretavizcaya, F. Castro and F. Gennari, "Mechanochemical Synthesis of Magnesium Aluminate Spinel Powder at room temperature," *J. Am. Ceram. Soc.*, vol. 87, no. 11, p. 2020-2024, 2004.

- [86] Z. Zhihui and L. Nan, "Influence of Mechanical Activation of Al<sub>2</sub>O<sub>3</sub> on Synthesis of Magnesium Aluminate Spinel," *Science of Sintering*, vol. 36, pp. 73-79, 2004.
- [87] S. Meir, S. Kalabukhov, N. Froumin, M. Dariel and N. Frage, "Synthesis and Densification of Transparent Magnesium Aluminate Spinel by SPS Processing," *J. Am. Ceram. Soc.*, vol. 92, no. 2, p. 358–364, 2009.
- [88] N. Jiang, Q. Liu, T. Xie, P. Ma, H. Kou, Y. Pan and J. Li, "Fabrication of highly transparent AlON ceramics by hot isostatic pressing post-treatment," *Journal of the European Ceramic Society*, vol. 37, no. 13, pp. 4213-4216, 2017 .
- [89] S. Huang, F. Gao, Q. Li and X. Chenga, "AlON phase formation in hot-pressing sintering Al<sub>2</sub>O<sub>3</sub>/AlN composites and their oxidation behavior," *Journal of Alloys and Compounds*, vol. 685, pp. 309-315, 2016.
- [90] X. Li, J. Luo and Y. Zhou, "Spark plasma sintering behavior of AlON ceramics doped with different concentrations of Y<sub>2</sub>O<sub>3</sub>," *Journal of the European Ceramic Society*, vol. 35, no. 7, pp. 2027-2032, 2015.
- [91] J. QI, Y. WANG, T. LU, Y. YU, L. PAN, N. WEI and J. WANG, "Preparation and Light Transmission Properties of AlON from nanosized Al<sub>2</sub>O<sub>3</sub> and AlN," *The Minerals, Metals & Materials Society and ASM International*, vol. 42, no. A, p. 4075–4079., 2011.
- [92] E. Kroke, L. Loeffler, F. F. Lange and R. Riedel, "Aluminum Nitride Prepared by Nitridation of Aluminum Oxide Precursors," *Journal of the American Ceramic Society*, vol. 85, no. 12, pp. 3117 - 3119, 2002.
- [93] T. Suehiro, N. Hirosaki, R. Terao, J. Tatami, T. Meguro and K. Komeya, "Synthesis of Aluminium Nitride Nanopowders by Gas-Reduction-Nitridation Method," *Journal of the American Ceramic Society*, vol. 86, no. 6, p. 1046–1048, 2003.
- [94] C. Chiang, "1. Ph.D Thesis: Synthesis of ultrafine aluminum nitride powder using a new carbothermal reduction process.," Rutgers The State University of NJ, New Brunswick NJ, 1993.
- [95] T. Yamakawa, J. Tatami, T. Wakihara, K. Komeya and T. Meguro, "Synthesis of AlN Nano-powder from  $\gamma$ -Al<sub>2</sub>O<sub>3</sub> by Reduction–Nitridation in a Mixture of NH<sub>3</sub>–C<sub>3</sub>H<sub>8</sub>," *J. Am. Ceram. Soc.*, vol. 89, no. 1, pp. 171-175, 2006.
- [96] T. Suehiro, J. Tatami, T. Meguro, S. Matsuo and K. Komeya, "Synthesis of spherical AlN particles by gas-reduction nitridation method," *Journal of the European Ceramic Society*, vol. 22, p. 521–526, 2002.
- [97] T. Yamakawa, J. Tatami, K. Komeya and T. Meguro, "Synthesis of AlN powder from Al(OH)<sub>3</sub> by reduction-nitridation in a mixture of NH<sub>3</sub>-C<sub>3</sub>H<sub>8</sub> gas," *J. Eur. Ceram. Soc.*, vol. 26, no. 12, pp. 2413-2418, 2006.

- [98] X. Yuan, X. Liu, F. Zhang and S. Wang, "Synthesis of  $\gamma$ -AlON Powders by a Combinational Method of Carbothermal Reduction and Solid-State Reaction," *J. Am. Ceram. Soc.*, vol. 93, no. 1, p. 22–24, 2010.
- [99] Y. Wang, Q. Li, S. Huang, X. Cheng, P. Hou, Y. Wang and S. Y. G. Chen, "Preparation and properties of AlON powders," *Ceramics International*, vol. 44, p. 471–476, 2018.
- [100] M. Su, Y. Zhou, K. Wang, Z. Yanga, Y. Cao and M. Hong, "Highly transparent AlON sintered from powder synthesized by direct nitridation," *Journal of the Euro. Cer. Society*, vol. 35, p. 1173–1178, 2015.
- [101] L. Zhang, H. Luo, L. Zhou, Q. Liu and J. L. W. Zhang, "Preparation of  $\gamma$ -aluminum oxynitride phosphor with Eu doping by direct nitridation in ammonia and post-annealing," *J. Am. Cer. Soc.*, vol. 101, p. 3299–3308, 2018.
- [102] S. Kikkawa, N. Hatta and T. Takeda, "Preparation of Aluminum Oxynitride by Nitridation of a Precursor Derived from Aluminum–Glycine Gel and the Effects of the Presence of Europium," *J. Am. Ceram. Soc.*, vol. 91, no. 3, p. 924–928, 2008.
- [103] H. Fukuyama, W. Nakao, M. Susa and K. Nagata, "New Synthetic Method of Forming Aluminum Oxynitride by Plasma Arc Melting," *J. Am. Ceram. Soc.*, vol. 82, no. 6, p. 1381–1387, 1999.
- [104] B. Naderi-Beni and A. Alizadeh, "Development of a new sol-gel route for the preparation of aluminum oxynitride nano-powders," *Ceramics International*, vol. 46, p. 913–920, 2020.
- [105] G. Ye, J. Shang, D. Zhang, M. Liang and Y. Chen, "Synthesis and Oxidation Behavior of MgAlON Prepared from Different Starting Materials," *J. of the Am. Cer. So.*, vol. 93, no. 2, pp. 322–325, 2010.
- [106] B. Ma, Y. Wang, W. Zhang and Q. Chen, "Pressureless sintering and fabrication of highly transparent MgAlON ceramic from the carbothermal powder," *Journal of Alloys and Compounds*, vol. 745, pp. 617–623, 2018.
- [107] S. Bandyopadhyay, G. Rixecker, F. Aldinger and H. S. Maiti, "Effect of Controlling Parameters on the Reaction Sequences of Formation of Nitrogen-Containing Magnesium Aluminate Spinel from MgO, Al<sub>2</sub>O<sub>3</sub>, and AlN," *J. of the Amer. Cer. Soc.*, vol. 87, no. 3, pp. 480–482, 2004.
- [108] W. Dai, W. Lin, Y. O. A. Yamagushi, J. Yu and Z. Zou, "Synthesis of Magnesium Aluminum Oxynitride by Carbothermal Reduction Nitridation Process," *Journal of the Ceramic Society of Japan*, vol. 115, no. 1, pp. 42–46, 2007.

- [109] S. Pichlbauer, H. Harmuth, Z. Lencés and P. Sajgalík, "Preliminary investigations of the production of MgAlON bonded refractories," *Journal of the European Ceramic Society*, vol. 32, p. 2013–2018, 2012.
- [110] X. Cheng, L. Liu, G. Qiu, Z. Bai, M. Guo, F. Cheng and M. Zhang, "Low temperature and pressureless synthesis of MgAlON: qualitative analysis and formation evolution," *Int. J. Mater. Res.*, vol. 111, no. 7, pp. 537-545, 2020.
- [111] F. Chen, F. Zhang, J. Wang, H. Zhang, R. Tian, Z. Zhang and S. Wang, "Hot isostatic pressing of transparent AlON ceramics with Y<sub>2</sub>O<sub>3</sub>/La<sub>2</sub>O<sub>3</sub> additives," *Journal of Alloys and Compounds*, vol. 650, pp. 753-757, 2015.
- [112] L. Henkel, D. Koch and G. Grathwohl, "MgAl<sub>2</sub>O<sub>4</sub>-Spinel Synthesized by High-Energy Ball Milling and Reaction Sintering," *J. of the Am. Cer. Soc.*, vol. 92, no. 4, pp. 805-811, 2009.
- [113] M. Mouyane, B. Jaber, B. Bendjemil, J. Bernard, D. Houivet and J. G. Noudem, "Sintering behavior of magnesium aluminate spinel MgAl<sub>2</sub>O<sub>4</sub> synthesized by different methods," *Int. J. of Applied Ceramic Technology*, vol. 16, no. 3, pp. 1138-1149, 2019.
- [114] A. Talimian, V. Pouchly, H. F. El-Maghraby, K. Maca and D. Galusek, "Impact of high energy ball milling on densification behaviour of magnesium aluminate spinel evaluated by master sintering curve and constant rate of heating approach," *Ceramics International*, vol. 45, no. 17, pp. 23467-23474, 2019.
- [115] N. Obradović, W. Fahrenholtz, S. Filipović, D. Kosanović, A. Dapčević, A. Đorđević, I. Balać and V. Pavlović, "The effect of mechanical activation on synthesis and properties of MgAl<sub>2</sub>O<sub>4</sub> ceramics," *Ceramics International*, vol. 45, no. 9, pp. 12015-12021, 2019.
- [116] S. Peddarasi and D. Sarkar, "Mechanochemical effect on synthesis and sintering behavior of MgAl<sub>2</sub>O<sub>4</sub> spinel," *Materials Chemistry and Physics*, vol. 262, pp. 1-8, 2021.
- [117] B. Ma, W. Zhang, Y. Wang, X. Xie, H. Song, C. Yao, Z. Zhang and Q. Xu, "Hot isostatic pressing of MgAlON transparent ceramic from carbothermal powder," *Ceramics International*, vol. 44, no. 4, pp. 4512-4515, 2018.
- [118] R. M. German, *Powder Metallurgy & Particulate Materials Processing*, Metal Powder Industries Federation, 2005.
- [119] Z. Feng, X. Huang, D. Chen, Z. Liao, J. Qi and T. Lu, "Pressureless sintering of transparent AlON ceramic with assimilable  $\gamma$ -Al<sub>2</sub>O<sub>3</sub> as sintering promoting additives," *J. of the Am. Cer. Society*, 2022.
- [120] Z. Feng, J. Qi, X. Guod, Y. Wang, XiuxiaCao, Y. Yu, C. Meng and T. Lu, "A new and highly active sintering additive: SiO<sub>2</sub> for highly-transparent AlON ceramic," *Journal of Alloys and Compounds*, vol. 787, pp. 254-259, 2019.

- [121] R. Zhang, H. Wang, M. Tian, Y. Wang, M. Liu, H. Wang and G. Zhang, "Pressureless reaction sintering and hot isostatic pressing of transparent MgAlON ceramic with high strength," *Ceramics International*, vol. 44, no. 14, pp. 17383-17390, 2018.
- [122] H. Boussebha, S. Bakan and A. Kurt, "Dynamic / thermochemical method: A novel approach in the synthesis of B<sub>4</sub>C powder," *Open Ceramics*, vol. 6, no. S1, pp. 1-7, 2021.
- [123] Z. Yıldızlı, «Synthesizing TiB<sub>2</sub>, B<sub>4</sub>C and BN ceramic powders using dynamic / thermochemical method,» MSc Thesis, Sakarya University, 2019.
- [125] A. O. K. Engin B. Türker, "TiN Powder Synthesis using Dynamic CRN Method," *Afyon Kocattape University FEMÜBİD*, vol. 14, pp. 565-569, 2014.
- [126] H. Boussebha, E. Akcan and A. O. Kurt, "Syntheses of AlN Nanopowder," in *SERES'18*, Eskişehir, Turkey, 2018.
- [127] L. Zhang, L. Zhang, Z. Lin, Y. Jiang, J. He, W. Cai and S. Li, "Synthesis of β-SiAlON Nanopowder by Ammonolysis of Alumina–Silica Gel," *J. Am. Ceram. Soc.*, vol. 97, no. 1, p. 40–43, 2014.
- [128] M. Yan, Y. Li, L. Li, Y. Sun, S. Tong and J. Sun, "In-situ synthesis and reaction mechanism of MgAlON in Al<sub>2</sub>O<sub>3</sub>-MgO composites produced in flowing nitrogen," *Ceramics International*, vol. 43, no. 17, pp. 14791-14797, 2017.
- [129] H. Boussebha, N. Mutlu, N. Canikoglu and A. O. Kurt, "Synthesis of submicron AlN powder using dynamic/thermochemical method," *Internation Journal of Applied Ceramic Technology*, vol. 19, no. 6, pp. Pages 2967-2978, 2022.



## **CURRICULUM VITAE**

Name Surname : Hamza Boussebha

### **EDUCATION:**

- **Undergraduate** : 2011, Annaba University, Department of Materials Science, Materials Science and Engineering
- **Graduate** : 2013, Annaba University, Department of Materials Science, Materials Science and Engineering

### **PROFESSIONAL EXPERIENCE AND AWARDS:**

- He worked as a logistics supervisor at NAXCO Group between 2014 and 2015
- He was awarded a full scholarship to pursue a PhD at Sakarya University
- He worked as foreign language tutor and IELTS coach with different private institutes.
- He is currently working as foreign trade special and export at ESKA VALVE AŞ

### **PUBLICATIONS, PRESENTATIONS AND PATENTS ON THE THESIS:**

- Syntheses of Aluminum Nitride Nano powder; International Ceramic Conference Eskisehir, Turkey (SERES'18); SERES'18 Conference Proceeding Book.
- AlON Synthesis Possibility from Al(OH)<sub>3</sub> via Dynamic CRN; European Ceramic Society Workshop for Young Ceramist Proceedings; ISBN: 978-88-7586-599-3
- Synthesis of submicron AlN powder using dynamic/thermochemical method International Journal of Applied Ceramic Technology, ACerS.
- MS&T 2022 Pittsburgh Pennsylvania. Workshop for glass and Ceramics Students.

### **OTHER PUBLICATIONS, PRESENTATIONS AND PATENTS:**

- Simulation Model of The Growth Kinetics of Fe<sub>2</sub>b Layers with Consideration of The Boride Incubation Time Effect; Surface Review and Letters; <https://doi.org/10.1142/S0218625X19501270>
- A Technique for the Production of Submicron Boron Carbide Powder Afyon Kocatepe University Journal of Science and Engineering; ISSN: 2149-3367.
- The corrosion kinetics of cordierite based ZrO<sub>2</sub> composites obtained from natural zeolite in dilute HCl acid solution, Journal of Composite Materials.
- Dynamic / thermochemical method: A novel approach in the synthesis of B<sub>4</sub>C powder; ECerS Open Ceramics.